UNIVERSITA' DELLA CALABRIA

Dipartimento di INGEGNERIA MECCANICA, ENERGETICA E GESTIONALE

Scuola di Dottorato

PITAGORA

Indirizzo

INGEGNERIA MECCANICA

CICLO

XXVII

TITOLO TESI

DEVELOPMENT, MODELING AND TECHNICAL ANALYSIS OF POLYMERIC FUEL CELL PROPULSION SYSTEMS FOR HYBRID ELECTRIC VEHICLES

Settore Scientifico Disciplinare ING-IND/09

Direttore: Ch.mo Prof. LEONARDO PAGNOTTA

Firma

Supervisore: Ch.mo Prof. PETRONILLA FRAGIACOMO

Firma

Dottorando: Dott. DOMENICO DE LUCA

Firma

UNIVERSITY OF CALABRIA

DEPARTMENT OF MECHANICAL, ENERGY AND MANAGEMENT ENGINEERING
DIMEG

PhD in Mechanical Engineering

School "Pitagora"

XXVII Cycle

PhD Thesis

Development, modeling and technical analysis of polymeric Fuel Cell propulsion systems for Hybrid Electric Vehicles

Coordinator

Prof. Leonardo Pagnotta

Supervisor

Prof. Petronilla Fragiacomo

Candidate

M. Eng. Domenico De Luca

RESEARCH FIELD: ING-IND/09

ACADEMIC YEAR 2014/15

To my family,

where the love come true.

Acknowledgments

The author would like to thank the following people that gave special support to the Research: Prof.ssa Petronilla Fragiacomo, for her fundamental support, Prof. Walter Theodor Czarnetzki, for the fruitful period in Germany, M. Eng. Waldemar Schneider, for his technical advices, Ing. Giovanni Pede, for his collaboration, Prof.ssa Maria Angela Gentile, Prof. Maria Francesca Camodeca and Prof. Mariarosa De Rosa for their trust, the secretary employees of my high schools, in particular Mr. Nuccio, for their disposability, Prof. John Broughton, for his language suggestions, M. Eng. Giuseppe De Lorenzo, M. Eng. Francesco Pizzonia, M. Eng. Orlando Corigliano and M. Eng. Amelia Mirandola, for their help, Prof. Sergio Rizzuti and Prof. Leonardo Pagnotta, for their guidance in school "Pitagora", all industrial and research partners of European projects, for cooperation and for giving me chances to improve and to continue this Research, and undoubtedly my wife Ersilia, for her love and patience.

Abstract

One of the major consumers of oil with concerns about climate change, pollutions and depletion of fossil fuels is the transportation sector. The predictions about the increasing trend of numbers of vehicle, considering two-wheeled and four-wheeled ones, imply a special focus for alternative fuels which are sustainable and environmental friendly into the future. In this context hydrogen is expected to play a lead role. The Proton Exchange Membrane Fuel Cell appear as the best technology in the long term to produce electrical energy on board, while the hybrid electric configuration for powertrains appear the most suitable arrangement for energy optimization.

The main purpose of the Research is the theoretical evaluation of newly designed hybrid electric powertrains equipped with Fuel Cells. These studies were carried out through numerical modeling and simulation in Matlab/Simulink® environment. The results allow a deeply analysis of the Fuel Cell stacks and the hybrid electric configurations with a special focus on the power flows, energy balance, consumptions, logic of control, water and thermal management, efficiency, etc., in order to improve the overall behaviour of sub-systems and of the entire powertrain and in order to correctly dimension various components. The use of simulation and numerical modeling is beneficial in terms of cost and time in comparison with real prototyping. So, it can be considered as the first step in the design and testing of these type of vehicles.

The Matlab/Simulink® model consists of several block connected each other where the parameters which characterize each components are estimated under varying operating conditions in accordance with some external conditions. The simulations are carried out for several applications for a wide range of vehicle which comprise two-wheeled vehicles and cars both for different segments and uses in theoretical urban, sub-urban and motorway driving cycles. In the case of a two-wheeled vehicle, such as a Fuel Cell powered bicycle, the driving cycle taken into consideration is not theoretical but real, since it is obtained directly from measurements on board.

Sommario

Uno dei maggiori settori di consumo di petrolio e combustibili fossili è il settore dei trasporti. Questo comporta conseguenze negative per ciò che riguarda l'inquinamento ambientale ed i cambiamenti climatici. Le previsioni di un aumento mondiale del numero di veicoli a due ruote ed a quattro ruote, implicano una speciale attenzione per i combustibili alternativi e sostenibili dal punto di vista ambientale. In questo contesto l'idrogeno gioca un ruolo chiave. Le celle a combustibile, infatti, ad elettrolita polimerico si presentano come la più promettente tecnologia nel lungo periodo per produrre energia a bordo dei veicoli. Tale tecnologia trova applicazione nei veicoli ibridi in cui i flussi energetici sono ottimizzati.

L'attività di ricerca svolta ha avuto come principale obiettivo l'analisi numerica di sistemi a propulsione innovativa equipaggiati con celle a combustibile. Questi studi sono stati condotti attraverso la definizione di modelli matematici di simulazione numerica in ambiente Matlab/Simulink®. I risultati consentono una dettagliata analisi delle celle a combustibile e delle configurazioni di veicoli ibridi con particolare riferimento ai flussi di potenza, al bilancio energetico, ai consumi, alla logica di controllo, all'umidificazione della membrana, al controllo termico, all'efficienza, ecc., al fine di dimensionare correttamente i vari componenti. L'utilizzo della simulazione numerica consente un'analisi più veloce ed economica rispetto alla realizzazione dei prototipi. Pertanto, essa può essere considerata come il primo passo nella progettazione e nella sperimentazione di questi veicoli.

Il modello in Matlab/Simulink® consiste in un modello a blocchi dove i vari parametri operativi sono stimati in diverse condizioni operative nel rispetto di alcuni vincoli predefiniti. Le simulazioni sono svolte per diverse applicazioni per una vasta gamma di veicoli che comprendono veicoli a due ruote ed automobili di diversi segmenti per tragitti, definiti teoricamente, urbani, misti ed extra-urbani. Nel caso specifico di una veicolo a due ruote, derivato da una bicicletta elettrica con l'aggiunta di una cella a combustibile, i cicli di guida presi in considerazione non sono teorici, ma reali, in quanto ottenuti direttamente tramite misurazioni a bordo del veicolo.

Table of contents

List of Figures

List of Tables

Nomenclature, abbreviations and subscripts

Nomenclature (Latin letters)

A_{cell}	Cell area	[cm^2]
$A_{vehicle}$	Frontal surface of vehicle	[m^2]
C	battery capacity	[Ah]
C_r	Rolling coefficient	[-]
C_x	Drag coefficient	[-]
E_{Nernst}	Nernst voltage	[V]
E_0	theoretical battery cell voltage	[V]
F	Faraday constant	[C/mol]
F_{AERO}	aerodynamic resistance (force)	[N]
F_{GRAV}	gravitational resistance (force)	[N]
F_{INERT}	inertial resistance (force)	[N]
F_{ROLL}	rolling resistance (force)	[N]
h	energy flow of reactants	[W]
HD	degree of hybridization	[-]
HHV	High heating value	[kJ/kg]
i	Current density	[A/cm2]
i_L	Limiting current density	[A/cm2]
i_0	Exchange current density	[A/cm2]
I	Current	[A]
I_{BATT}	battery current	[A]
I_{FC}	fuel cell current	[A]
k	Mass transport (concentration overpotential)	[-]
LHV	Low heating value	[kJ/kg]
m	mass of vehicle	[m]
$\dot{m}$	Mass flow rate	[g/s]
mm	Molecular mass	[g/mol]
n	number of electrons in a atom of hydrogen	[-]
N_{cells}	Number of cells	[-]
OCV	Open circuit voltage	[V]

p	Operating pressure	[atm]
p_{air}	Air pressure	[atm]
p_{H2}	Hydrogen pressure	[atm]
p_{H2O}	Water pressure	[atm]
p_{O2}	Oxygen pressure	[atm]
pp	partial pressure	[atm]
p_{sat}	Saturation pressure	[atm]
P_{AUX}	power of auxiliaries	[W]
P_{BATT}	power flow of battery	[W]
P_{cell}	Cell power	[W]
$P_{CHG(max)}$	maximum power charging battery	[W]
P_{ED}	power flow requested by ED	[W]
P_{ED_avg}	Average power request by ED	[W]
P_{EM}	power flow of electrical machine	[W]
$P_{EM\text{-}nom}$	nominal power of EM	[W]
P_{FC}	Fuel cell stack power	[W]
$P_{FC\text{-}max}$	maximum power of FC	[W]
P_{LOST}	power lost during braking	[W]
P_{REC}	power recovered during braking	[W]
q	charge of particles	[C/mol]
$\dot{Q}$	Heat generated (thermal power)	[W]
r	Internal resistance	[Ω/cm2]
R	Universal gas constant	[J/mol·K]
sh	Specific heat	[J/mol·K]
slope	slope of the road	[-]
SOC	state of charge of battery	[-]
SOC_L	state of charge lower limit	[-]
SOC_U	state of charge upper limit	[-]
St	Stoichiometric ratio	[-]
t	time	[s]
t_{tot}	time of the mission	[s]
T	Operating temperature	[°C]
T_K	Operating temperature in Kelvin	[K]
Tambient	Ambient temperature	[°C]

Tinlet	Inlet temperature	[°C]
$v_{vehicle}$	speed of vehicle	[m/s]
V_{act}	Activation overpotential	[V]
V_{cell}	Cell voltage	[V]
V_{con}	concentration overpotential	[V]
V_{BATT}	battery voltage	[V]
V_{FC}	fuel cell voltage (stack)	[V]
V_{ohm}	Ohmic overpotential	[V]
V_{th}	Theoretical voltage	[V]
x	Mole fraction in a chemical compound	[-]

Nomenclature (Greek letters)

α	Transfer coefficient (activation overpotential)	[-]
α_1	Amplification constant (concentration overpotential)	[AV/cm2]
ΔG	Gibbs free energy change	[J/mol]
ΔH	Enthalpy change	[J/mol]
ΔS	Entropy change	[J/mol•K]
ΔV	Overpotential	[V]
η_{EM}	efficiency electrical machine	[-]
$\eta_{INVERTER}$	efficiency inverter	[-]
η_{TRASM}	efficiency mechanical transmission	[-]
η_{FC}	Fuel Cell efficiency	[-]
ϕ	Relative humidity	[-]
ρ	Air density	[kg/m^3]

Abbreviations and subscripts

act	Activation
BATT	Battery
BoP	Balance of Plant
BP	Bipolar plates
CL	Catalyst Layer
conc	Concentration

DM	Diffusion media
EM	Electrical Machine
ED	Electric Drive
EPC	Electronic Power Converter
EV	Electric Vehicle (purely)
FC	Fuel Cell
FCEV	Fuel Cell Electric Vehicle
FCHEV	Fuel Cell Hybrid Electric Vehicle
FCH JU	Fuel Cell Hydrogen Joint Undertaking
HEV	Hybrid Electric Vehicle
HV	Hybrid Vehicle
ICE	Internal Combustion Engine
MEA	Membrane electrode assembly
OEM	Original Equipment Manufacturer
ohm	Ohmic
PEM	Proton Exchange Membrane
PEMFC	Proton Exchange Membrane Fuel Cell
PHEV	Plug-in Hybrid Electric Vehicle
PMU	Power Management Unit
RESS	Rechargeable Energy Storage System

1. Introduction

1.1 Motivation

Owing to the limitation of fossil fuels and high consumption and pollution for transportation, the vehicle industry is looking for other sources of energy. A Fuel Cell Hybrid Electric Vehicle (FCHEV) could be a suitable solution considering the state of the art of electric motors, power electronics, energy storage systems and fuel cell stacks. Since the integration of all these components is a new challenge for the manufacturer, simulation before prototyping is beneficial in terms of cost, design and performance.

Proton Exchange Membrane Fuel Cells (PEMFCs), which convert the chemical energy stored in hydrogen fuel directly to electrical energy with water as the only product, are seen as one of the most promising technology for clean and efficient power generation in the twenty-first century. In fact, PEMFCs are able to reduce our energy use, pollutant emissions and dependence on fossil fuels [1].

PEMFC are the most popular type of fuel cell and they are set to become the power source of the future. The interest in PEMFC has increased during the last couple of decades due the limitation of fossil fuels and their pollution concerns. Especially, when fueled with hydrogen that is obtained from renewable energy resources, PEMFCs are characterized as zero-emission energy generating technology [2].

The improvement in FC technology helps to achieve the main purpose of “zero emission” in the passenger vehicle market. The design of “zero emissions” vehicles can be facilitated through the optimization of the components in order to minimize the consumptions with particular reference to the functions of the vehicles, the areas where they are driven and their use with different driving style. In the last years, it has been demonstrated that FC vehicles are very efficient but they need to be designed for a specific task, called “mission”, in order to reduce the cost and to increase the efficiency. In fact, some parameters, such as the average

power used by the vehicle and the minimum energy storage capacity, are dependent on the mission [3] [4].

Interest in FCHEVs derives from several technical and economic considerations. In fact, a purely electric vehicle presents characteristics, such as the autonomy range and recharging time, which limit the adaptability of the vehicles to longer and more demanding missions. Hybrid vehicles allow the autonomy to be increased due to the on-board stored hydrogen. Furthermore, the hydrogen refueling time is lower than the recharging time of the batteries. On the other hand, a hybrid vehicle requires a more complex architecture due the presence of two different power sources [5] [6].

This Research presents the simulation of a powertrain for FCHEVs in order to dimension the Fuel Cell (FC) as primary source of energy and to investigate the power flows during both motoring and recuperative braking. For this purpose a Matlab/Simulink® model has been built up which can be used for a wide range of applications. The results of simulation show which of the following is the best powertrain configuration for several vehicles: a bike in which the traction force is provided by both electric motor and the pedaling of the cyclist, a bike in which the traction force is provided only by an electric motor without pedaling, a motorcycle for 2 passengers and cars which belong to the European segments A-B-C-D-E. All of these vehicles are equipped with a Proton Exchange Membrane fuel Cell (PEMFC) and a Lithium-Ion battery. The presence of human force during the motion can be also taken into consideration.

Specifically, the specific consumption, the total consumption in a definite route, the state of charge of battery (SOC), the battery voltage and the amount of energy generated by FC will be monitored. The model validation will be done by comparison between the obtained results and scientific articles in the literature.

1.2 Scope of the research

Fuel Cell (FC) technology appears to be a very promising solution to replace petroleum-based vehicles with the aim of reducing the combined issues of air pollution and rapidly depleting oil. The main technological and economic barriers influencing the penetration of this technology into the mass market regard hydrogen infrastructures, the degradation and durability of some components and the high cost of FC stacks. The adoption of a hybrid electric powertrain in which the power required for propulsion can be provided from both a

primary source of energy and a Rechargeable Energy Storage System (RESS) allows the dimensioning of the FC in terms of the average value of power required, because the remaining rate needed for peak power is provided by the RESS and, consequently, the cost of the powertrain is reduced.

Two-wheeled vehicles, such as electric bicycles, are very popular in dense urban areas where traffic is an everyday challenge. This is especially true for China and the Asian Pacific area where these vehicle types are a practical and economical means of transportation compared to Internal Combustion Engine (ICE) driven vehicles. Consequently, many Original Equipment Manufacturers (OEMs) and research centers have created prototypes of bicycles powered by FC in order to analyze the benefit of hydrogen technology in transportations [7].

Historically, in the 1970s many OEMs started to develop Electric Vehicles (EVs) powered by batteries due to the oil shortage. However, these electric vehicles powered solely by battery had a restricted driving range. Meanwhile, automotive manufacturers have moved in the direction of Hybrid Electric Vehicles (HEVs) based on ICEs because they are considered a good solution in the short and medium term, whereas FCHEVs are considered a good solution in the long term due their high efficiency and zero emissions [8] [9].

This interest has arisen globally in recent years due to the pressing environmental concerns, representing a revolutionary change in vehicle design philosophy [10].

In fact, many scientific researches about the development of two-wheeled vehicles equipped with FC have been published in the last ten years, such as Hwang who published the test results of a PEMFC powered prototype bicycle in which the FC stack consisted of 40 cells which has a power of 300W with an efficiency up to 35% and a distance-to-fuel ratio of 1.35 km/g [11].

In further projects two-wheeled vehicles have been tested and presented with the aim to optimize the behavior of the powertrain, to increase the efficiency of the system and to extend the autonomy of vehicles [12-18].

The Proton Exchange Membrane Fuel Cell (PEMFC) is the most promising technology for automotive applications due to many attractive features, such as low operation temperature, quick start-up, sustained operation at a high current density, low weight, compactness, sufficient stack life time and suitability for discontinuous operation [19].

PEMFCs have recently passed the demonstration phase and have partly reached the commercialization stage on account of rapid development and an impressive research effort

worldwide. However, the remaining challenges that need to be overcome mean that it will be several years before full commercialization can take place. While each challenge has been focused on differently according to each application, there are three main challenges that are common to each use: supply of high-purity hydrogen, cost reduction of the system and various technological problems. Moreover, the development of FCHEV requires the on-board integration of a fuel cell system and electric energy storage devices, with an appropriate energy management system [20] [21].

1.3 Methodology

The main portion of the Research is based on computer simulations. The characteristics of the Hybrid Electric powertrain and of the PEMFC system are implemented by using Matlab/Simulink® models as simulation tool for process modeling and energy system analysis. A component library, which includes models of Fuel Cell, Lithium-Ion batteries, driving cycles, control units, humidifiers, auxiliaries, etc., has been created. The physical, electrochemical and thermodynamic equations that describe all occurring phenomena are inserted in these models.

The design procedure consist of the following steps:

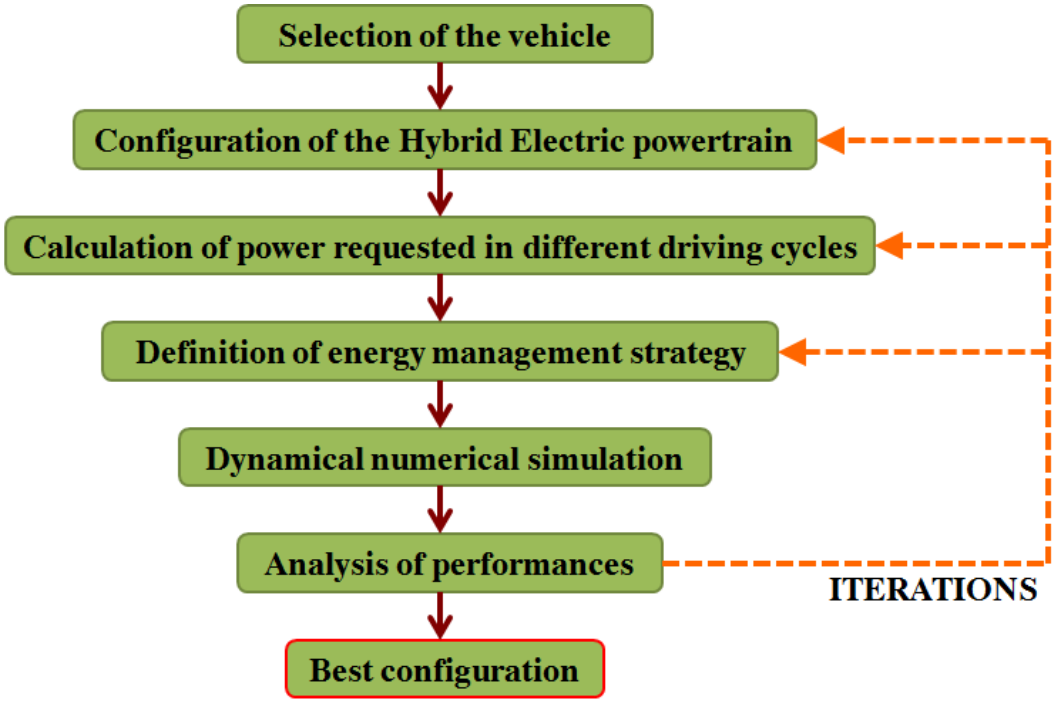

Fig. 1.1: Design procedure of the Research

As indicated in the Fig. 1.1, some iterations will be done after each simulation in order to assess the specifications of the newly powertrains to enhance the performance and reduce their disadvantages. This procedure could be used for a wide range of vehicles with similar topologies of the balance of plant and the auxiliaries devices. The size of the system will be optimized in different driving conditions and for a wide range of applications. For instance an enhanced analysis of two-wheeled vehicle and four-wheeled vehicle will be carried out through the simulation of the real transportations targets.

The dynamic interactions among all components of a FC system make it difficult to design newly designed FCHEVs because each of the design parameters must be carefully chosen for better fuel economy, enhanced safety, exceptional drivability and a competitive dynamic performance. Since prototyping and testing each design combination is cumbersome, expensive and time consuming, numerical modeling and simulation are indispensable for concept evaluation and analysis of FCHEVs. Also, the development of PEMFCs requires the simulation of the entire system under different loading conditions, pressures of reagent gases and temperature.

According to Fig. 1.2, the numerical model can be classified in steady-state, quasi-steady and dynamic. In this thesis two different model are built up and presented: the first one for simulation of PEMFCs (a steady-state model in zero-dimension) and the second one for simulation of FCHEVs (a quasi-steady model in backward-facing).

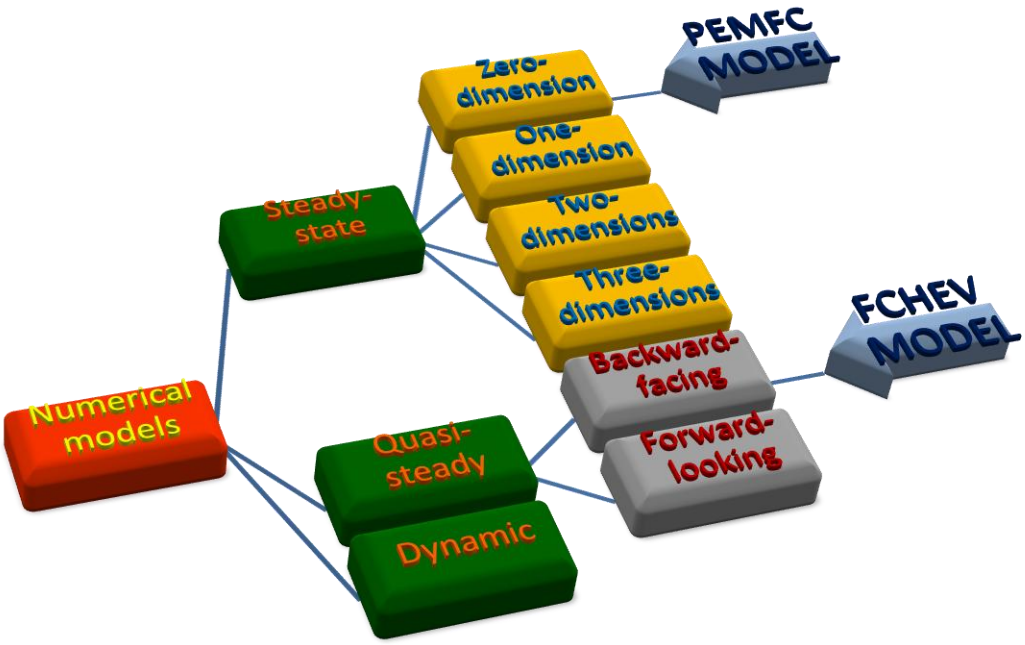

Fig. 1.2: Numerical model classification

1.4 Overview of the thesis

The proceeding of PhD thesis is classified in the following chapters:

Chapter 1 presents the statement of purpose for this Research and the methodology used.

Chapter 2 provided the background of Fuel Cell technology and the balance of plant. The Fuel Cell theory is explained with a special attention to the basic structure, the electrochemistry and the thermodynamics.

Chapter 3 describes the layout of the studied hybrid electric architectures with a special focus on the energy management, the rechargeable energy storage system, the operating parameters and the experimental and theoretical driving cycles.

Chapter 4 presents the model of the Fuel Cell stack.

Chapter 5 explain the modeling of hybrid electric powertrains with the descriptions of the Matlab/Simulink® models.

Chapter 6 describes the results of simulations for FC stacks (theoretical analysis compared with the data provided by manufactures), two-wheeled vehicles (bike and motorcycles) and four-wheeled vehicles (cars of European market segments).

Chapter 7 present the conclusions of the thesis including some comments about the results of simulations, as well as starting points for further research.

2. Proton Exchange Membrane Fuel Cell technology

2.1 Fuel Cell basics

Proton Exchange Membrane (PEM) and its use in Fuel Cell (FC) is an attractive technology for the sector of transport applications such as in cars and buses because of the high power densities and the low temperatures which allow the requirement of FCs in transportations.

Basically, the operation temperature is around 80 °C, while, in contrast to other FC technologies, a solid membrane is used as electrolyte. Moreover, the sealing, the assembly and the handling is not as complicated as in other FCs. A further advantage of the low operating temperature is that faster startups can be realized, which is very important for transport applications. Consequently, a PEMFC is seen as the main candidate for transportation applications [22] [23].

The future society based on the hydrogen as energy carrier refers to the vision of using hydrogen as a clean energy source and is anticipated to compete with coal, natural gas and gasoline as a fuel for power generation and transportation applications. Importantly, hydrogen is an energy carrier and not an energy source because it is not available directly in nature as pure gas but it must be produced by using other energy sources.

When the electricity is generated through renewable resources such as wind power, hydropower and solar photovoltaic cells and then it is used for electrolysis of water, in this case the hydrogen produced is virtually carbon-free. In the energy supply chain for industrial, commercial and residential application as well as for transportations the hydrogen may be able to store energy from intermittent renewable sources, such as solar and wind power plants where the demand of electricity does not follow the same trend of the generated power. Thus, electricity obtained from renewable sources can be used for electrolysis of water in order to produce hydrogen which will be easily stored.

One of the most promising way to use hydrogen is for automotive applications instead of fuel obtained from oil. It use consist in a internal combustion engine (ICE) as fuel for combustion or, alternatively, when used in FCs, as reactants to produce directly electricity which will be provided to an electric motor for traction. FCs are the promising technology in long term because they are far more efficient than the ICEs and hold several other advantages: they produce only heat and water as exhaust products and, in comparison to batteries, FCs do not discharge and provide power as long as fuel is supplied [24] [25].

2.1.1 Basic structure and characteristics

The structure of a PEMFC consists of proton exchange membranes, diffusion media, catalyst layers, flow field plates, gaskets and end plates, as indicated in Fig. 2.1. The combination of the membrane, diffusion media and the catalyst layer is also called the membrane electrode assembly (MEA). Due to the reason that a single cell is only able to generate a small voltage and current the FCs are connected in parallel or series to obtain an increase in voltage, current and power output. These combinations of unit cells are called a stack [26] [27].

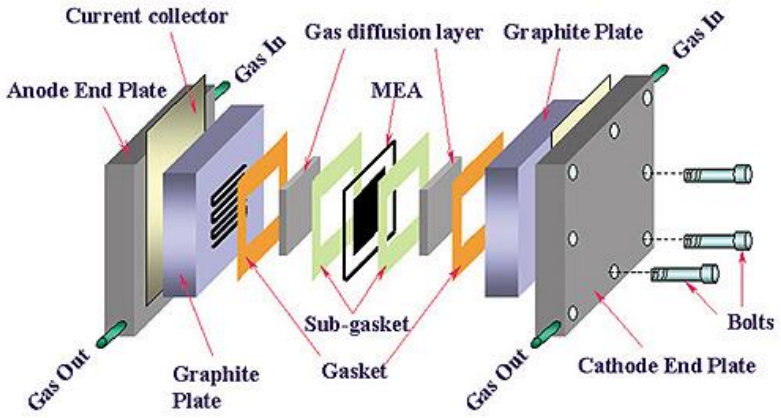

Fig. 2.1: Basic structure of a single cell [26]

During the operation of a PEMFC, shown in Fig. 2.1, hydrogen is forced into the gas flow fields at the anode while air is forced into the gas flow fields at the cathode. These reactants are compressed and, in most cases, humidified to prevent a drying out of the membrane. Usually, the humidification is applied only on the cathode side. Then, gases flow through the respective Diffusion Media (DM) and diffuse into the respective Catalyst Layer (CL). The used catalyst in PEMFCs is platinum. At the CL of the anode hydrogen is then oxidized,

forming protons and electrons, at which the protons moving through the ion conductive membrane and the electrons are conducted by the carbon support in the CL to the current collector of the anode and then over an external circuit to the current collector at the cathode. On the other, side in the cathode CL oxygen is reduced and then forms water with protons and electrons. Afterwards, this product water is transported out of the cathode CL by the flowing air.

During the whole operation also heat is generated due to inefficiencies. This heat has to be conducted out of the fuel cell to avoid overheating. The polymer membrane only resists a temperature rise up to roughly 95 °C [28].

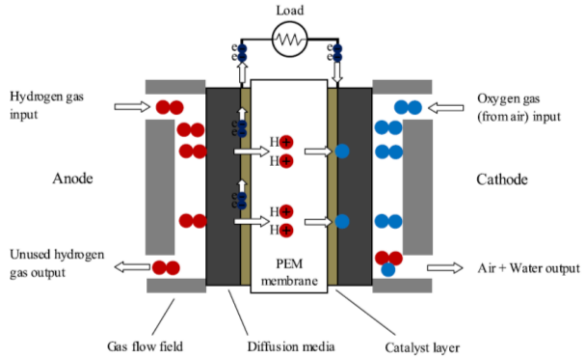

Fig. 2.2: Schematic view of fuel cell operations [28]

The membrane in a PEMFC is a thin layer of a solid electrolyte with a thickness in the range of 10÷100 µm. The main tasks for the membrane are to conduct protons from the anode to the cathode and to prevent a transport of electrons through the membrane. Hence a good material for membranes must be highly conductive for ions and a good isolator. Moreover, it must be chemically and thermally stable as well as mechanically robust. The most used material with the current technologies is based on Nafion, a perfluorosulfonic acid. For the reason of higher physical strength it has a backbone structure of polytetrafluoroethlene (PTFE). Two major transports mechanisms are taking place in the membrane that is the proton and water transport. However, there is a connection between both, because water in the membrane is necessary for the proton transport [29].

The catalyst layer (CL) are very thin layers with a thickness of around 10 µm. This is the location where the hydrogen oxidation reaction (anode) and the oxygen reduction (cathode) takes place. The CLs consist of three different phases, carbon support with dispersed platinum catalyst particles on the surface, ionomer and void space. This structure is important for the electrochemical reaction.

The diffusion media (DM) is usually made of two different layers, the macro-porous layer and the micro-porous layer. The main tasks of these layers are the electronic connection between electrode and bipolar plate, protection of the CL from corrosion or erosion, mechanical support to the membrane electrode assembly (MEA), transfer of reactants and heat and water removal [30].

Gas flow fields distribute the reactants for the chemical reaction and remove the generated water. The gas flow fields are designed in many different types of flow fields, such as parallel, serpentine, pin-type or metal foam designs.

The tasks of the bipolar plates (BPs) which contain the gas flow fields are to provide mechanical strength to the MEA and to guarantee a good conductivity for heat and electron transport. The BPs are made of materials like non-porous graphite or stainless steel.

The main advantages of FC systems are:

- No pollutants
- High efficiency
- Scalable design
- No moving parts
- Low maintenance
- Various methods of supplying fuel
- Low noise

On the other hand, FC systems presents some limitations, such as:

- High cost
- Catalyst degradation with time
- Need of not still available fueling infrastructure

Although future markets for FC include portable, transportation and stationary sectors, these advantages and limitations make the FC technology very suitable for transportation applications. The transportation market will benefit from FC because fossil fuels will become scarce and expensive. Moreover, in most developed countries legislation is becoming stricter about controlling emission of vehicles. Consequently, FC allow a new type of vehicle that are more efficient and environmental friendly than vehicles powered by other fuels [31].

2.1.2 Fuel Cell electrochemistry and thermodynamics

A PEMFC fuel cell consists of a negatively charged electrode (anode), a positively charged electrode (cathode) and an electrolyte membrane. Hydrogen is oxidized on the anode and oxygen is reduced on the cathode. Protons are transported from the anode to the cathode through the electrolyte membrane and the electrons are carried to the cathode over the external circuit [32].

The equation (2.1) shows the basic chemical reaction of a fuel cell, that is reverse to the electrolysis process.

$$H_2 + \frac{1}{2}O_2 \rightarrow H_2O + electricity + heat \qquad (2.1)$$

The equations (2.2) and (2.3) shows the reactions that take place at the anode and cathode.

$$H_2 \rightarrow 2H^+ + 2e^- \quad \text{(at the anode)} \qquad (2.2)$$

$$\frac{1}{2}O_2 + 2e^- + 2H^+ \rightarrow H_2O \quad \text{(at the cathode)} \qquad (2.3)$$

These reactants are transported by diffusion to the electrode surfaces, while the water and the waste heat which are generated into the cell must be continuously removed. This process present some critical issues which must be overcome.

The performance of a fuel cell is defined through its polarization curve. In such a graph the cell voltage is plotted over the current or current density. To calculate the performance P_{cell} of one cell the cell voltage V_{cell} has to be multiplied with the current I:

$$Vcell \cdot I = Pcell \qquad (2.4)$$

Usually, the highest power output is in the middle of the current axis where the product of cell voltage and current reaches its maximum.

In case of the operating conditions require a high efficiency of the FC system, then the operation point has to be shifted to small currents. The reason for that is the irreversibility at higher currents, which result from electrochemical processes. So, more heat is generated instead of electrical energy with higher currents. This aspect is explained numerically in the

chapter 6 where a numerical simulation is carried out for electrochemical processes of a FC stack. Mathematically, the waste heat $\dot{Q}$ is calculated by following equation:

$$\dot{Q} = (V_{th} - V_{cell}) N_{cells} \cdot I \qquad (2.5)$$

Regarding the efficiency, it is important to describe how electrochemical and thermodynamic processes governing the FCs. Fundamentally essential for that is the definition of the Gibbs free energy as it is defined as the amount of energy available to do external work. In the case of fuel cells this energy is used to move electrons around an external circuit and thus produce electricity [23].

The following equation shows the maximum obtainable electrical energy within a fuel cell, which is given by the change in Gibbs free energy ΔG of the electrochemical reaction:

$$\Delta G = \Delta H - T \cdot \Delta S \qquad (2.6)$$

The enthalpy change ΔH represents the total available thermal energy. If the entropy produced during the electrochemical reaction is equal to zero, then a fuel cell reach a theoretic efficiency of 100 %. In this case, which is not real, all energy can be used. However, the entropy is always generated within the FC system and, consequently, the T·ΔS term denotes the unused amount of energy for direct purpose, but it is the amount of heat produced within a reversibly and real working FC system. The theoretical voltage V_{th} is calculated as if all the energy stored in the hydrogen fuel can be transformed into electrical energy with an efficiency of 100 %. Therefore, the Gibbs free energy change equals as well as the enthalpy change and this lead to the following equation for the theoretical voltage:

$$V_{th} = \frac{-\Delta H}{n \cdot F} \qquad (2.7)$$

If the higher heating value (HHV) is used then the result for is 1.48 V. In the equation (2.7), n refers to the number of involved electrons (2 for hydrogen) and F is the Faraday constant. The maximum achievable voltage of a fuel cell is called the open circuit voltage OCV. In that case the system is reversible or has no losses. The value of OCV is usually approximately 1.2 V,

though it is also dependent on partial pressures of the reactants and on the operation temperature:

$$OCV = \frac{-\Delta G}{n \cdot F} \tag{2.8}$$

OCV is also defined ideal voltage. The cell voltage V_{cell} is obtained as OCV minus all the voltage losses (activation, ohmic and concentration):

$$V_{cell} = OCV - V_{act} - V_{ohm} - V_{con} \tag{2.9}$$

The effects of irreversibilies influence the polarization curve for activation, ohmic and concentration losses with the trend shown in Fig 2.3.

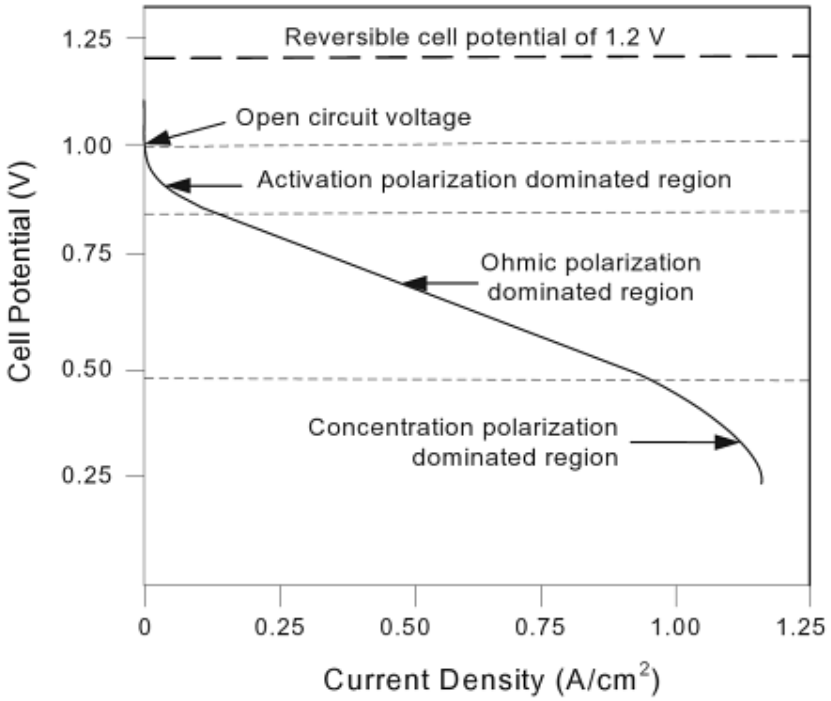

Fig. 2.3: Generic trend for polarization curve due to the activation, ohmic and concentration losses

The losses for activation, ohmic and concentration are also called overpotentials or overvoltages in the literature.

The activation losses are required to provide a given rate of electrochemical reactions: while the kinetics of the hydrogen oxidation reaction has been considered to be very rapid, the reaction at the cathode is rather slow and thus has the biggest contribution to the activation losses. The activation losses are referred to the part of the polarization curve on the left side (small current density). The activation losses are mainly calculated by Tafel equations which are logarithmic relationship between losses and current density. With the increasing of temperature the chemical reaction are faster and the activation losses are lower.

The ohmic losses are due to the proton transport within the membrane and electrodes, to the electrical resistance of the electrodes and to the contact resistances. Low conductivity is a result of an high resistance inside the cell. The value of conductivity depends on the water content. The ohmic losses are calculated with the equations indicated in paragraph 4.2.1 where the parameters used are two: the current density *i* and the internal resistance *r*. The resistance r depend on other parameters: the current density, the membrane thickness and the proton conductivity. The conductivity, therefore, depends on the temperature and the water content. Since a water management has to ensure an adequate level of humidification, the water content, in the model, could be assumed as constant or it could be connected in the Simulink® panel to the block of the water management.

The concentration losses are due to the mass transport phenomena that occur at high current density. Those are mainly driven by current density, chosen materials, geometry of the fuel cell and temperature. These are mass-transport-related losses due to hindered transport of the reactants to the catalyst site. Hence the design of the electrodes and the acting partial pressure of the reactants in the CL are important effects. And also there is a strong dependency of the current density. In fact, the concentration losses exponentially increase at high current densities because an increased amount of water within the cathode increase the flow resistance of the reactants in the partially flooded layers. The main effect is that more oxygen molecules have to move through the same cross section [33].

Normally, the efficiency of a fuel cell (based on voltage calculations) can be defined as the cell voltage divided by the open circuit voltage:

$$\eta_V = \frac{V_{cell}}{OCV} \tag{2.10}$$

More in detail, the efficiency in the ideal case is obtained by dividing the maximum output work by the enthalpy input:

$$\eta_{FC} = \frac{\Delta G}{\Delta H} \tag{2.11}$$

If the values used are respectively -237.2 kJ/mol and -285.8 kJ/mol for ΔG and ΔH, the result is equal to 83% which represent the maximum thermodynamic efficiency under standard conditions.

The equation (2.10) is obtained from the relationship between Gibbs free energy and enthalpy in case of hydrogen, as indicated in (2.12):

$$\eta_{FC} = \frac{P_{out}}{P_{in}} = \frac{n \cdot F \cdot V_{cell}}{n \cdot \Delta H} = \frac{V_{cell}}{OCV} or \frac{n \cdot F \cdot V_{cell}}{\dot{m} \cdot LHV} \tag{2.12}$$

2.2 Proton Exchange Membrane Fuel Cell for automotive applications

The automotive applications can have benefits from Fuel Cells because the fossil fuels, that are mostly used in this sector, in the next future will became scarce and, consequently, expensive. Moreover, the legislation is introducing increasingly stringent limits to the emissions of vehicles. In this context, zero emissions vehicles are seen as a promising solution, especially in the long term, to replace traditional vehicles based on Internal Combustion Engines (ICEs). So, FCs allow to have powertrain more efficient and environmental friendly which can be applied for a wide range of applications [34].

Proton Exchange Membrane Fuel Cells (PEMFCs) are shown as the potential candidate for automotive applications because they allows compact design and achieves a high energy to weight ratio. The principal advantage of them is the ability to operate at moderate temperatures in the range of 60÷80°C with a quick start-up. The efficiency of PEMFCs is above 50%, while an internal combustion engine (ICE) have an efficiency of around 30% (gasoline) or 40% (Diesel) [35].

Moreover, PEMFCs enable low noise and vibration operation, even during rapid accelerations and in some cases could be of 50% lower than the corresponding ICEs. In respect, PEMFCs contribute the reach less environmental emissions emitting in the atmosphere only water

vapor as exhaust. In Fig. 2.4 are shown the projected GHG pollutions for different types of light duty vehicles in the coming years [36-38].

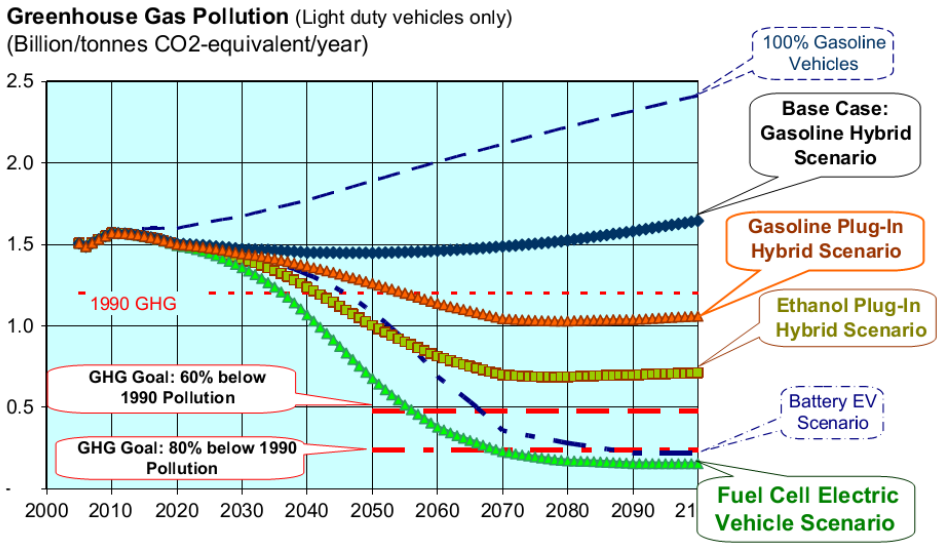

Fig 2.4: Prediction of greenhouse gas pollution [36]

The main issues in commercialization of the PEMFCs are high manufacturing costs and complex water management systems. A further challenge are varying seasonal ambient temperatures. During winter, the fuel cell stack is more susceptible to damage caused by formation of ice within the stack. Heating of the stack before cold start-up is also usually recommended by the manufacturers to prevent freeze damage. Moreover, at colder ambient conditions, the cell takes more time to reach the operating temperatures and the stack performs inefficiently during this period.

The thermal management is also critical for the stack life. In fact, lower temperatures obstruct the performance of the fuel cell, while, on the other hand, excessive heat could cause damage to the stack. The management of the stack requires control of operating temperatures through a cooling system.

Moreover, the reactants require blowers and pumps that consume around 15% of the power produced by the fuel cell. Another challenge is the cost of these fuel cells. At present, the estimated service life of PEMFCs operating in a vehicle is in the range of 2000–4000 hours. Reaching a goal of 5000 hours require advanced manufacturing techniques. So, more durable stacks require increased production costs. There are plans to reduce this cost by 2020 as

indicated in the paragraph 3.5. Currently, the fuel cells cost significantly higher than ICEs and until mass-produced, they will not be competing with the engines used currently [39].

Importantly, Fuel Cell Vehicles (FCVs) have the advantage to only require storage for the fuel. An indicator about one important parameter such as the travel distance for vehicles with different energy storages and corresponding weight of the vehicles is indicated in Fig. 2.5. It can be observed that in order to have larger driving range, the mass of the vehicle with batteries increases substantially. In this context, FCVs can afford to conquer longer distances and can be regarded similar to ICE-based cars.

Obviously, as indicated in the paragraph 2.2 the hybridization of the vehicle, in fuel cell hybrid electric vehicles (FCHEVs) allow to have both advantages of purely electric vehicles (EVs) and fuel cell vehicles (FCVs) [38].

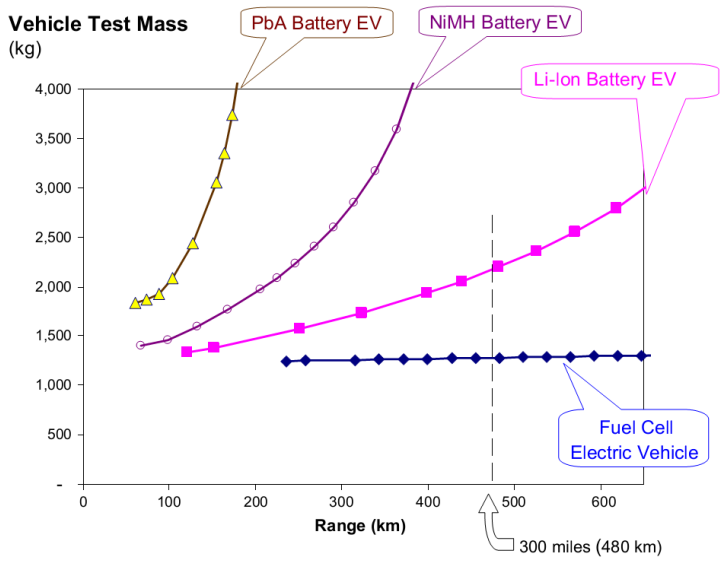

Fig 2.5: Trend of vehicle mass over autonomy for different energy storage systems [38]

Hydrogen is a high energy content fuel. Still, its low density presents many technical challenges in on board storage design. One approach of avoiding such a problem is on board reforming of hydrogen. Pure hydrogen is the preferable fuel of choice as other fuels can cause decomposition and degradation of the membrane. Also, PEMFCs are very sensitive to carbon monoxide and, in case of presence of not desiderated substances, it require additional purification system which increase the costs [40].

On board compressed hydrogen storage in cylinders seems to be a feasible storage option. At the moment, the price of hydrogen is about twice to that of gasoline and there is also a need to develop the hydrogen infrastructure for availability and supply of fuel to dispensing outlets. Refuelling stations for hydrogen to support the increasing number of vehicles are very expensive to build presently, but it is a technical solution under development in several research programmes.

In comparison to FCVs, the charging unit for the plug-in hybrid electric vehicles (PHEVs) is cheaper at the moment; however the charging times are very high compared to the refuelling of hydrogen. Moreover, storage volume occupied by the batteries is many folds more than required for the PEMFCs. The logarithmical curves of storage volumes for batteries place limitations in terms of size of the vehicle. In comparison, the hydrogen tank pressurized at 700 bar takes the least of the volume (see Fig. 2.6), and is more appropriate for light duty vehicles where size of the automobile is one of the main concerns [38].

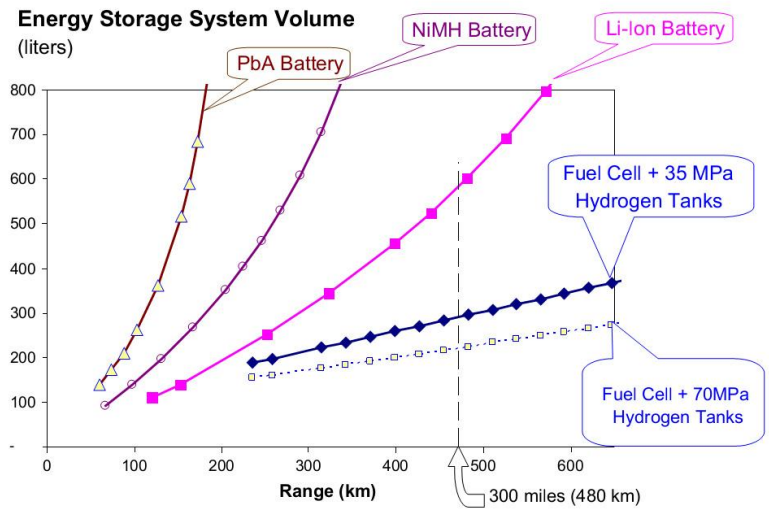

Fig 2.6: Trend of energy stored on board over autonomy for different energy storage systems [38]

2.3 Balance of Plant

The equipment of the Balance of Plant (BoP) include all necessaries components to allow FC operations, such as humidifier, air blower, pumps, heat exchangers, cooling circuit, flow valves and control unit. In fact, while pressurized hydrogen is provided to the anode, air is

compressed, cooled and humidified before entering to the cathode side, as the following figure show:

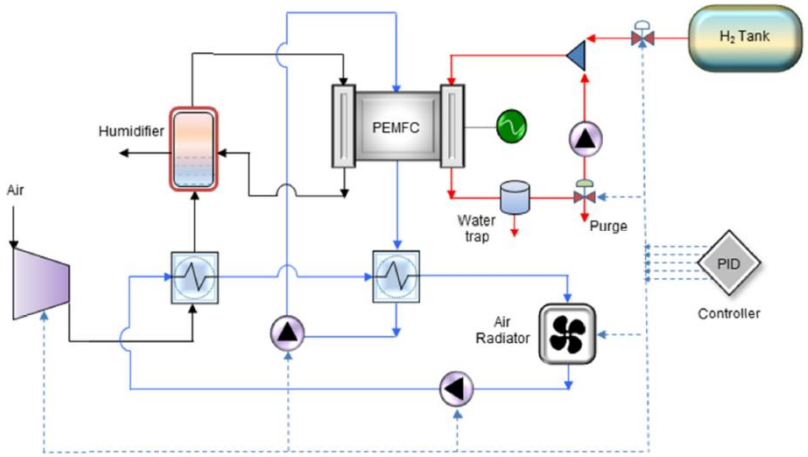

Fig. 2.7: Balance of Plant of a FC stack [41]

BoP components are critical for correct functioning of the stack due they are able to regulate three important aspects of the system: reactant supply, water management and heat management [41].

The principle of functioning of a FC stack consist of providing electrical power in a wide range of operating and environmental conditions. This principle of functioning is constrained inside a specific limitations: in fact the performance depends on a number of operating conditions such as current density, reactant stoichiometry, relative humidity, inlet pressures, temperature, etc. Consequently, each of these conditions has a big influence on the performance.

For instance, operating the FC stack below the minimum theoretical stoichiometry leads to premature durability issues. Stoichiometry is the ratio of real flow rate to the flow rate required to support the reaction. The minimum value of theoretical stoichiometry required is 1 for both hydrogen and oxidant. Although, the performances are not sensitive to stoichiometry at low currents, it is a critical at high currents.

Transportations installations require the overcome of the following obstacles in the development of BoP:

- Cost reduction: recently the introduction of new materials and production methods has increased the reliability of FC systems and, at the same time, reduced the cost of BoP plant per kW/FC system.

- Performance: in terms of time response, noise levels, consumptions, weight and space constraints.
- Reliability: for a prognostics and health management.
- Extreme environment conditions: low or high levels of temperature and humidity.
- Efficiency: start-stop procedure, dynamic variations, transient, degradation process.
- Packaging: for the allocation of all needed components on board vehicles.

The BoP components have the important role to assure the proper performances of the FC through the optimization of the mass flow rates, water injection and removal and voltage output control. Usually, the complexity of the BoP depend on the size of the FC: a larger FC require a more complex BoP.

More of the components shown in Fig. 2.7 are used to distribute air and hydrogen into and out the FC. The reactants must be modified during several processes before entering in the FC at the required conditions. Thus, blower, compressors, pumps and humidifier must be used in order to deliver the gases into the FC at the correct temperature, pressure, humidity and flow rate.

2.3.1 Humidifier

Since reactants need to be humidified before entering into the stack, the humidifier humidify the inlet air through the water produced by chemical reaction inside the fuel cell. The humidity needs to be increased to avoid local dry out of the fuel cell membrane at the air inlet. The water production through the catalytic hydrogen combustion in the fuel cell exceeds the water demand for cathode humidification and therefore a closed water-balance can be easily achieved. The humidification is performed through shell and tube or plate membrane humidifiers or direct water injection.

A model will be described in chapter 4 in order to define the correct way for water management in the humidification process and for the estimation of the water injection flow rate.

Theoretically, it is crucial for performances and durability that the content of water must be adequate within the membrane: in fact the proton conductivity depends directly on the water content and a deficiency of water in the membrane cause the degradation reducing the

durability. But too much water reduce the performance leading to a flooding of the electrodes and blocking the pores in the diffusion media.

The water management is a challenge in a PEMFC because the ohmic heating at high currents cause the drying out of the membrane. Although some FCs does not need humidification, it is always necessary in the larger FCs where the air or the hydrogen or both of them must be humidify before entering into the cell.

2.3.2 Air blower, compressor and pumps

Air blowers, compressors, recirculation pump and water pumps are BoP components which are very important in order to guarantee the correct behavior of the whole FC system and in order to reach high performance levels. All of these components need to be regulated by the control unit.

Usually, the air is provided to the FC through a blower which is driving by an electrical motor. The air blower needs to supply air to FC stack. For start-up a battery provide the power to the blower, while a part of the power output of the FC will be used to keep the blower running. This amount of energy must be taken into consideration in the overall energy balance of the system.

As the air compressor requires substantial energy to provide the required airflow, efficiency of the air compressor is of particular importance. Furthermore, the air compressor needs to accelerate rapidly to ensure low response time for the fuel cell system. Theoretically, a greater concentration of oxygen per volume and per time increases the efficiency of the FC. At high pressure, a lower mass flow rate is required and less water for humidification is needed.

Pumps need in a FC system in order to move water at a certain pressure. It is important to choose a correct pump in accordance to efficiency, reliability, corrosion-free and the ability to work at certain values of temperature, pressure, mass flow rates.

2.3.3 Heat exchangers

Heat exchangers extract the heat produced within the FC stack and maintain the desired operating temperature which is critical for performances and durability. In fact, the cathode air requires conditioning before it enters the fuel cell stack. The temperature needs to be adjusted as close as possible to the fuel cell stack temperature to avoid local cold spots at the air inlet. The state-of-the-art strategy for cathode air pre-heating is through a heat-exchanger.

The heat exchanger needs to efficiently dissipates the thermal energy generated by the fuel cell stack. This is particularly important for automotive systems due to the high power stack and limited volume available for the heat exchanger. Furthermore, the heat exchanger control has to be tightly integrated with the anti-freeze start-stop system by allowing fine control of the thermal energy in particular for sub-zero operating conditions.

2.3.4 Cooling circuit and anti-freezing system

The freeze-start and system storage at freezing conditions of PEM fuel cells continues to be a challenge resulting in high technical system efforts, additional system components and therefore additional system weight and cost. The freeze-start represents an unavoidable degradation of the fuel cells, which can lead to a reduced service life, declining performance and severe damage or even destruction of the fuel cell system by the formation of ice crystals. Under normal operation the fuel cell system has two byproducts: water and heat. Under low temperatures the excessive water can freeze thus permanently damaging the system and stopping the reaction by blockage. For a successful introduction of fuel cells in many markets or applications an applicable solution for the freeze start and the storage of the fuel cell at freezing environmental conditions is necessary especially in the field of portable and mobile applications.

2.3.5 Flow valves

A valve is placed between the hydrogen tank and inlet manifold of anode which enables, disables and adjust the hydrogen supply. This regulatory valve change the value of the hydrogen pressure from high values to the desired one. The amount of hydrogen regulated by this valve equals the stoichiometric hydrogen required of the cell. Stoichiometric ratio is defined as the amount of reactant supplied to the amount which is consumed in the reaction.

Flow and pressure of oxidant into the cathode is regulated by the blower. The amount of stoichiometric oxygen for the fuel cell reaction is manipulated by a controller which regulates the electrical power of the blower, and hence compression and air flow.

2.3.6 Control Unit

Fuel Cell Control Unit controls BOP(Balance of Plant) of the fuel cell system for electricity generation, controls the vehicle in response to the driver’s intention, including acceleration

and breaking, and distributes generated electricity or electricity of sub-power supply unit such as high voltage battery.

A power control unit of a fuel cell hybrid vehicle includes a first switching unit, a second switching unit, and a control unit. One terminal of the first switching unit is connected to a fuel cell stack and to an anode of a DC/DC converter in parallel, and the other terminal is connected to an inverter. One terminal of the second switching unit is connected to the inverter and to a cathode of the DC/DC converter in parallel, and the other terminal is connected to a cathode of the fuel cell stack. The control unit switches contact points of the first and the second switching units to selectively supply a voltage from one of the fuel cell stack and a battery to a motor.

2.3.7 Turbines

When the FC system produce, at the outlet side, a gas which is hot and pressurized, a turbine can be used in order to use the amount of energy of the outlet gas. The turbine has the opposite function of the compressor and all consideration expressed for compressors are also valid for turbines but with different direction of the power flows: in fact, while a compressor must be more efficient as possible in order to reduce its consumption of electricity, a turbine must be more efficient as possible in order to recover more energy. By the way, due its inefficiencies a turbine can recover only a portion of work available and this amount is not possible to cover the required power by other BoP components.

For instance, an example of the functions covered by compressor and turbine is shown in fig. 2.8. In this a scheme a FC stack operating at its voltage, temperature and pressure levels is combined with some BoP components. The air stoichiometry is defined as well as the efficiencies of BoP components. A model for this configuration could be built up starting from the model described in chapter 4. In fact, the model can be expand to more other components which are not considered in this research. These new possibilities for calculations and simulations could include the amount of power required by compressor, the temperature change of air during compression, the need of humidification and if it is useful to use a turbine or not.

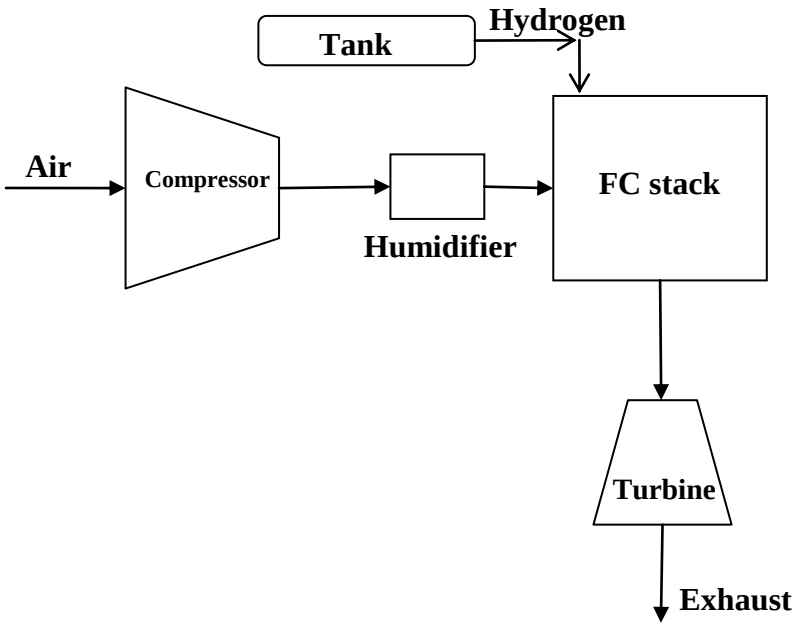

Fig. 2.8: Compressor and turbine in a FC system

3. Hybrid Electric Vehicles

3.1 Hybrid Electric configurations

A Hybrid configuration for a vehicle is when the propulsion energy is available from at least two different sources of energy allocated on board of vehicle. When at least one of these sources of energy is electric and it is directly used for propulsion the configuration is called Hybrid Electric.

In accordance with this general definition, obtained from CEN EN 13447, a Hybrid Vehicle (HV) has a powertrain which create at least two path of energy flow between the wheels and the energy storages. These flows are unidirectional and bidirectional depending on the typology of energy storage (gaseous or liquid fuel used in energy converters, electrochemical storage, ultra-capacitors, etc.). A Hybrid Electric Vehicle (HEV) is a HV where at least one of energies used for propulsion is electric. Purely EV are considered the best solution as alternative powertrain because they are emission free, quiet and efficient. The main problem is the low energy content of batteries and long recharge time that causes a limitation of the autonomy of vehicles. As a result, FCHEV is a valid combination of the benefits of EVs and the traditional ones [42].

Regarding technical aspects, HEVs can be classified into different families according to the topology of the system. In the case of use of Fuel Cell (FC), as the primary source of energy, the “series” hybrid configuration must be adopted. In this configuration the sum of the power from the primary converter and RESS is electrical and the power is transferred to the wheel only by an Electric Machine (EM) [43] [44].

In this thesis the design of a “series” hybrid configuration will be developed. A “series” hybrid configuration, shown in Fig. 3.1, consists of a primary converter and a rechargeable energy storage system that provides electric power to an electric motor.

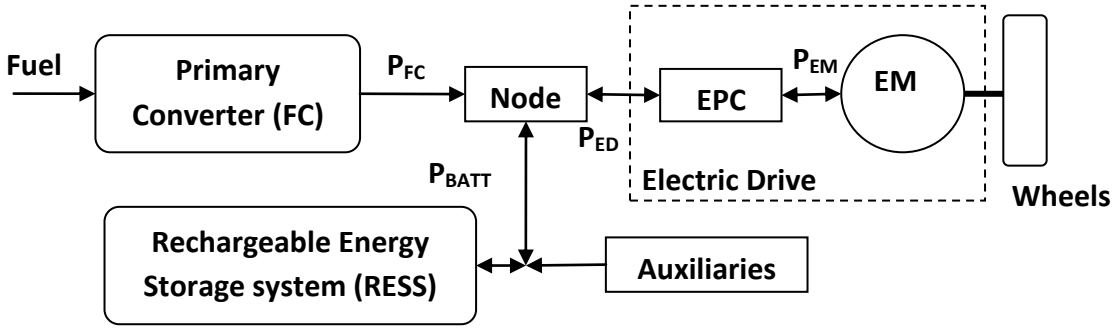

Fig. 3.1: General scheme of a "Series" Hybrid Vehicle

The Electric Motor (EM) works as generator during braking in order to recover energy. The FC system consists of an FC stack with all its auxiliary devices, needed to supply hydrogen to the anode and air to the cathode, to humidify and to cool. An Electronic Power Converter (EPC) is connected between the stack and electrical node to regulate the voltage level. The primary converter is fully decoupled from the driven wheels and, consequently, it can be operated at high efficiency work condition or other selected work conditions, selected through the optimization of the logic of control [45].

The "Series" configuration meets three special conditions:

- two energy sources on board;
- the source that generates energy from fuel is called Primary Converter (PC) and it is characterized by an unidirectional energy flow;
- the secondary source is constituted by a Rechargeable Energy Storage System (RESS) which delivers and stores energy with a bidirectional energy flow.

The power requested from Electric Drive (ED) and needed for propulsion can be provided, within certain limits, by the combination of the primary and the secondary sources: this arbitrariness can be exploited to obtain special objectives such as reducing consumption or emissions. The techniques and the methodologies used to reach the specific objective of dimensioning of the system are the main objective of this Research.

The Primary Converter (PC) transforms the primary energy fuel into the electrical power. Obviously this type of conversion can be achieved through a FC system or alternatively in many different ways. Its output power is delivered to a DC-bus, which consist into an electrical node, where the combination of electric powers coming from the two different sources is obtained.

The Rechargeable Energy Storage System (RESS) typically consists of an electrochemical battery pack. The Electric Drive takes electrical energy from the node and transforms it into mechanical energy, available at wheels. Normally it is constituted by an Electronic Power Conditioner (EPC) and a three-phase Electrical Machine (EM) operating as motor during traction phases, and as generator during braking.

Series hybrid drive trains offer several advantages: for instance, since the Primary Converter is fully decoupled from the driven wheels, it can be operated at high efficiency work conditions which can be further improved by optimal design and control. Consequently, simple control strategies may be used as a result of the mechanical decoupling provided by the electrical transmission. Also, electric motors have a near-ideal torque-speed characteristics, so they do not need multi-gear transmissions. Furthermore, instead of using one single motor and a traditional differential gear, two motors can be used, each of them powering a single wheel. The ultimate refinement would be the usage of four motors, thus making the vehicle an all-wheel-drive without the expense and complexity of differentials and drive shafts running through the frame.

On the other hand, the "series" hybrid electric configuration presents some disadvantages: for instance, the various subsystems add further weight and cost and the traction motor must be sized to meet maximum requirements since it is the only system propelling the vehicle.

3.1.1 Two-wheeled and four-wheeled vehicles considered in this research

In this Research, the modeling will be set and carried out for a wide range of vehicles that comprises the two-wheeled and the four-wheeled ones. Regarding the impact of these different type of vehicles, it must be noticed how they are diffused worldwide. A two-wheeled vehicle, also called motorcycle, is one of the most important transportation modes whose design varies greatly to suit a range of different journeys: urban, long distance, commuting, off-road and sport. Although the number of four-wheeled vehicles is higher, two-wheeled vehicles are also one of the most affordable forms of motorised transport. In fact, in the non-car-centric cultures of India, China and Southeast Asia, where more than half of the people in the world live, two-wheeled vehicles outnumber four-wheeled ones. Statistically, as indicated in Fig. 2.2, about 200 million motorcycles are in use worldwide or about 33 motorcycles per 1000 people. By comparison, there are about 1 billion cars in the world or about 141 per 1000 people, with about one third in service in Japan and the United States. In the developed world,

motorcycles are frequently owned in addition to a car and, thus, used primarily for recreation or when traffic density means a motorcycle confers travel time or parking advantages as a mode of transport [46] [47].

Fig. 3.2: Number of two-wheeled and four-wheeled vehicles per 1000 people [46]

Some studies about the use of FCs in two-wheeled vehicles began to appear in the scientific literature at the beginning of the twenty-first century [48].

In fact, researchers and engineers created prototypes of scooters equipped with FCs taking the Asian market into consideration, in which there are more than 18 million scooters sold every year [49].

Since scooters are so popular and are usually equipped with a two-stroke internal combustion engine, they cause serious environmental air pollution and a big effort was encouraged by governments to make vehicles more environmentally friendly [50].

In the early studies of FC scooter the PEMFCs emerged as the best FC technology to produce the primary energy on board. In subsequent studies, in which prototypes were produced, the use of PEMFCs was confirmed and the FCs were connected with batteries in hybrid systems. For instance, prototypes of the FC scooter were presented in the 2004 by Hwang, in 2007 by PHB-Hydrogen bike and by the Fuel Cell Institute of University of Esslingen, in 2010 by SiGNa Chemistry, in 2011 by Suzuki and in 2012 by Asia Pacific Fuel Cell Technologies [51-56].

3.2 Fuel Cell Hybrid Electric Vehicles

3.2.1 Layout

The primary converter is a PEMFC, while the RESS is a Lithium-Ion battery which is chosen for its good performance characteristics in terms of power density (W/kg) and energy density (Wh/kg). In HEVs, the size of the RESS is defined in order to provide sufficient energy storage capacity (Wh) and adequate peak power ability (W). The size requirement of RESS varies significantly according to the characteristics of different power-trains such as pure

Electric Vehicles (EVs), Hybrid Electric Vehicles (HEVs) and Plug-in Hybrid Electric Vehicles (PHEVs). The EM, although it is the only component propelling the vehicle with a size able to meet the maximum power requirement, has a near-ideal torque-speed characteristic which means a multi-gear transmission need not be adopted. Importantly, the EM works as a generator during braking in order to recover energy. In the electrical node the combination of electric powers coming from the two different source is obtained [57].

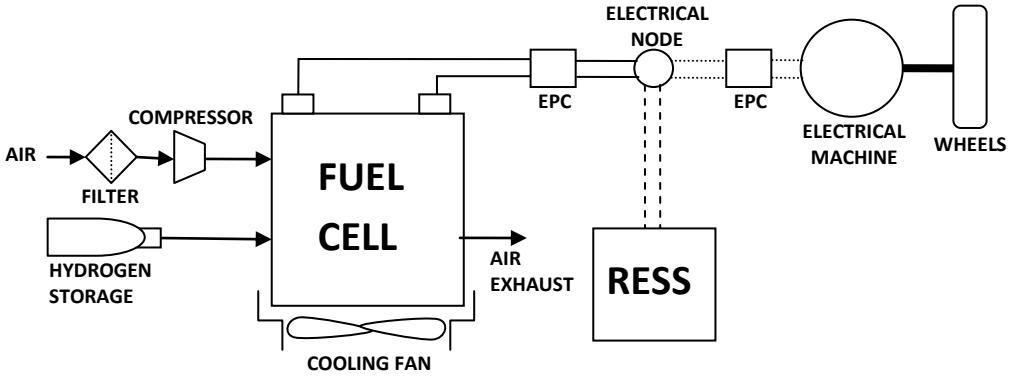

Fig. 3.3: Scheme of "series" hybrid configuration with FC for a vehicle

A "Series" Hybrid Electric powertrain, shown in Fig. 2.3, contains a primary source of energy, such as an FC, an RESS, such as a Lithium-Ion battery, and an Electrical Motor (EM). Since the required power for propulsion (P_{ED}) and auxiliaries (P_{AUX}) can be provided from both RESS and FC, a Power Management Unit (PMU) is needed for the purposes of handling and optimizing the power flows control strategy [58].

The presence of a storage system allows dimensioning of the primary energy source regarding the average required power because the remaining power can be provided by the RESS. Thus, an important parameter in FCHEVs is the Hybridization Degree (HD) which is defined by the ratio between the installed maximum power source of FC and the nominal power of the EM, as indicated in the following equation [59] :

$$HD = \frac{P_{FC}}{P_{ED}} \qquad (3.1)$$

In terms of HEV classification, the full spectrum of series HEV, see Fig. 3.4, starts from pure-electric vehicles (EV) to full-power fuel cell vehicles (FCEV). FCHEVs, hybrid vehicles in

which the primary generator is a fuel cell, can certainly be classified according to the aforementioned HEV classification [60].

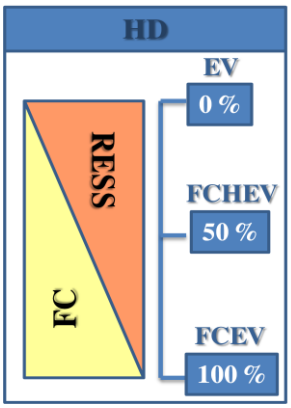

Fig. 3.4: Hybrid classification overview considering the Hybridization Degree (HD)

Generally, the maximum power of the EM is higher than the nominal power because the maximum power can be provided for a limited time while the nominal power can be provided continuously. According to equation 3.1, vehicles with a high degree of hybridization mainly use the storage unit for recovering energy and helping the power management strategy. In comparison, vehicles with a low degree of hybridization present a dimension of the primary source sufficient to generate the average value of the requested power left in the battery to deliver the needed power for high requests. The degree of hybridization is equal to 0 % in the case of EV and to 100 % in the case of Fuel Cell Electric Vehicles (FCEV), while the value can change according to ideas of the vehicle designer in the case of hybrid architecture.

The differences in duty cycles of urban buses, generally repeated and therefore easily foreseeable, and cars, unpredictable mixed urban and extra urban cycles, make very difficult to define a general optimal hybridization degree. As a result of the high power primary energy source vehicles with high hybridization degree mainly uses the storage unit for braking energy recovery and management of acceleration quick transients. Indeed, these vehicles have a small storage capacity compared with vehicles with lower hybridization degree. The power fluxes within the FCHEV drive system are concept considering a vehicle mission of time length t_{tot}, during which the Electric Drive require a certain power (P_{ED}) expressed as function of the time. So, the average value of requested power, which must be delivered by the primary converter, is equal to:

$$P_{ED\_avg} = \frac{1}{t_{tot}} \int_0^{t_{tot}} P_{ED}(t)dt \qquad (3.2)$$

What are the advantages of HEVs versus conventional vehicles? Because of the secondary power source, generally a battery pack, HEVs can reduce the transients in the primary converter, thus attaining fuel economy or emission reductions. Also, the primary converter can work at point of maximum efficiency during the cycles, thus its size can be reduced. Last, in a HEV the braking energy can be recovered.

Summarizing, in a hybrid electric vehicle the storage system must be able to [61]:

- recover the braking energy;
- level the peak power required enabling the generator to deliver a constant power which could be set on the average required power;
- deliver continuously the additional power required to compensate the maximum request by ED.
- to store enough energy to avoid the complete discharge in the most challenging driving cycles.

An FC system consists of an FC stack with all its auxiliary devices, needed to store and supply hydrogen to the anode and to supply, compress and humidify air to the cathode. Moreover, it comprises a cooling circuit, as shown in Fig. 3.5 [62].

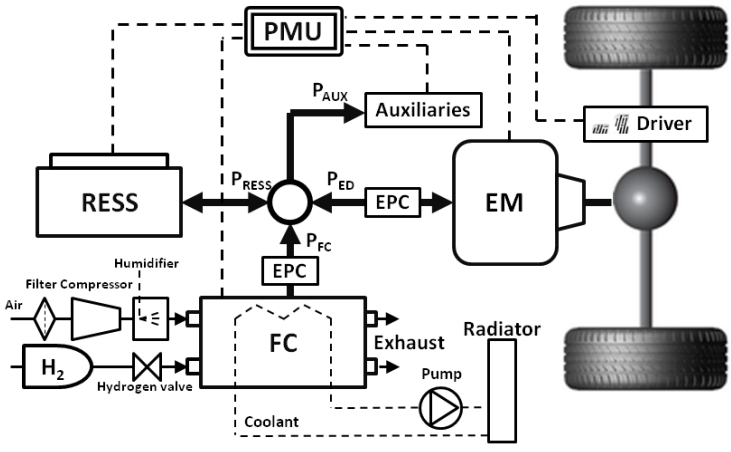

Fig. 3.5: General arrangement of a powertrain for FCHEV.

The System of a FCHV is separated into four different system levels like one can see in Fig. 3.6. These levels are the Air System, Hydrogen System, Thermal System and Electrical System.

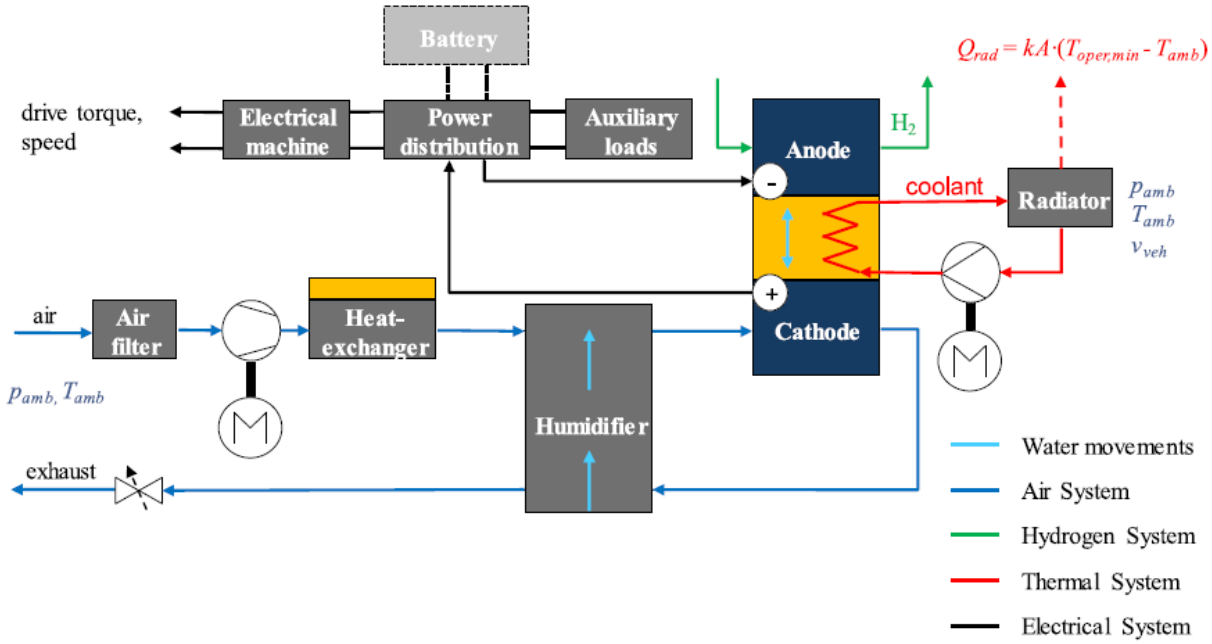

Fig. 3.6: Topology of PEMFC system for FCHEVs.

In the *Air System* the oxygen is provided at the cathode. As a first step the air, at ambient conditions, is separated from undesirable particles in the filter and then it is compressed by a compressor. Then, a heat exchanger is used to cool down the air because of the increase of temperature during the compression. This help to prevent thermal damage to the humidifier and to the membrane. Usually, an external humidification is needed and therefore a humidifier is placed before the cathode, which uses the wet air at the outlet of the cathode for the humidification of the inlet. At the end of the Air System there is a throttle for enabling the compressor to build up the desired operating pressure.

In the *Hydrogen System* the hydrogen is supplied at the anode. For the pressurization of the hydrogen gas no compressor is needed because it is stored at high pressure levels. So, the pressure needs to be reduced till the desired pressure by a control valve. The hydrogen is circulated by a jet-pump or a recirculation blower in order to avoid hydrogen losses. In some cases, a humidification is also needed using the wet gas of the outlet.

In the *Thermal System* all transformations needed to ensure that the operating temperature remain at values less than 95 °C a needed are done. Moreover, in it the generated thermal energy of the system is released to the surrounding. Basically, a coolant is circulated inside the system by a coolant pump. The radiator is a crucial component which rejects the heat to the ambient air. Compared with Internal Combustion Engines (ICEs) cars the cooling of fuel cell systems is more challenging because the difference between operating and ambient temperatures is lower.

In the *Electrical System* the electricity is controlled, converted and distributed within the powertrain. Firstly, the generated electricity in the FC is converted to two different voltages because for the traction grid a high voltage is needed, while for the onboard supply system only a voltage of 12 V is required. Afterwards, the electricity is supplied to the electrical motor and the auxiliary units [63].

3.2.2 Rechargeable Energy Storage System (RESS)

Recently, lithium batteries have been introduced in hybrid electric vehicles due their characteristics of energy density, power density, no memory, low losses and slow discharge when not used. Usually, Lithium-Ion and Lithium-Polymer are taken into consideration.

In a Lithium-Ion battery ions move from negative electrode to the positive electrode during discharge and back when charging through the electrolyte and separator diaphragm.

Rechargeable Energy Storage systems (RESSs) are devices which store energy in various forms such as electrochemical, kinetic, pressure, potential, electromagnetic, chemical, and thermal. The main characteristics required for automotive applications are:

- the amount of energy in terms of specific energy and energy density;
- the electrical power;
- the volume;
- the mass;
- reliability;
- durability;
- safety;
- cost;
- recyclability and environmental impact.

Thus, the following characteristics should be considered for a correct selection of a RESS:

- specific power;
- storage capacity;
- specific energy;
- response time;
- efficiency;
- self discharge rate and charging cycles;
- sensitivity to heat;
- charge-discharge rate life time;
- environmental effects;
- initial and operating cost;
- maintenance.

For purely Electric Vehicles (EVs), batteries with an amount of stored energy in the range of 5÷30 kWh for cars and up to 100 kWh for buses are required. Some characteristics for different type of RESS are shown in Fig. 3.7.

Battery Chemistry	**Type Primary (P) Secondary (S)**	**Cell Voltage (V_{cell}) / V**	**Theoretical (practical) Specific Energy / Wh.kg^{-1}**	**Useful Energy Density / Wh.l^{-1}**
Alkaline zinc manganese dioxide (Zn/MnO_2)	P	1.5	358(145)	400
Lithium iodine (Li/I_2)	P	2.8	560(245)	900
Alkaline nickel cadmium (NiCd)	S	1.3	244(35)	100
Nickel metal hydride (NiMH)	S	1.3	240(75)	240
Lead acid (Pd/A)	S	2.1	252(35)	70
Sodium sulphur (Na/S)	S	2.1	792(170)	345
Sodium nickel chloride ($Na/NiCl_2$)	S	2.6	787(115)	190
Lithium-ion (Li-ion)	S	4.1	410(180)	400

Fig. 3.7: Characteristics of various type of battery

Theoretically, a battery is an electrochemical cell that transforms chemical energy into electrical energy. It is made of an anode and a cathode which are separated by an electrolyte. Electrons are generated at the anode and flow towards the cathode through the external circuit while, at the same time, protons flow throughout the electrolyte.

Generally, the two most prominent types of battery used in EVs are Nickel Metal Hydride (NiMH) and Lithium-Ion (Li-ion). NiMH batteries are in most cases used as secondary energy sources in hybrid electric vehicles, such as in Toyota Prius, where they are used in conjunction with an Internal Combustion Engine (ICE), while Lithium-Ion batteries are used as primary energy sources in EVs, such as in the Nissan Leaf. The Nissan Leaf is a purely Electric Vehicle powered by 12 x 4 cells (48 modules) providing a capacity of 24 kWh and taking up to 8 hours to fully charge from a standard domestic outlet from zero State-of-Charge (SoC), or 30 minutes from a 3-phase AC socket. The cost of the vehicle is around 35,000 $.

NiMH batteries are used in over 95% of all HEVs due their presence on the Toyota Prius. Their major advantages are safety, environmental acceptability, low maintenance, high power and energy densities, cost. Moreover, NiMH batteries are preferred in industrial and consumer applications due to the design flexibility in a range between 30 mAh and 250 Ah.

NiMH batteries are currently priced at 250 $ to 1,500 $ per kWh, hence the total price of the battery pack for a Toyota Prius varies between 600 $ and 3,000 $ per vehicle.

The structure of NiMH batteries, shown in Fig. 3.8, include an anode of hydrogen absorbing alloys (MH), a cathode of nickel hydroxide ($Ni(OH)_2$) and a potassium hydroxide (KOH) electrolyte [64].

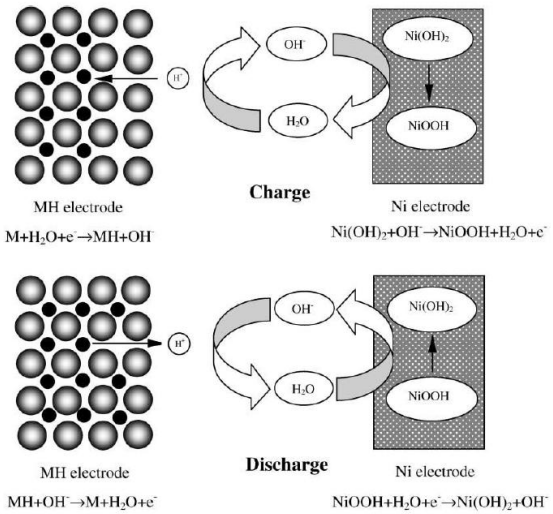

Fig. 3.8: Schematic view of the structure of a NIMH battery [64]

Lithium-ion batteries are light, compact and operate with a cell voltage of 4V with a specific energy in the range of 100÷180 Wh/kg. The anode is made of graphite and the cathode is made of Lithium Metal Oxide. The electrolyte is typically a lithium salt. A scheme of the operational principles, which the overall reaction is reported below, is shown in Fig. 3.9.

$$xLi^{+} + xe^{-} + LiCoO_2 \rightarrow Li_2O + CoO \qquad (3.3)$$

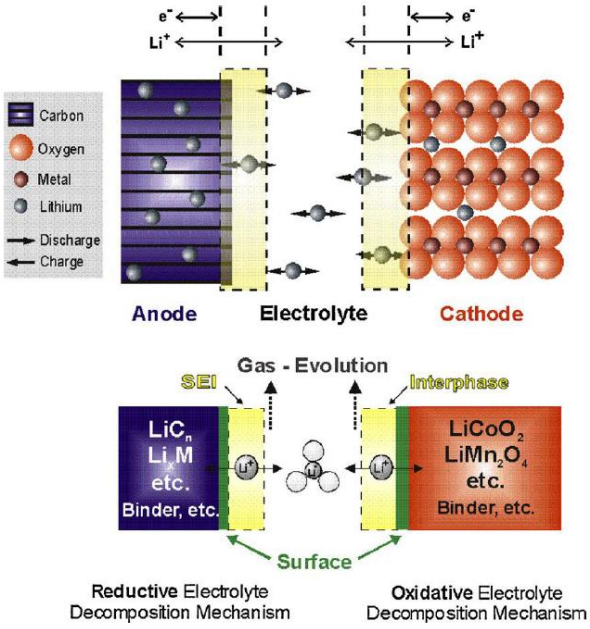

Fig. 3.9: Operational principles of a Lithium-ion battery [64]

Although a Lithium-ion battery store more energy than a NiMH battery, it have major issues such as costs (1,000 $ per kWh), wide operational temperature ranges, materials availability (Lihium), environmental impact and safety. It is observed that Lithium-Ion batteries suffer from electrolyte decomposition leading to the formation of oxide films on the anode and severe oxidative processes at the cathode due to overcharging.

A comparison between different types of batteries in terms of energy density ids reported below.

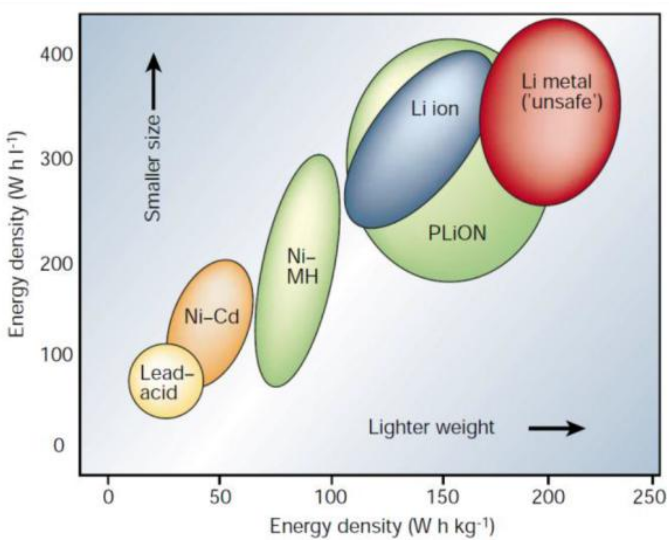

Fig. 3.10: Comparison between different types of battery [64]

Historically, Lithium-ion operational principles and chemical structure has not progressed much since their introduction to the market in the early 1990s by Sony and Asahi Kasei following the pioneering work from Whittingham, Tarascon, Armand and Scrosati. By the way, technical developments are urgently required, especially for performing and durable material chemistries for both the electrodes and the electrolytes. The objective is to find materials with high performance and durability. Currently worldwide efforts of researcher focus on the replacement of graphite and $LiCoO_2$ with alternative high capacity and low cost materials and on the replacement of ethylene carbonate–dimethyl carbonate with other electrolytes which do not suffer from decomposition under oxidative regimes.

The supply of Li-ion batteries now exceed the demand, but the market is growing from 1.5 $ billion in 2011 to more than 9 $ billion in 2015. The previsions say that the market for Lithium-Ion batteries in the automotive sector will reach over 50 $ billion by 2020.

Scarcity of lithium was once thought of as a looming concern for the electrification of vehicle fleets. However, it should be noted that only around 1% of a lithium-ion battery is made by Lithium by weight, implying around 0.08 kg of Lithium per kWh of storage capacity. That means approximately 1÷2 kg per EV. At present, Lithium is not recycled due to excessive cost and energy requirements; however, if future supply shortages lead to increasing material prices, the recycling of these batteries will become standard [64].

3.3 State of the art of alternative transportation systems including FCHEVs

It is expected that alternative fuels will play an always more prominent role in the next decades with the objective of gradually substituting fossil fuels. However, there is currently a need of attractiveness of fuel alternatives for consumers. Such as, alternative fuel vehicles only represented 3.4% of the European car fleet in 2012 and the use of alternative fuels in heavy duty vehicles and maritime and aviation modes is negligible.

In Europe, the transportation sector is responsible for 32% of final energy consumption (352 Mtep) in 2012, as indicated in Fig. 3.11.

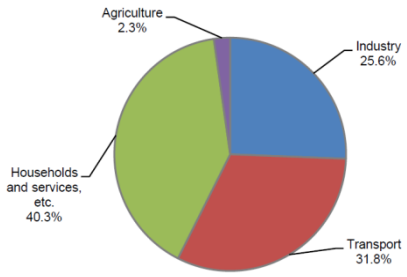

Fig. 3.11: European energy consumptions for sectors [65]

In the transportation energy demand the road transport is the largest energy consumer with a 72.3% of the total. Aviation is the second largest consumer with a 12.4%, followed by international maritime transport with a 11.5%. Rail transport accounts for 1.8% (60% of which is used for electric traction), and finally inland navigation consumes only 1.1%.

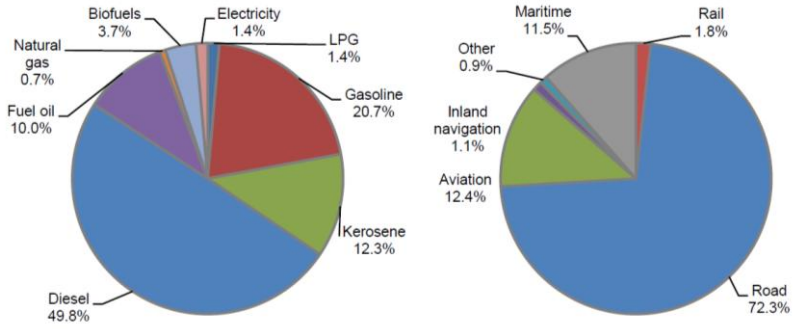

Fig. 3.12: Energy demand in transportation for European market [65]

Moreover, in 2012, European transport depended on oil products for about 94% of its energy needs. Europe imports around 86% of its crude oil and oil products from abroad, with a bill up to 1 € billion per day.

The dependence of transportations on oil and fossil fuels must be reduced and, also, the energy sources must be diversified. As seen in the above figures, almost all energy consumed in air and waterborne transportations is petroleum-based in 2012. The percentage of road transportations is of 94% petroleum-based, while the percentage of rail transportations is of 40% petroleum-based. However, in the medium and long term, most fuels should be renewable in order to reduce the GHG emissions.

The different elements for description of fuels are:

- overall specifications;
- availability and potential production capacity;
- GHG and other emissions;
- energy consumption;
- maturity of fuel production;
- costs;
- maturity of vehicle/vessels and infrastructure technology;
- market size;
- supply infrastructure;
- market aspects.

The electricity and the hydrogen are two main carrier of energy that are studied in this Research. Their main characteristics including the state-of-art are described as follow.

Electricity is an energy carrier that can be converted from a wide variety of primary energy sources. A certain quantity of electricity can be produced from renewable energy sources, offering a nearly zero emission pathway, although this is not always the case, such as when a combination of renewable and non-renewable sources are used.

At present, electricity for transportation sector is mainly used in the railways with a percentage of 76% on the final energy use in transportations. In fact, 54% of the railway lines are electrified in Europe. The growing trend in the use of electricity in transportations imply a positive impacts on local air pollution. Importantly, the production of pollutants may be in other areas than those of usage. For instance, if the EVs are used in towns, their electricity supplier are based in the countryside. For this reason, the electrification of public transport in urban areas is expanding rapidly in order to reduce local air pollution and noise levels in urban areas. The full electrification of heavy-duty vehicles and buses through batteries cannot happen in the short term, but a partial electrification by the use of plug-in and hybrid technologies represent the current strategy and it is giving good results in terms of reduction of noise and pollution.

The electricity generation mix in Europe is changing significantly: it now includes an increased share of decentralized and variable renewable energy sources. More than 27% of the capacity installed in 2013 came from renewable sources, such as hydroelectric, wind and solar. Significant energy storage will be needed to accommodate growing shares of renewable energy sources that, due to their variability, could present challenges to balancing supply and demand on the grid. In this context, EVs could be a solution as part of a smart grid. EVs have zero-tailpipe emissions and they can also give a contribution to reduction of GHG emissions in case of power stations based on renewable sources of energy.

FCHEVs and hydrogen provide, also, an alternative proposal for transportations. Similar to electricity, hydrogen is an energy carrier that can be produced from a wide variety of primary energy sources. Currently, hydrogen is predominantly produced by steam reforming of methane using a chemical transformation, but hydrogen can also be produced from renewable or nuclear energy using electrolysis. Moreover, hydrogen can also produced by bio-methane reforming or by organic feedstock.

The technology for hydrogen production is mature and efforts are directed to have a more cheaper production. Also some efforts are requested for a necessary hydrogen refuelling station infrastructure.

The raise of irregular renewable energy sources, especially solar and wind energy, is causing challenges in the management of energy infrastructures. So, the use of energy storage systems is needed in order to have a grid stability. Hydrogen is considered as one of most prominent solutions for large scale and long-term energy storage. The technical development which must to be overcome in order to have a mature technology are in a always more advanced phase. One of the key solutions is by conversion of electricity to hydrogen, which is already possible through electrolysis.

Europe, U.S.A. and Japan are considered as technology leaders in Fuel Cell and Hydrogen applications. One of the qualities of hydrogen is that it can be produced from virtually any primary energy source. Productions systems could differ each other in terms of cost, environmental performance, efficiency and technological maturity. Importantly, for the use of hydrogen in fuel cells the hydrogen has to be purified to a high level, involving removal of impurities that could impact fuel cell performance. Hydrogen is stored in tanks under very high pressure up to 700 bars.

While hydrogen has very high energy content per kilogram and it is very light in weight, even when highly compressed or liquefied. Therefore, it does not have high energy content per liter or space required to store it.

Due to current limits in battery capacity and driving range which is, currently, in the range of 100÷200 km for a small or medium car, EVs are considered as the most suitable powertrain for smaller cars and shorter trips, such as urban and suburban driving cycles. Some studies of driving cycles show how the most travel have an average daily distance of 50 km, which match with the driving range of EVs. Considering the long time in which the cars are not in motion, the driving range can be increased if customers charge EVs regularly while the EVs are parked at the office or at home. Occasional longer driving range is also important to reach a wide market and a fast charging of battery, which need to be further developed, could help this purpose. The Tesla Model S in 2012 with a range of over 400 km has taken the market by surprise and has encouraged the development of long range EVs in large and luxury car segments.

The improvement of the driving range of EVs up to 400÷500 km is a key factor for the success of this technology in the upcoming years. By the way, the development of low cost electric vehicles with a short driving range remain the big challenge for the introduction of EVs in the large market. The EVs for these purposes include also the two-wheeled vehicles.

The reasons are the mobility issues in big and crowded cities. The increase trend of electric motors in road transport for cars and buses is reaching a market maturity, but the full electrification of vehicles do not seem a realistic option in the near future. However, these technologies should be considered in a long term perspective.

EVs and PHEVs holds great promise for passenger cars and light vehicles, while the point of view for buses and heavy-duty vehicles is different. The recent developments in EVs and battery technologies show that the capacity and the range of new vehicles become longer. Currently, there are EVs, such as Tesla S, with ranges above 400 km, while other manufacturers are looking for similar long range EVs. For instance, Audi R8 e-tron in 2016 with a 450 km range, Audi Q6 SUV, Porsche 717 with a 500km range in 2019, Landrover, and Jaguar F-Pace SUV, 500 km range. Other manufacturers are expected to follow.

In the recent past there was a rapid increase in the number of new EVs and PHEVs, as well as in recharging infrastructure, although sales are still limited if compared to the total vehicle sales as indicated in Fig. 3.13. Therefore, expectations are high for the future.

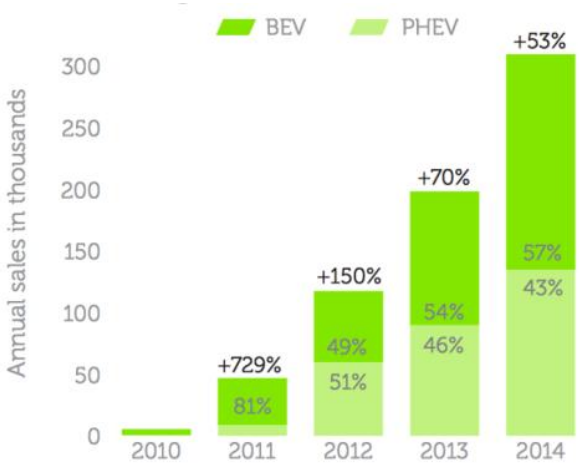

Fig. 3.13: EVs sales in recent past [65]

The market sales of EVs in some countries are indicated in following figure.

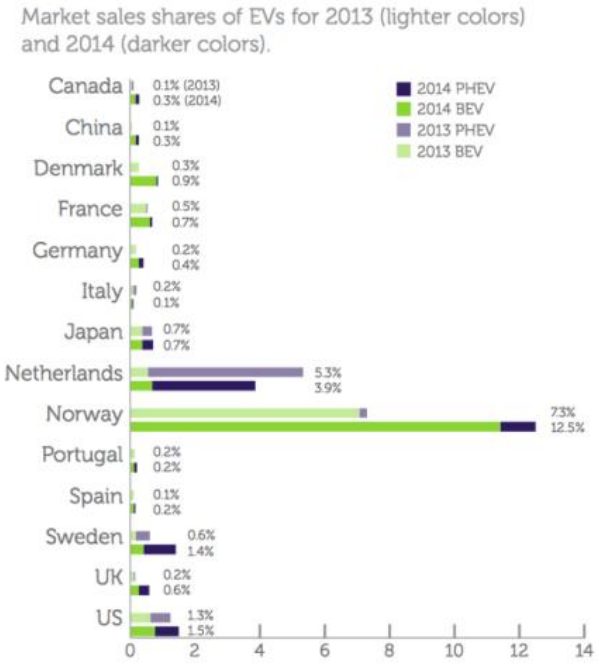

Fig. 3.14: EVs sales in some countries [65]

In 2014 almost 90000 electric cars were sold in Europe of which 55000 were purely EVs equipped with only a battery and an electric motor. As shown in previous figure, the percentage of the market penetration of EVs, including also PHEVs, where below 1% in most countries, except for Norway and Netherlands. While the high rate in Norway comes from purely EVs sales, the high rate in the Netherlands comes from PHEVs sales.

In essence, a FC is very similar to a battery because it generates electricity from an electrochemical reaction without combustion. However, a battery can store a limited amount of energy and once depleted it must be recharged using an external supply. A FC is supplied with hydrogen fuel which once depleted must be refueled allowing a significantly longer distance in comparison with a battery. Summarizing, a FC is similar to an ICE coupled with an alternator although a FC do not use a combustion, but oxidizes hydrogen electrochemically with water vapor as the only exhaust product. Moreover, FCHEVs are intrinsically more efficient than ICE-based cars with TTW (tank to wheel) efficiency over than 40% considering the state-of-art of 2015. A FC is also similar to an ICE-based vehicle because it can be refueled in some minutes for a driving range of more than 600 km. Also, the power and the driving range of the car can be set independently since the first depends on the size of the FC and the electric motor, while the driving range depends on the size of the tank. An hybrid architecture combines a fuel cell (from 0 to 100%) and a battery (from 100% to 0 %)

with a different levels of hybridization degree. Particularly, the “range extender” approach allows to add a FC in an existing EV, with a certain value of hydrogen stored.

FCs also have can be used as on-board auxiliary power units (APUs) for road and non-road applications such as in shipping or aviation.

Historically, the first FCHEV passengers vehicle was developed in 1997. Since then, significant technological advancements have been achieved. The FC technology has been introduced in public transport and in light duty two-wheeled and four-wheeled vehicles. Car manufacturers introduced small demonstration prototypes and fleets in the period between 2000 and 2008. In 2009, all of the main manufacturers, such as Daimler, Ford, General Motors, Fiat, Honda, Hyundai-Kia, BMW, Renault-Nissan and Toyota, addressed the transportation sector requesting a hydrogen infrastructure and concentrating their efforts in the development of the technology with the intent to commercialize a significant number of FCHEVs. When the technology appeared mature, safe and ready for applications in road transport, the commercialization process has begun within some specific market segments. Currently, there are already more than 500 FCHEVs operating in Europe, mainly in Germany, Scandinavia, UK, Netherlands and France, while fleets of FC buses for public transport has already started in London, Hamburg, Cologne, Milan, Oslo and other cities.

FCEHVs have been applied in a wide range of demonstration projects throughout the world. The technological barriers identified as critical for the success of FCs in vehicles have mostly been resolved. These includes start-up and operation in temperatures down to -30°C, driving range up to 400 km, refuelling times less than 3÷5 minutes for passenger cars and less than 10÷15 minutes for buses, reliability of 95% and performance as well as ICE-based vehicles. However, to become fully commercially possible, the costs of FCHEVs still need to be reduced and lifetimes increased. Regarding to the lifetime, it has been increased from a few hundred operating hours to several thousand operating hours, but more improvement are expected in term of durability and lifetime.

Owing to significant improvements in technology which consist primarily in a cost reduction and in a lifetime increase, some car manufacturers have already announced the market introduction of FCHEVs for 2015 and for the following years. In particular, Toyota has started to sell the Mirai model in Japan in December 2014 at a cost of 57400 $. Some such vehicles are expected to be sold in Europe in 2015 while Hyundai is already offering its iX35 for either lease or sale in the UK and Scandinavia since late 2014.

The current cost of the vehicles depend on the country and model and could oscillate between 55000 and 80000 €. The sales of the Toyota Mirai, word that in Japanese means "future", began on 15 December 2014. The Japanese government plans to support its commercialization with a subsidy of 19600 $. Sales are starting in the US with a price of 57500 $ without government incentives. Sales in Europe are scheduled to start soon, but only in UK, Germany and Denmark in a first stage. Daimler is expected to propose a model in 2017, but the price is not yet estimated. Hyundai has put it FC-based iX35 model on the Dutch, Norwegian and Danish market at a price of 66000 €.

A resume table of major global manufacturers, which are including the FCHEVs as part of their product portfolio, are listed in the Fig. 3.15 [65].

Producer & Vehicle	Key specifications	Availability - cost
Daimler - **B-Class F-CELL** **First released 2009/2010 Vehicles currently running in Germany, Norway, California**	Mercedes Benz B-Class F-CELL 100 kW Peak Output 70 kW Continuous Output 1,4 kWh Lithium-ion battery 380 km range (NEDC) 3.7 kg H2 storage	About 200 Mercedes Benz B-Class F-CELLs are operated in customer hand in Germany, Norway and California. The vehicles are leased to the customer on a monthly leasing rate.
Honda - **FCX Clarity** - **FCX Concept launched in December 2014 and due to go into production in November 2015**		The FCX Clarity has been on (selective) lease to private drivers in California since 2009 First sales to be made in Japan in March 2016 followed by sales in California and Europe (UK, Germany, Scandinavia)
Hyundai: - **ix35 Europe** - **Tucson USA** **Production: up to 5,000 pa** **First released 2013. Vehicles currently running in Europe (Germany, Belgium, Denmark, Norway, UK), South Korea and California**	Small SUV 100kW fuel cell & 60AH battery 365mile (584km) range 5.6kg H2 storage	USA – California: lease only at $499/month plus taxes for 36 months, inclusive of fuel and maintenance Europe – UK purchase at £53,105 inclusive of UK specific purchase support for ULEVs. Lease option also available
Toyota - **Mirai** **Production: 3,000 pa** **First released 2014. Vehicles being deployed in Japan, Europe (UK, Germany, Denmark) and California**	Executive 4 door saloon car (similar to Lexus GS300 size and spec.) 114kW fuel cell & 16.5AH battery 300mile (483km) range 5kg H2 storage	USA – California: Purchase cost at $58,325 plus taxes or lease at $499 per month with $3,649 initial deposit. Europe – based on 66,000 Euro plus local taxes. Equivalent to £63,104 in the UK, before purchase support (£5,000) under the ULEV scheme. Japan – sales began on 15 December 2014 at a price of ¥6.7 million (~US$57,400) before a subsidy of ¥2 million (~US$19,600).[

Fig. 3.15: Product portfolio of FCHEVs for major manufacturers [65]

Since the electric propulsion is involved in different ways in road vehicle, such as in purely electric vehicles (EVs), hybrid electric vehicles (HEVs) and Fuel Cell Hybrid Electric Vehicles (FCHEVs), there are different stages of development of technology, as indicated in Fig. 3.16 [66].

Types of EV	PEV	HEV	FCEV
Energy source	(i) Battery	(i) Battery/ultracapacitor (ii) Internal combustion engines	(i) Fuel cells
Propulsion technique	(i) Electric motor drives	(i) Electric motor drives (ii) Internal combustion engines	(i) Electric motor drives
Characteristics and feature	(i) Zero emission (ii) Short driving range (iii) Higher initial costs	(i) Low emission (ii) Longer range (iii) Complex	(i) Zero emission (ii) Highest initial costs (iii) Medium driving range
Major techniques	(i) Electric motor control (ii) Battery management (iii) Charging device	(i) Electric motor control (ii) Battery management (iii) Managing multiple energy sources and optimal system efficiency (iv) Components sizing	(i) Fuel processor (ii) Fueling system (iii) Fuel cell cost
Regenerative braking	(i) Yes	(i) Yes	(i) Yes

Fig. 3.16: Major characteristics of different type of electrification in vehicles [66]

Generally, an additional equipment is required to convert petrol into motion in a traditional ICE-based vehicle: engine, radiator, transmission system, fuel delivery lines, lubrications components, exhaust, catalytic converter, etc. In contrast, the source of energy (batteries) in purely electric comprises the majority of the powertrain part, because motor, wiring and transmission are relatively small. FCHEVs is between these two extremes due to the weight and volume of FC stack and its Balance of Plant and due to the high pressure storage tank.

Fig. 3.17 demonstrates the impact that system weight and conversion efficiency have on the specific energy of petrol, hydrogen and Lithium-Ion batteries, using data from four modern vehicles. In all cases, the effective specific energy is substantially reduced from the values that get typically reported.

	Conventional	Hybrid	Hydrogen	Battery
Reference vehicle	Volkswagen Golf VI	Toyota Prius III	Honda FCX Clarity	Nissan Leaf
Fuel weight (kg)	40.8	33.3	4.1	171[a]
Storage capacity (kWh)	500	409	137	24
Specific energy (Wh primary / kg fuel)	12,264	12,264	33,320	140[a]
Storage system weight (kg)	48	40	93	300[b]
Specific energy (Wh primary / kg of storage)	10,408	10,261	1,469	80
Net power (kW)	90	100	100	80
Power plant and auxiliary weight (kg)	233	253	222	100
Specific energy (Wh primary / kg total equipment)	1,782	1,398	315	60
Average conversion efficiency	21%	35%	60%	92%
Effective storage capacity (kWh useable)	105.0	143.1	82.0	22.1
Specific energy (Wh useable / kg total equipment)	374	489	260	55

Fig 3.17: Comparison of petrol, hydrogen, electrical storage systems in four vehicles [66]

An accurate assessment of future propulsion systems requires a complete vehicle cycle analysis, commonly called a well-to-wheels (WTW) analysis. In the WTW analysis there is the energy uses and emissions associated with fuel production, called well-to-tank (WTT), and the energy use and emissions associated with vehicle operation, called tank-to-wheels (TTW).

A WTW pathway traces from the original energy source through conversion, distribution and storage, to the wheels of the car. In Fig. 3.18 are reported the typical WTT and WTW efficiencies for conventional and electric vehicles [64].

Vehicle Type	Well to Tank	Tank to Wheel						Well to Wheel
BEV	32%-100%	Charger 90%	Battery 92%	Inverter 96%	Motor 91%	Mechanical 92%	66.5%	21.3%-66.5%
H_2 FCEV	75%-100%	Fuel Cell 51.8%		Inverter 96%	Motor 91%	Mechanical 92%	41.6%	31.2%-41.6%
Hybrid	82.2%	30.2%						24.8%
Diesel	88.6%	17.8%						15.8%
Petrol	82.2%	15.1%						12.4%

Fig. 3.18: Tipical WTT and TTW for vehicles [64]

California is the state leader in U.S. as FC development. In fact, in California there are most of FC applications for stationary and transportations sectors. Especially, the state has prioritized the development of a network of hydrogen fueling stations to support the roll out of commercialized fuel cell electric vehicles, which started in 2014 with the delivery of the first Hyundai Fuel Cell vehicles to lease customers.

California is also a national and international leader in the control of air pollution and greenhouse gas (GHG) emissions from mobile and stationary sources. The California Air Resources Board (ARB), founded in 1967, is tasked with protecting the public from exposure to toxic air contaminants and GHGs. The agency is a key player in providing leadership in implementing and enforcing air pollution control rules and regulations with the expected scenario for transportations indicated in the figures 3.19 and 3.20. [67]

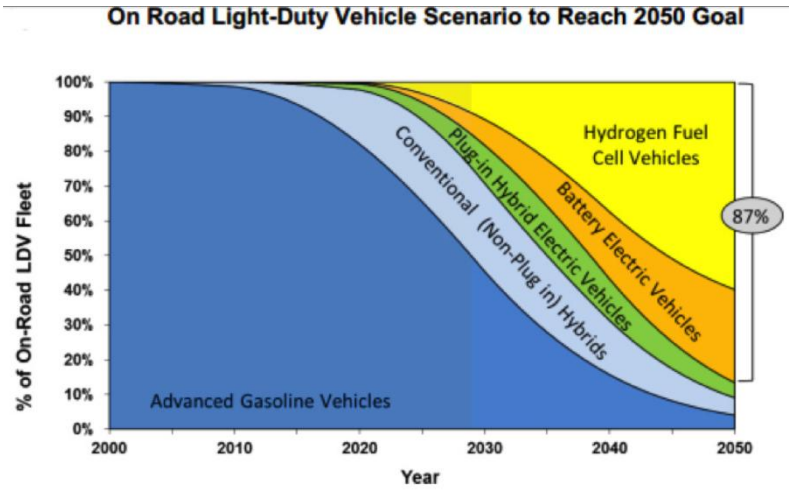

Fig. 3.19: Scenario for light-duty vehicles in California [67]

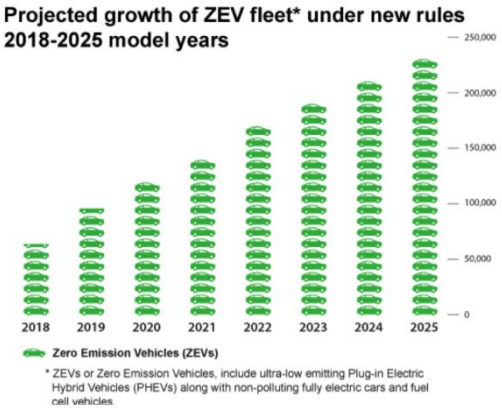

Fig. 3.20: Scenario of ZEV (Zero Emission Vehicles) in California [67]

Historically, since the invention in 1838, FCs had been used in various applications such as in spacecraft, submarine, road vehicles and stationary power plants. The first FC that powered a vehicle was produced by General Motors (GM) in 1966, called GMC Electrovan. It was the result of two year development effort lead by Dr. Craig Marks and utilized 32 fuel cell modules with a continuous output of 32 kW and a peak power of 160 kW. The Electrovan achieved a top speed of 70 MPH and had a range of 120 miles. However, the whole fuel cell system turned the 6-seat van into a 2-seater due to the large hydrogen and oxygen tanks along with the piping. After test driving in the GM facility and being shown off to journalists, the project was discontinued due to the prohibitive cost and lack of hydrogen infrastructure at that time.

Almost thirty years later, the fuel cell technology was revisited by automakers. Daimler-Benz introduced the NECAR 1 (New Electric Car) to the public in 1994. The 50 kW PEMFC was manufactured by Ballard which has become one of the leading PEM fuel cell manufacturers. The NECAR 1 utilized a compressed hydrogen tank that stored the gas at 300 bar and achieved a top speed of 56 MPH and range of 81 miles. The fuel cell and the storage system, like the GM Electrovan, also took up the entire cargo space and left only two-seat space in the van. NECAR 2, introduced two years later was featured a fuel cell system one third of the weight of its predecessor.

During 1996 to 1999, several major automakers such as Toyota, GM, Mazda, Ford, Honda, Nissan, and Volkswagen also brought fuel cell vehicles projects to fruition. They employed fuel cells ranging in power from 10 to 75 kW and demonstrated vehicle ranges of up to 310 miles. Many of these auto companies had set goals to commercialize fuel cell vehicles in first decade of twenty-one century, but none of these goals were realized.

In 2002, Toyota launched its first FCHEVs (called FCHV) in US and Japan. Its powertrain comprised a 90 kW FC and a nickel-metal hybrid battery. At low speed the FCHV runs on battery alone. The fuel cell and battery supplied power in tandem when higher performance was required. The combined range of the fuel cell and battery was 155 miles. Since then, eight major automakers have put in significant efforts to test the performance of the FC vehicles. In the Fig. 3.21 are listed demonstration projects of FCHEVs.

Year	Automaker	Model	Engine	FC Power (kW)	Range (miles)	Max speed (mph)	Hydrogen Pressure (Bar)	Note
2002	Toyota	FCHV	Fuel cell/ battery hybrid	90	180	96	350	18 leased in California and Japan
2002	Daimler	A-Class F-CELL	Fuel cell/ battery hybrid	85	90	87	700	60 vehicles in US, Japan, Singapore, and Europe started in 2003
2002	Ford	Advanced Focus FCV	Fuel cell/ battery hybrid	85	180	n/a	350	30 fleet vehicles in Sacramento, Orlando, and Detroit
2002	GM	Advanced HydroGen3	Fuel cell	94	170	100	700	6 placed in Washington DC
2002	Nissan	X-TRAIL	Fuel cell/ battery hybrid	75	n/a	78	350	3 leased to Japanese government
2004	Hyundai	Tucson	Fuel cell/ battery hybrid	80	185	93	350	Demonstration project in the US between 2004-2009 and in Korea between 2006-2010
2004	Kia	Sportage	Fuel cell	80	185	93	n/a	Demonstration project in the US between 2004-2009 and in Korea between 2006-2010
2006	GM	Equinox FCEV	Fuel cell/ battery hybrid	93	200	100	n/a	Leasing started in 2007. 100 vehicles in California, New York, and Washington DC
2007	Honda	FCX Clarity	Fuel cell	100	354	100	350	Small scale production of 200 vehicles between 2008-2010, Leasing in Southern California and Japan
2008	Kia	Borrego/Mojave FCEV	Fuel cell/ super capacitor	115	426	93	700	Leasing to Seoul, Korean residents starting in 2009
2008	Toyota	FCHV-adv	Fuel cell/ battery hybrid	n/a	97	n/a	n/a	Limited leasing in Japan started in 2008. More than 100 leased in Connecticut, California and New York.
2009	Daimler	Mercedes-Benz B-Class F-CELL	Fuel cell	90	239	105	n/a	Small series production started in 2009. 70 Deployed in Los Angeles and San Francisco by 2012
2011	Hyundai	Tucson IX	Fuel cell/ battery hybrid	100	403	n/a	700	Tested 50 vehicles in 2011
2012	Hyundai	ix35	Fuel cell/ battery hybrid	100	365	100	n/a	Leasing in Sweden and Denmark started in 2012

Fig. 3.21: Demonstration projects of FCHEVs [68]

Since Toyota and Hyundai have announced their commercially available FCHEVs, with the specifications of Fig. 3.22, which will be used where the public hydrogen fueling stations are located. Both models show similar ranges that exceed the best battery electric car in the current market, such as Tesla S-85 with 265 miles in range. The fueling time for both models is comparable to gasoline vehicles, which presents a significant advantage over the battery electric car which requires at least 30 minutes to get around 80% of its range capacity. Importantly, Toyota plans are to lower the price to achieve an anticipated full scale market penetration in the decade of 2020s.

Maker	Model	Fuel Cell Power (kW)	Range (miles)	Fueling Time	Price	Note
Hyundai	Tucson Fuel Cell	100	265	<10 min	Lease at $499/month, $2999 due at signing	Price includes fuel and maintenance
Toyota	Mirai	unrevealed	435	3 min	¥ 7 million in Japan ($68600)	n/a

Fig. 3.22: Specifications of commercially available FCHEVs [68]

In 2013, Ford, Nissan, and Daimler signed a joint venture for developing FCHEVs to be commercialized by 2017. A GM and Honda partnership is also aiming to bring FCHEVs to the market by 2020. A timeline with main steps in FCHEVs development is shown in Fig. 3.23 [68]

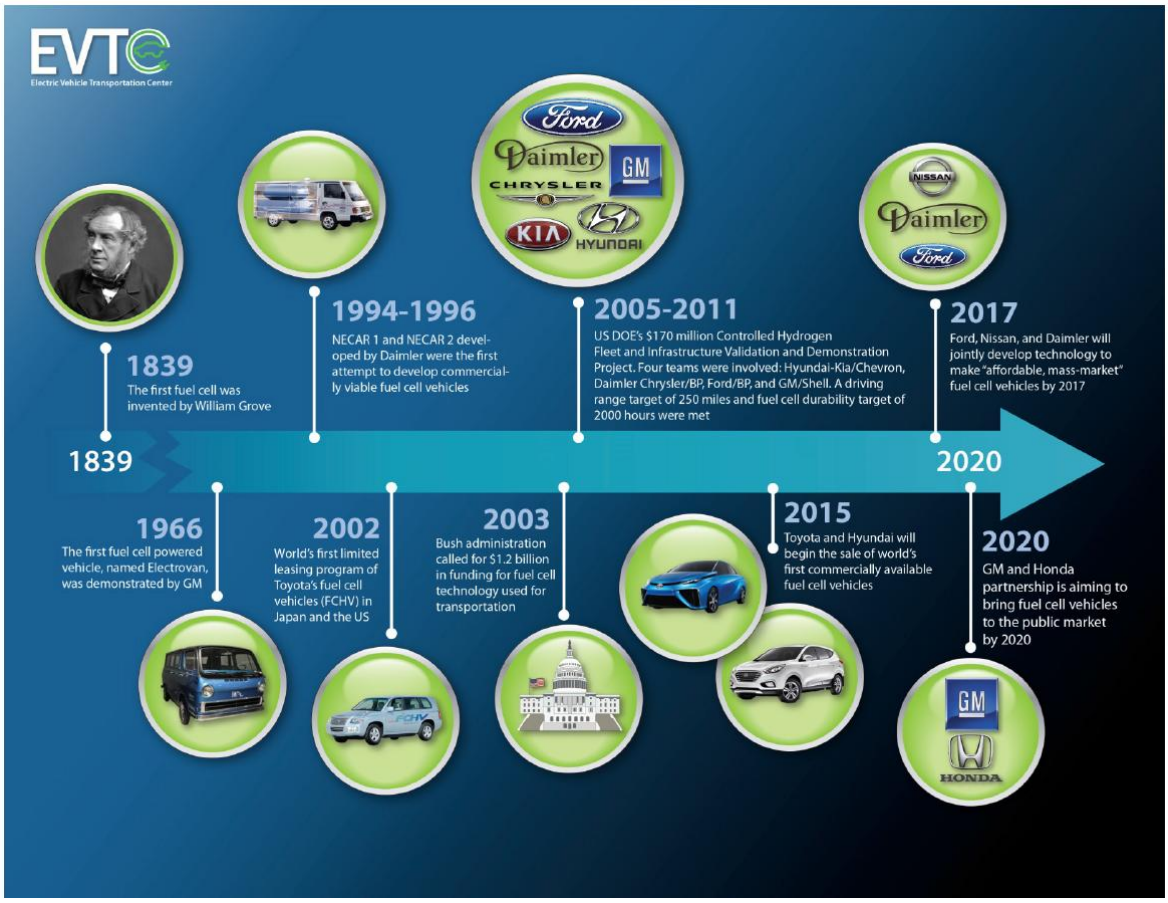

Fig. 3.23: Timeline of main steps of FCHEVs development [68]

3.4 State of the art of research and innovation programmes

The European Union though its research and innovation funded programmes has set ambitious long-term targets for hydrogen systems and technologies. The targets which are planned to reach for 2020 comprising an increase in the share of renewable energy, improvements in energy efficiency and dramatic reductions in greenhouse gas emissions of 20%. The actions in the field of Fuel Cells and Hydrogen are under the supervision and control of Fuel Cell Hydrogen Joint Undertaking (FCH JU) which is a partnership of public and private companies, research centers, universities and institutions [69].

The FCH JU was established in May 2008 with a lead role of Fuel Cell and hydrogen technologies in the provision of medium and long term solutions to energy challenges of European Community. The budget for 2008-2013 amounted to around EUR 940 million, jointly funded by the European Commission and Europe's fuel cell and hydrogen industry and research communities. With these funds, the FCH JU has carried out a Research and Technology Development (RTD) programme, associated with the Seventh Framework Programme (FP7). This programme is supporting basic and applied research and demonstration activities across a range of applications in the transportation and energy sectors, such as in hydrogen production, distribution and storage, early markets, cross-cutting activities, commercialization, safety, manufacturing, regulations, codes and standards (RCS), pre-normative research ((PNR)), socio-economic analysis, education and training.

Due to the success of the FP7, the FCH JU was renewed in June 2014 as part of Horizon 2020. The budget is now set at EUR 1.33 billion with activities focusing on two innovation pillars: transportation and energy. The topics of these two innovation pillars are set out in the Multi Annual Work Programme (MAWP) which is schematic represented in Fig. 3.24.

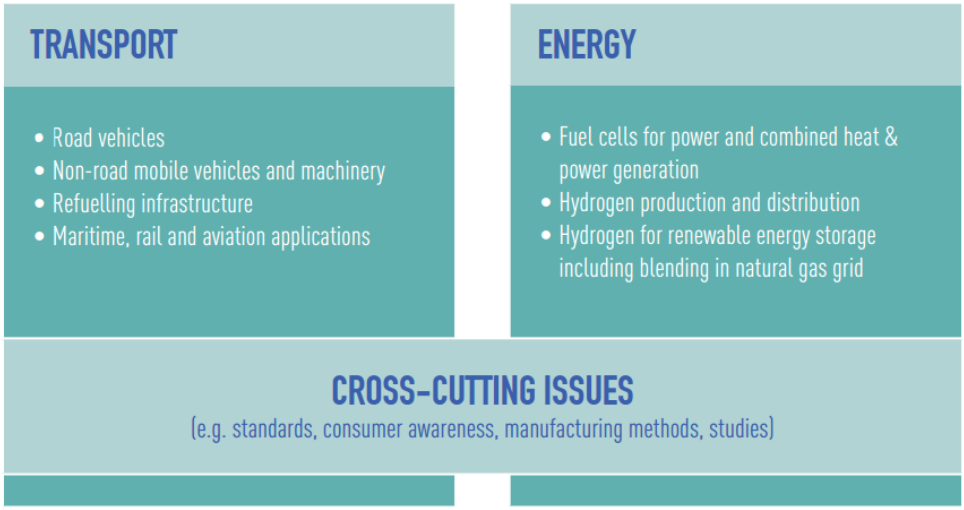

Fig. 3.24: two main pillars in MAWP [69]

The objective of the transport pillar is the acceleration of the commercialization FCs for use in a wide range of transport applications. In fact, FCs play a lead role to the pollution reduction in transportations giving the possibility to achieve a zero-emissions impact of vehicles. The focus of this pillar in H2020 is on reducing the production costs of fuel cell systems and increasing their lifetime so that they are competitive with conventional technologies. These improvements will contribute directly to successful commercialization, to the expansion of hydrogen refuelling infrastructure across Europe and to demonstrate and test the durability, robustness, reliability, efficiency and sustainability of technologies, and ease of customer use.

Through the actions of FP7 substantial progress has been made towards large scale deployment of fuel cell vehicles in Europe:

- more than 200 cars will be demonstrated on Europe's roads in a number of European states in four projects: H2MOVES, HYTEC, SWARM and HYFIVE;
- six hydrogen refuelling station installations in HYFIVE project;
- cost per vehicle has been reduced;
- more than 45 buses have been deployed across Europe in three projects: CHIC, High V.LO City and HYTRANSIT. Additionally, 20 buses will be deployed under a fourth project, 3EMOTION, which is starting in 2015. These projects have reached a reduction in cost per bus over time, an improvement in fuel consumption and an expansion of the geographical coverage across Europe;

- more than 400 Material Handling Vehicles (MHVs) are planned for use across the European states in four projects: HyLIFT-DEMO, MobyPost, HyLIFT-Europe and HAWL;
- four Auxiliay Power Unit (APU) applications are being developed and validated in six projects: FCGEN, DESTA, SAPIENS, PURE, HYCARUS and SAFARI.

Regarding the action about research, the focus areas of FCH JU are related to following aspects

- membranes through activities to develop and improve membranes for transportation cells and stacks, catalysts through improvements to raise performance levels and reduce costs in PEMICAN, ARTEMIS, IMPACT, IMMEDIATE, IMPALA, CATHCAT, CATAPULT, NANOCAT and SMARTCAT projects;
- bipolar plates through developments and improvements to materials for better performing components in STAMPEM, IRAFC and COBRA projects;
- manufacturing and process development through activities to support the near-term production of components and subsystems in AUTOSTACK, LIQUIDPOWER and AUTOSTACK-CORE projects;
- methodology and tools through the creation and development of modeling and other tools to help industry to undertake projects in PUMAMIND;
- system and balance of plant (BoP) components through development and improvement of components for better performance and reduced cost;
- advanced refuelling components and storage through activities to develop the hydrogen refuelling process alongside storage options in PHEDRUS;
- storage development in SSH2S, COPERNIC and HYCOMP projects.

The objective of the energy pillar is the acceleration of the commercialization of in the fields of fuel cells for stationary applications and in the field of production, storage and distribution of hydrogen. This pillar is responsible for developing and demonstrating a number of different technologies and tends to be less concentrated than the transportation pillar. The scope is to advance the technologies of fuel cell stacks, BoP and complete systems to the point where they are able to compete effectively with current power and heat-generation technologies. The case of hydrogen production, storage and distribution there are three objectives: to develop

and demonstrate hydrogen production using electrolysis with renewable power for energy storage and grid balancing, to develop low-carbon hydrogen production from other resources such as direct solar and biological and to develop and demonstrate technologies for hydrogen storage, handling and distribution efficiently and effectively throughout the energy value chain.

Cross-cutting projects support the commercialization activities of the two FCH JU pillars (transport and energy). They are critical to the overall FCH JU strategy. They consist on market support measures, public awareness, educational activities, socio-economic assessment, tools and demonstrations [70].

Since the sustainable, secure and competitive energy supply and transport services are at the heart of the strategy for a low carbon economy till 2020, the innovation and deployment of new clean technologies are essential for a successful transition to a new sustainable economy as indicated in ten milestones which define the reasons of such attention to hydrogen and fuel cell technologies:

1) Fuel cell and hydrogen technology is vital for the future European economy.
2) Decisive action is needed now to maintain Europe's global technology leadership for the future.
3) A purely market-driven approach alone will not enable the introduction of clean technologies.
4) Public Private Partnership is the appropriate structure to support the technological shift.
5) Joint public/private effort needed for FCH technology breakthrough across sectors reach €17,9 billion for 2014-2020.
6) Investment focus is twofold: improving the competitiveness of FCH technology solutions and increasing the share of renewable sources in the hydrogen production mix.
7) Combined public and private investment is needed for all stages of the innovation cycle, from R&D to first-of-a-kind commercial references.
8) Bringing clean technologies to the point of market breakthrough might require a shift from technology to sector support.
9) New financial instruments are needed to finance first-of-a-kind commercial applications and support market introduction.

10) Fuel Cell and Hydrogen technologies should benefit from various European programmes.

The role of fuel cells and hydrogen in transport is crucial: FCEVs provide a clean alternative and clear advantages for mobility for all travel circumstances, urban, intercity and longer-distance. There are no major performance compromises to be made by the user in terms of size, driving range or speed, refuelling time or other driving comforts in comparison to traditional cars. In fact, FCHEVs have no emissions, are silent and hydrogen can be produced from all renewable energy sources. FCHEVs has a Total cost of Ownership (TCO) advantage over EV and PHEV in heavy-long distance car segments. Presumably, if investments are well coordinated over the next 10 years, FCHEVs could be fully commercial by and competitive with Internal Combustion Engines (ICE) by 2025. Generally, the objectives of FCH JU in transport sector till 2020 are two: firstly, improve and validate hydrogen vehicle and refuelling technologies to the level required for commercialization decisions by 2015 and a mass market roll-out as from 2020 and, secondly, demonstrate competitive FCHEVs and infrastructure solutions, by contributing around 500,000 FCHEVs and around 1000 public hydrogen refuelling stations to the transition of the transport sector into electric drives [71].
In 2009, both the European Union and G8 leaders agreed that CO_2 emissions (GHG) must be cut by 80% by 2050 and global warming stay below the safe level of 2ºC. But 80% decarburization overall by 2050 requires 95% decarburization of the road transport sector, as indicated in the following graph:

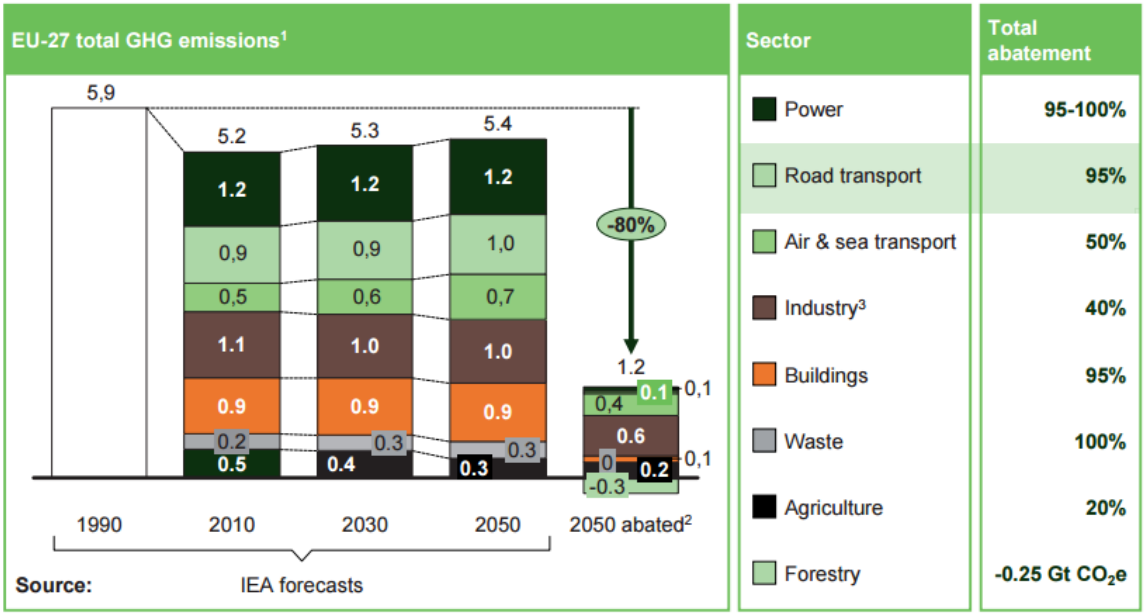

Fig. 3.25: Greenhouse Gas (GHG) emissions abatements [71]

Decarburization may be achieved through efficiency, bio-fuels and electric power-trains. With the number of passenger cars set to rise to 273 million in Europe and to 2.5 billion worldwide by 2050, decarburization may not be achievable through improvements in the traditional ICE or alternative fuels alone, but electric vehicles (EVs, FCHEVs and PHEVs) are necessary to achieve GHG reduction goals. The benefits of these electric vehicles over ICEs are:

- electric vehicles have zero emissions while driving;
- significantly improving local air quality;
- they can be made close to CO_2-free, depending on the primary energy source used;
- electric vehicles can be fuelled by a wide variety of primary energy sources including gas, coal, oil, biomass, wind, solar and nuclear;
- help to reduce oil dependency;
- while ICEs have the potential to reduce their CO_2 footprint considerably through improved energy efficiency, this is insufficient to meet the CO_2 reduction goal for 2050.

FCHEVs are almost technologically ready, although some further steps still need for improve efficiency and durability, but they are not commercially available due some recent developments, such as the implementation of 700 bar storage technology, address of safety concerns, cold start reached to -25ºC, or even lower, new materials (e.g. metallic bipolar

plates) which have optimized heat management in the stacks, better understanding of the mechanisms affecting durability, possibility to control and manage cell voltage. *f* Moreover, common standards for hydrogen refueling have been agreed: standard connections and safety limits and performance requirements have been established by several SAE22 and ISO22 standards. With more than 500 passenger cars covering over 15 million kilometers and undergoing 90,000 refueling, FCHEVs are now considered to have been comprehensively tested in a customer environment. The result: the focus has now shifted from demonstration to commercial deployment so that FCHEVs, like all technologies, may benefit from mass production and the economies of scale. A summary of these recent developments are indicated in the following scheme:

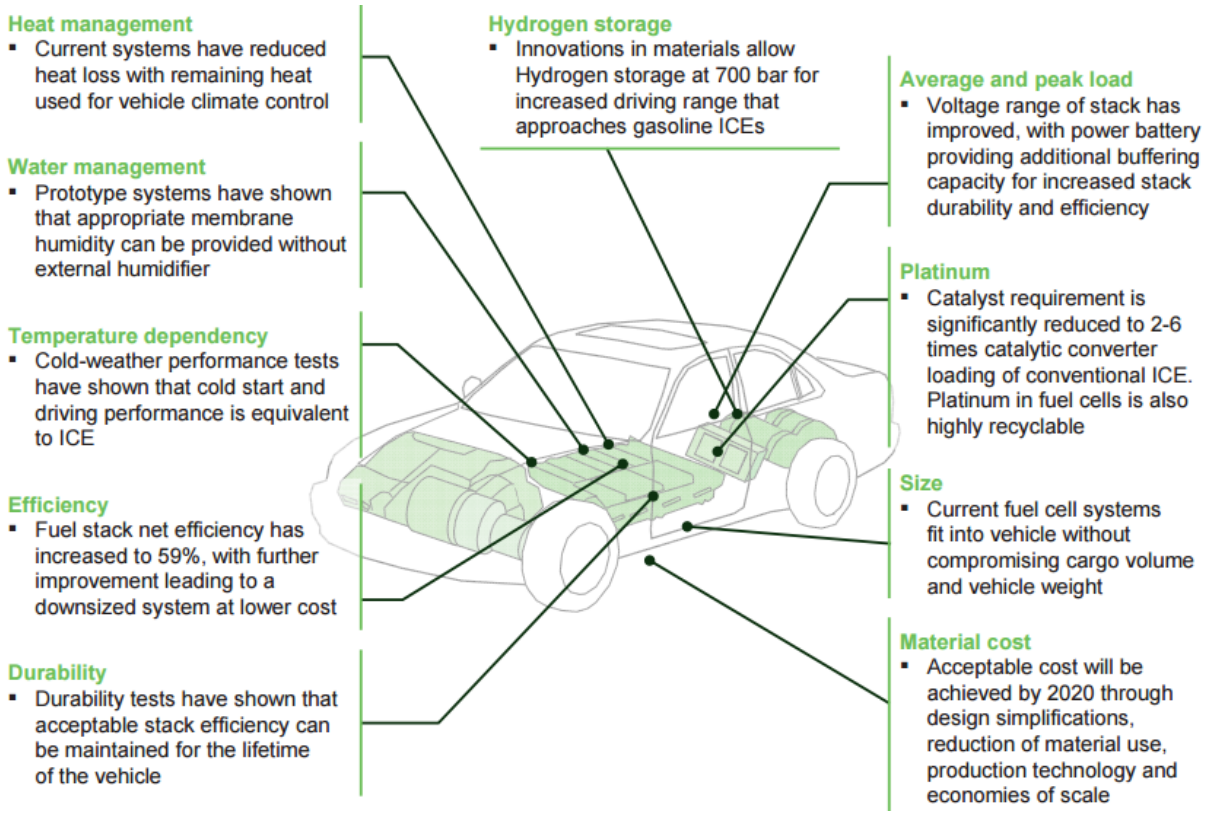

Fig. 3.26: Recent technological improvements of FCHEVs [72]

The benefits of electric vehicles go beyond the decarburization of road transport and energy security to address the key issue of air pollution in large and congested cities: the exhaust from ICEs not only emits CO_2, but also local pollutants such as carbon monoxide, hydrocarbons and nitrous oxides. Diesel vehicles also emit particulate emissions. Although these emissions are mitigated by catalytic converters, all pollutants that cannot be processed

are released into the atmosphere, degrading air quality and reducing the ability of large cities to meet air quality targets. On the other hand, these electric vehicles release zero emissions in their “tank-to-wheel” process, with emissions limited to the “well-to-tank” process: emissions depend on the primary energy source used and can be potentially reduced to zero. Finally, unlike ICEs, electric vehicles are virtually silent, also reducing noise pollution significantly [72].

4. Modeling of Fuel Cell stacks

4.1 Mathematical models in literature for FC modeling

Modeling is very helpful in the improvement of FC technology. The development of PEMFCs requires the simulation of the entire system under different loading conditions, pressures of reagent gases and temperature [73].

Modeling and simulation play an important role for the improvements, optimization and design of the FC systems. The models, that can build up using different tools, must be accurate and must be able to provide results quickly. The performance must be predicted under different operating conditions [74].

In the literature, several models have been published for FCs. These model differs each other from [75]:

- the number of dimension of the models (one, two or three);
- the dynamic, steady-state or quasi-steady analysis;
- the kinetics at anode and cathode (Tafel-type, Butler-Volmer, complex kinetics);
- anode and cathode phases (gas, liquid or a combination of them);
- mass transport;
- energy balance.

Some common assumption are used in the models, such as:

- ideal gas;
- incompressible and laminar flow;
- homogeneous and isotropic structures;

In this study, a Matlab/Simulink® dynamic model has built up in order to define the performance of PEMFCs in terms of voltage, efficiency and power, to analyze the mass flows of gases and water and to investigate the energy flow rates into the cell.

The model, that describes the behavior of PEMFC under transient conditions, is based on the thermodynamic and electrochemical equations available in literature. Since the simulation process is carried out using the current density as input signal and the operating conditions as input parameters, a parametric analysis has been done in different operating conditions.

4.2 Matlab/Simulink® model for FC stacks

The Matlab/Simulink® model proposed in this Research consist of the connected block shown in Fig. 4.1. The input parameters, which are operating temperature, inlet pressures of reactants, transfer coefficient, internal resistance, amplification constant, exchange current density, limiting current density, cell area and number of cell are indicated with the black/orange squares. Their values, which could be constant or variable, are inserted in the Matlab workspace and can be changed in order to carried on the simulation with new assumptions. The constant parameter, such as Faraday constant, universal gas constant or number of electrons per mole of hydrogen, are indicated with grey/blue squares. The input signal, which usually consist of the time in a simulation and which can be varied in a certain range with a certain accuracy, in this case is equal to the current density and it will be comprised in the range between 0÷1.40 with an accuracy of 0.01. So, the results will show how all operating parameters of the FC stack vary from 0 to 1.40 with an accuracy of 0.01, that means 0-0.01-0.02-…..-1.39-1.40. The blocks “V_act”, “V_ohmic” and “V_conc” allow to calculate the overpotentials for activation, ohm and concentration. These values are subtratted to the Nerst potential calculated in “V_Nernst” in order to calculate the real voltage in “V_cell”. The voltage is referred to a single cell and it will be used to calculate the power output by multiplying it with the number of cells, the current density and the cell area. Three more block allow to calculate the water injection for humidification, a mass balance and an energy balance [76].

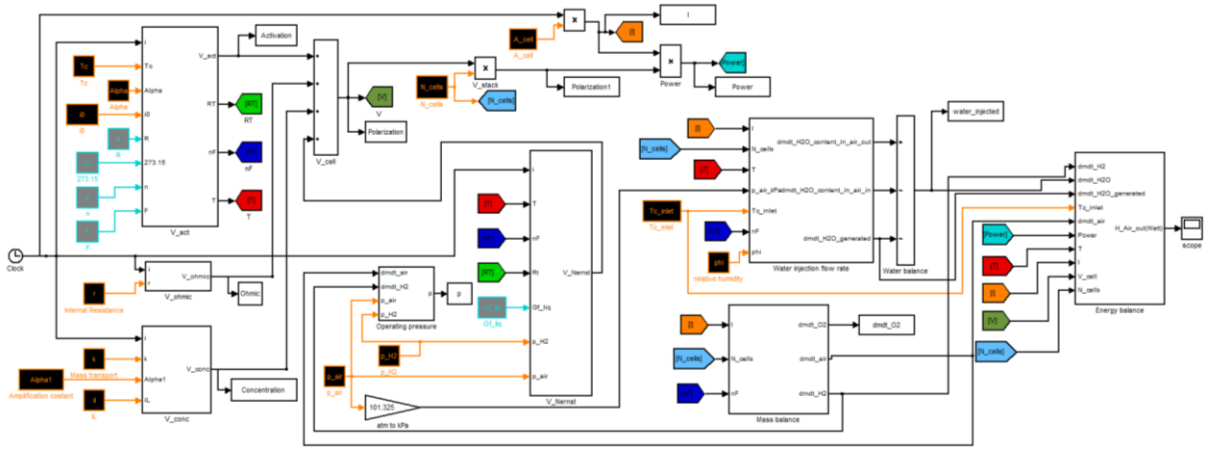

Fig. 4.1: Matlab/Simulink® model

Since the simulations are carried out in function of the current density and not of the time using parameters which are the same in the internal structure of the FC stack, the model is steady-state and one-dimensional.

The Matlab/Simulink® model can be simplify through the following flowchart where the calculations are described starting from the input values to the output ones.

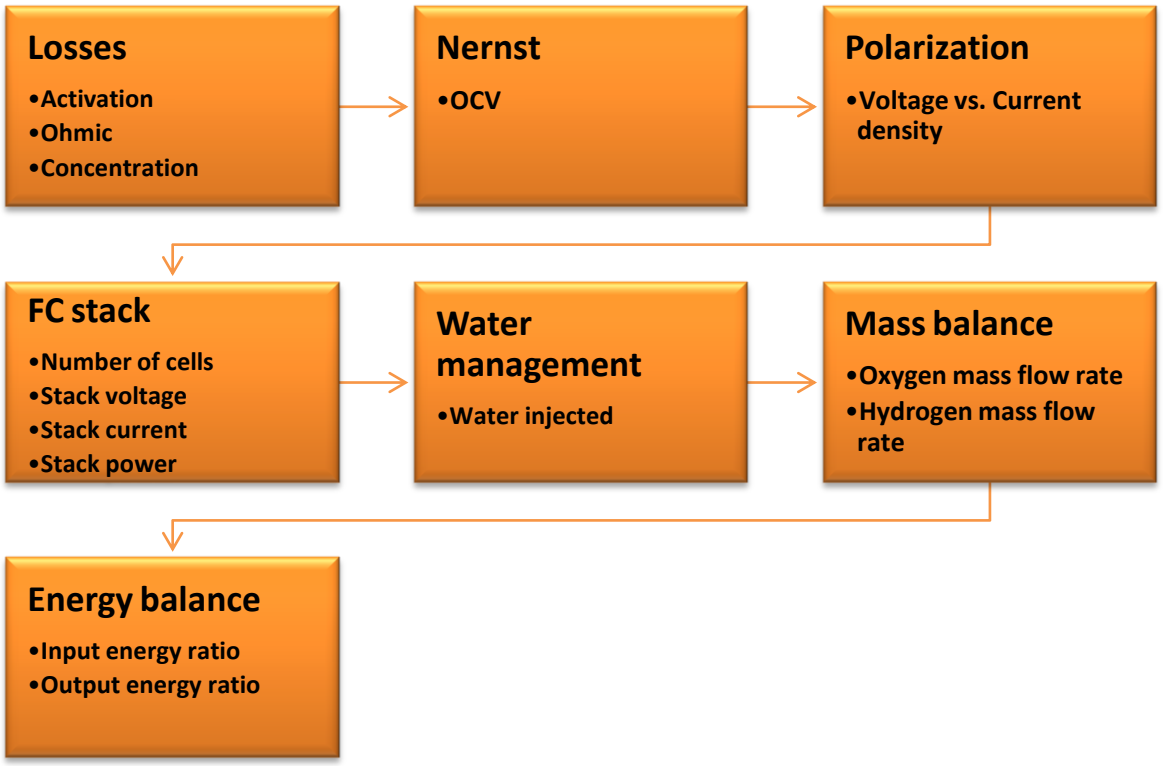

Fig. 4.2: Flowchart of FC model

4.2.1 Polarization curve

The performance of a PEMFC is characterized by polarization and power curves. All of these characteristics are usually plotted over current or current density. The manufactures provide the technical specifications of FCs through these type of diagrams [77].

The maximum obtainable electrical energy within a cell is given by the change in Gibbs free energy ΔG of the electrochemical reaction, according to equation (4.1) [78].

$$\Delta G = \Delta H - T(\Delta S) \tag{4.1}$$

This Gibbs free energy is a measure of the maximum electrical work obtainable from a chemical reaction at a certain value of temperature and pressure of reactants. So, the equation (4.1) represent the energy available in the FC at any constant temperature and pressure.

The enthalpy change ΔH represents the total available thermal energy. If there would be no entropy (ΔS=0) produced during the electrochemical reaction, then a FC reaches an efficiency of 100 % because all energy could be used. However, there will be always entropy generated within the system and so the term denotes the unavailable amount of energy. The electrical work produced by a reversible reaction is given from (4.2).

$$-\Delta G = \int V dq = n \cdot F \cdot OCV \tag{4.2}$$

Since the reaction becomes spontaneously if ΔG<0, an expression of OCV can be obtained through (4.3).

$$OCV = \frac{-\Delta G}{nF} \tag{4.3}$$

It can be seen that OCV is a function of the Gibbs Energy and consequently a function of temperature [34].

In addition, the effects of pressure and concentration of reactant gases must be considered. They are described by the Nernst equation (for hydrogen-oxygen fuel cell reaction).

$$E_{Nernst} = OCV + \frac{RT}{nF}\ln\left(\frac{p_{H_2O}}{p_{H_2}\cdot p_{O_2}^{0,5}}\right) \tag{4.4}$$

The value of ΔG at 353.15 K and 1 atm is equal to -228170 J/(K·mol). This value is used in Matlab/Simulink® model, in which the Nernst voltage is calculated in the following block:

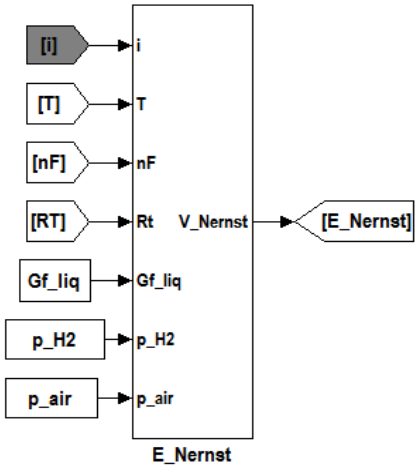

Fig. 4.3: Block diagram in Simulink® model used to calculate the Nernst voltage

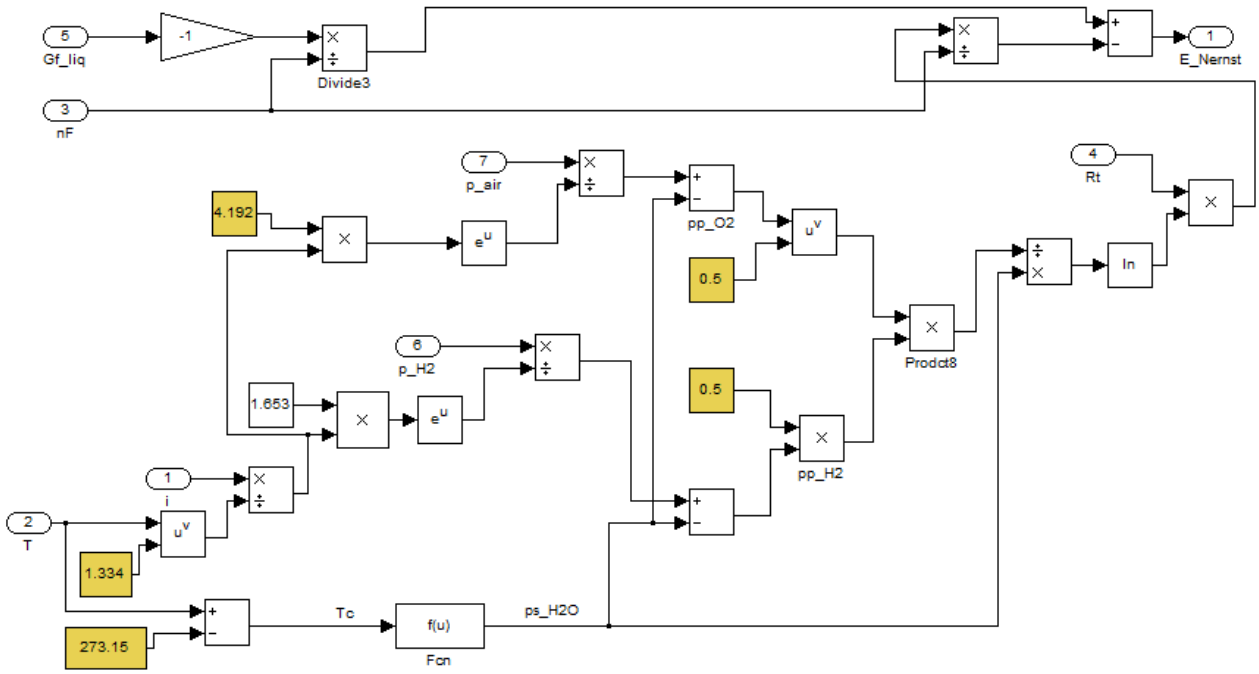

Fig. 4.4: Block diagram detailed in "E_Nernst" subsystem

The calculation of polarization curve is referred to a FC stack, characterized by an active area (cm^2) and a number of cells, which is operating at a predefined temperature. The values of inlet hydrogen and air pressure are known and inserted in the model. The other useful parameters for creating the polarization curve are:

- transfer coefficient α;
- exchange current density i_0;
- limiting current density i_L;
- amplification constant α_1;
- Gibbs function in liquid form G_{f_liq};
- constant for mass transport k;
- internal resistance R.

The Nernst voltage E_{Nernst} is calculated using the saturation pressure of water and the partial pressures of hydrogen, oxygen:

$$\log(p_{sat\_H2O}) = -2.18 + 0.03 \cdot T - 9.18 \cdot 10^{-5} \cdot T^2 + 1.45 \cdot 10^{-7} \cdot T^3 \quad (4.5)$$

$$pp_{H2} = 0.5 \cdot \left(\frac{p_{H2}}{\exp\left(\frac{1.65 \cdot i}{T_K^{1.334}}\right)} \right) - p_{sat\_H2O} \quad (4.6)$$

$$pp_{O2} = \left(\frac{p_{air}}{\exp\left(\frac{4.19 \cdot i}{T_K^{1.334}}\right)} \right) - p_{sat\_H2O} \quad (4.7)$$

The real cell voltage is lower than OCV because it is reduced at higher currents due to irreversible losses (or overpotential): the activation losses, ohmic losses and concentration losses [79].

$$V_{cell} = E_{Nernst} + \Delta V_{act} + \Delta V_{ohm} + \Delta V_{conc} \quad (4.8)$$

Since all losses are negative, the real cell voltage will be lower than Nernst voltage. Consequently, the actual work in a FC is less than the maximum available work due the irreversibilies of the process.

Activation losses are caused, in the first part of the polarization curve, by the slowness of the reaction near to the electrodes. Tafel equation (4.9) allow to calculate the activation losses.

$$\Delta V_{act} = -\frac{R \cdot T}{n \cdot \alpha \cdot F} \log\left(\frac{i}{i_0}\right) \tag{4.9}$$

The activation losses are calculated in the Simulink® model through the following block diagram:

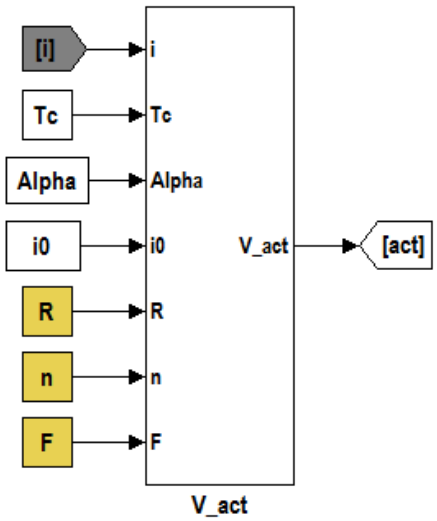

Fig. 4.5: Block diagram in Simulink® model used to calculate activation losses

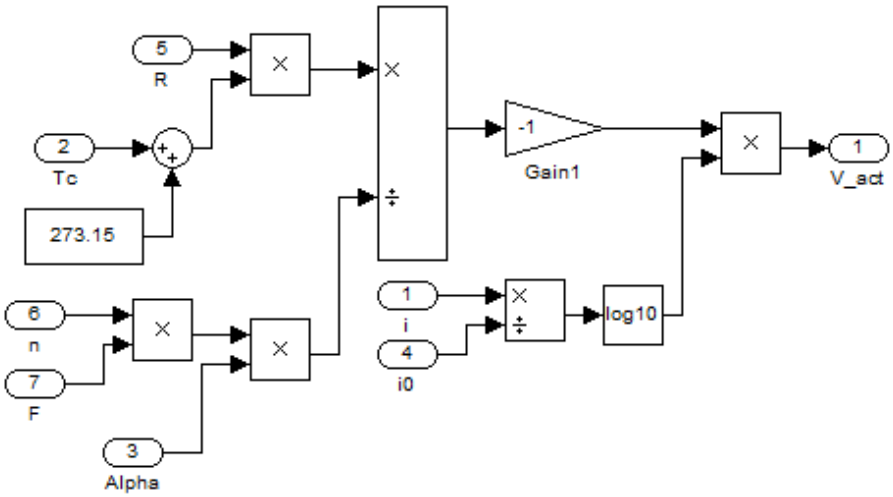

Fig. 4.6: Block diagram detailed in "V_act" subsystem

Ohmic losses are caused, in the middle part of the polarization curve, by resistance of electrolyte to the crossing of electrons. Ohm law (4.10) allow to calculate ohmic losses.

$$\Delta V_{ohm} = -r \cdot i \tag{4.10}$$

The ohmic losses are calculated in the Simulink® model through the following block diagram:

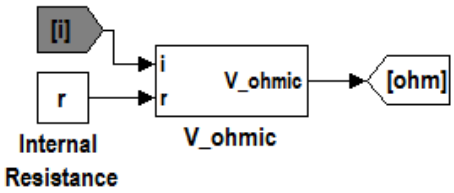

Fig. 4.7: Block diagram in Simulink® model used to calculate ohmic losses

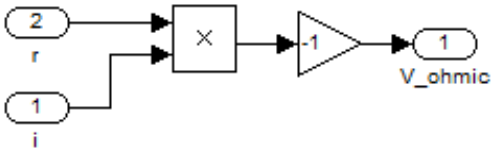

Fig. 4.8: Block diagram detailed in "V_ohmic" subsystem

Concentration or mass transport losses are caused, in the final part of the polarization curve, by the reduction of pressure of reactants during the chemical reaction. The equation (4.11) allow to calculate the concentration losses.

$$\Delta V_{conc} = \alpha_1 \cdot i^k \cdot \ln\left(1 - \frac{i}{i_L}\right) \quad \text{if} \quad 1 - \frac{i}{i_L} > 0 \quad \text{else} \quad \Delta V_{conc} = 0 \tag{4.11}$$

The concentration losses are calculated in the Simulink® model through the following block diagram:

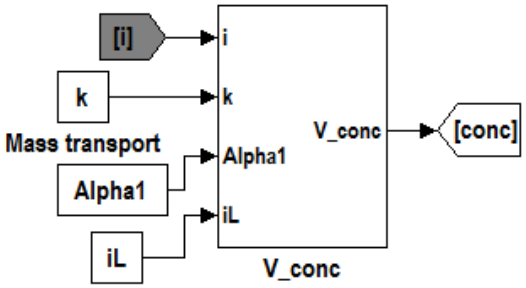

Fig. 4.9: Block diagram in Simulink® model used to calculate concentration losses

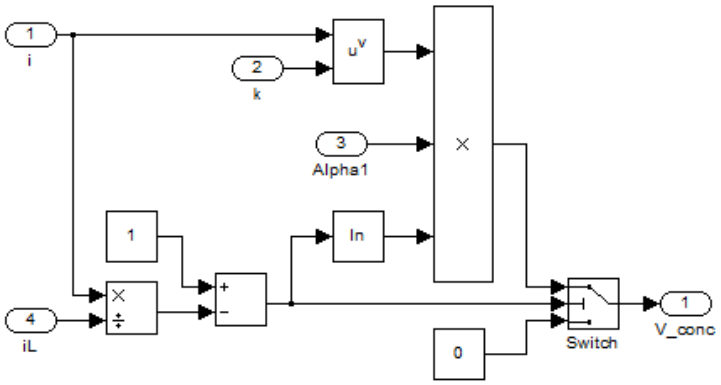

Fig. 4.10: Block diagram detailed in "V_conc" subsystem

The parameters used in the model in order to calculate the polarization curve are listed in Table 4-1 [80] [81].

Table 4-1. Parameters used in the calculations of polarization curve.

Constant	Letter	Value
Transfer coefficient	α	0.5
Internal resistance	r	0.19 Ω/cm^2
Amplification constant	α_1	0.085 AV/cm^2
Mass transport	k	1.1
Exchange current density	i_0	$1.2246 \cdot 10^{-7}$ A/cm^2
Limiting current density	i_L	1.4 A/cm^2

4.2.2 Stack power

In order to define the performances of a PEMFC, a calculation of the available power must be done.

The power provided from one single cell is obtained by the product of the cell voltage V_{cell} and the current I [82].

$$P_{cell} = V_{cell} \cdot I \tag{4.12}$$

In a stack with many cells connected in series the power generated is calculated with (4.13).

$$P_{FC} = V_{cell} \cdot I \cdot N_{cells} \tag{4.13}$$

The following block diagram contains the power calculation.

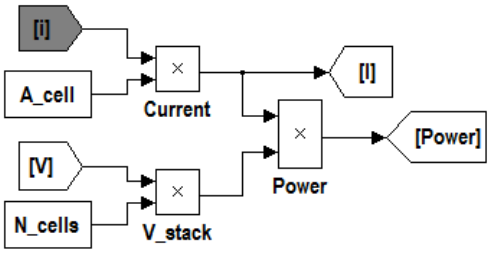

Fig. 4.11: Block diagram in Simulink® model used to calculate FC stack power

Several parameters must be considered when designing and modeling FCs. Since there are only two independent variables, voltage and current, the sizing of the stack is very simple In

fact, the output power can be easy calculated by the product of voltage and current, as indicated in the equation (4.12). When the design involve the current density instead of a current, the cell active area must be considered:

$$i = \frac{I}{A_{cell}} \tag{4.14}$$

As mentioned in the chapter 5.2.1, the cell voltage and the current density are related to the polarization curve. The manufacturers mostly use the values in the range 0.6÷0.8 as nominal cell voltage which must be multiplied by the number of cells to calculate the nominal voltage of the stack. So, the number of cells is usually defined by the voltage required , according to equation (4.15).

$$V_{FC} = V_{cell} \cdot N_{cells} \tag{4.15}$$

In the bipolar stack, the FC is constitute by several cells in series and the cathode of one cell is connected with the anode of the next cell.

4.2.3 Water management

The humidification level of the membrane needs to be controlled in order to maintain the correct ionic permeability. Normally some procedures can be employed to humidify the reactants, air and oxygen because it is essential to ensure adequate water content within the membrane for a good performance and durability of PEMFCs. On the contrary, too much water within the PEMFC lead to a flooding of electrodes, blocking the pores in the diffusion media or the flow channels [23].

The calculations of the water injection, in the model, is referred to a FC that generate a certain power at a voltage level thorough a mass flow of hydrogen at ambient temperature. The relative humidity of the air, the pressure of air and the stoichiometry ratio of oxygen play also a role in the calculations. Liquid water is injected into the air in order to humidify and also cool the FC.

The water injection flow rate can be estimated through the water mass balance.

$$\dot{m}_{H2Oin:\_the\_air\_inlet} + \dot{m}_{H2Oinjected} + \dot{m}_{H2Ogenerated} = \dot{m}_{H2Oin\_the\_air\_outlet} \quad (4.16)$$

The amount of water in air is:

$$\dot{m}_{H2O\_in\_the\_air\_inlet} = \frac{St_{O2}}{x_{O2}} \cdot \frac{mm_{H2O}}{n \cdot F} \cdot \frac{\phi \cdot p_{sat}}{p_{H2O} - (\phi \cdot p_{sat})} \cdot I \cdot N_{cells} \quad (4.17)$$

where St_{O2} is the stoichiometric ratio of oxygen (equal to 2), x_{O2} is the fraction of oxygen in air (equal to 0,2095), mm_{H2O} is the molecular mass of water (equal to 18,015), ϕ is the relative humidity and p_{sat} is the saturation pressure which is indicated in (4.18) [83].

$$p_{sat} = e^{(-5800{,}22T^{-1})+1{,}3914+(-0{,}0486T)+(0{,}4176T^{2})+(-0{,}1445T^{3})+(6{,}5459\ln(T))} \quad (4.18)$$

The amount of water generated is:

$$\dot{m}_{H2Ogenerated} = \frac{I}{n \cdot F} mm_{H2O} \cdot N_{cells} \quad (4.19)$$

And, the amount of water in the air at cell outlet is:

$$\dot{m}_{H2O\_in\_theair\_outlet} = \frac{(St_{O2} - x_{O2})}{x_{O2}} \cdot \frac{mm_{H2O}}{4 \cdot F} \cdot \frac{p_{sat}}{101325 - p_{sat}} \cdot I \cdot N_{cells} \quad (4.20)$$

in which the value of p_{sat} is expressed in Pa and it is related to outlet air temperature [84].
These equations allow to calculate the water injected (expressed in g/s) through the following diagram block:

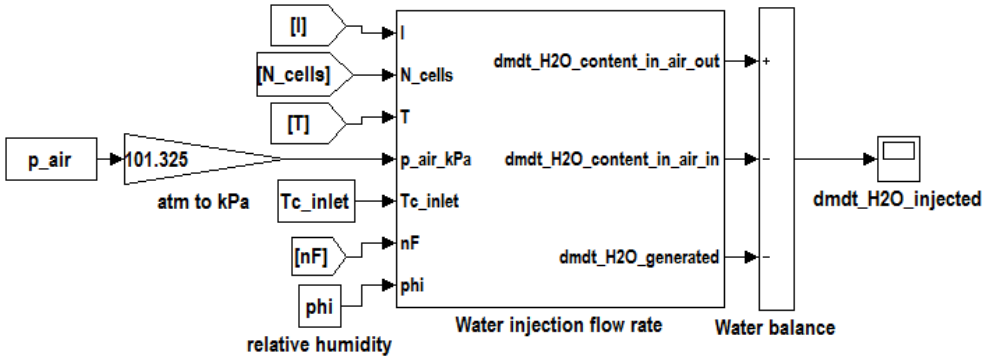

Fig. 4.12: Block diagram in Simulink® model used to calculate water injected

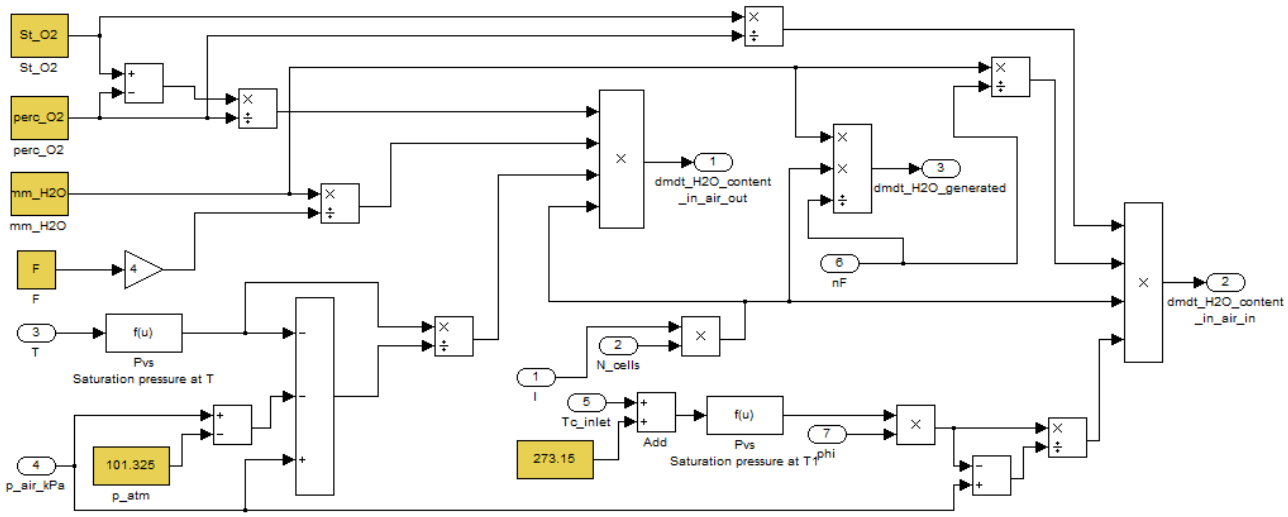

Fig. 4.13: Block diagram detailed in "Water injection flow rate" subsystem

4.2.4 Mass balance

Generally, the fuel cell mass balance requires that the sum of all of the mass inputs is equal to mass outputs, which can be expressed as equation (4.21) [85].

$$\sum(m_i)_{input} = \sum(m_i)_{output} \tag{4.21}$$

An example of mass balance is shown in fig. 4.12.

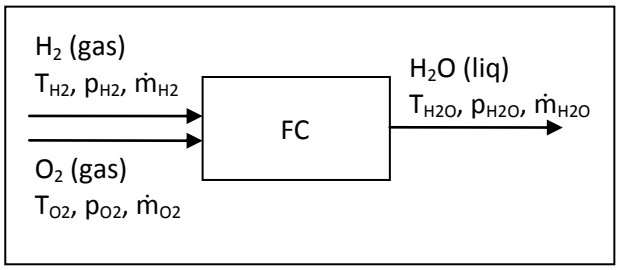

Fig. 4.14: Mass balance scheme for a FC

In order to have a proper working conditions, fuel and oxidants must be supplied continuously and, at the same time, water must be removed. Some calculations regarding mass flows need to be implemented in order to define the right values of these flow rates. As shown in the flow diagram of Fig. 4.14, hydrogen and oxygen enter into the cell at appropriate temperatures, pressures and mass flow rates. Then, they react completely in the cell and the product of the chemical reaction is water.

Generally, a mass balance consist of a balance between the input, assumed positive, the generation, assumed positive, the output, assumed negative and the consumption, assumed negative. The result of the arithmetic sum is equal to the accumulation which could be also equal to zero in certain cases.

These flow calculations are critical for determining the correct flow rates for a FC. The inlet flow rates for a PEMFC are (in which the flow rate are expressed in g/s):

$$\dot{m}_{H2\_inlet} = St_{H2} \cdot \frac{mm_{H2}}{2 \cdot F} \cdot I \cdot N_{cells} \tag{4.22}$$

$$\dot{m}_{O2\_inlet} = St_{O2} \cdot \frac{mm_{O2}}{4 \cdot F} \cdot I \cdot N_{cells} \tag{4.23}$$

$$\dot{m}_{air\_inlet} = \frac{St_{O2}}{x_{O2}} \cdot \frac{mm_{air}}{4 \cdot F} \cdot I \cdot N_{cells} \tag{4.24}$$

The diagram block with mass balance is the following:

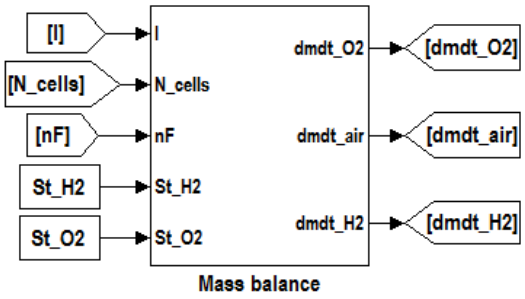

Fig. 4.15: Block diagram in Simulink® model used to calculate flow rates

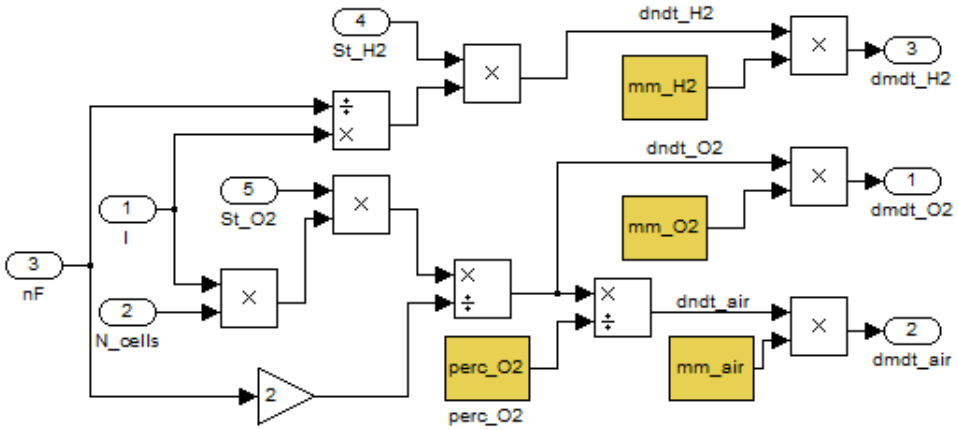

Fig. 4.16: Block diagram detailed in "Mass balance" subsystem

4.2.5 Energy balance

The energy flows into and out of each process in a FC system need to be analyzed in order to define the energy requirements for the process. The energy flows involved in that analysis are:

- composition, pressures and temperatures of reactants;
- work produced;
- heat loss;
- energy content in products of chemical reactions.

An example of energy balance can be summarized in the following scheme:

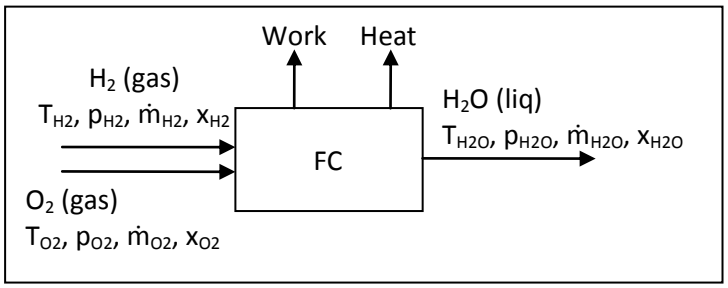

Fig. 4.17: Energy balance scheme for a FC

The overall energy requirements for the process can be evaluated stating from the expected power produced, the utilization of reactants and the heat loss. As indicated in fig. 4.15, the fuel and the oxidant enter into the cell at certain values of temperature and pressures, while after chemical reaction water, heat and electricity leave the cell.
Generally, an energy balance involve that the sum of energy inputs is equal to the sum of energy outputs [86] [87].

$$\sum(h_i)_{input} = \sum(h_i)_{output} + P_{FC} + \dot{Q} \tag{4.25}$$

where h_i are the enthalpies of the fuel, the oxidant and the water vapor, P_{FC} is the electrical energy generated and $\dot{Q}$ is the heat generated. All of these quantities, expressed in J/s, can be calculated with the following equations:

$$h_i = \dot{m}_i \cdot sh_i \cdot T_i \tag{4.26}$$

$$P_{FC} = I \cdot V_{cell} \cdot N_{cells} \tag{4.27}$$

$$\dot{Q} = (1{,}254 - V_{cell}) \cdot I \cdot N_{cells} \quad \text{(if the water leaves the FC as vapor)} \tag{4.28}$$

where sh is the specific heat (J/g·K) and ṁ is the mass flow rate (g/s). The enthalpy of hydrogen is referred to the high heating value (HHV) equal to 141900 J/g.

$$h_{H2} = \dot{m}(sh \cdot T + HHV) \tag{4.29}$$

While the enthalpy of water vapor is obtained with (4.30).

$$h_{H2O\_out} = \dot{m}_{H2O} \cdot sh_{H2O} \cdot T + 2500 \tag{4.30}$$

Finally, the energy balance is implemented in a Simulink® block diagram, as shown in fig. 4.23 and fig. 4.24, using the equation (4.31).

$$h_{H2} + h_{H2O\_in\_the\_air\_inlet} + h_{air\_inlet} - h_{H2O\_in\_the\_air\_outlet} - P_{FC} - \dot{Q} - h_{air\_outlet} = 0 \tag{4.31}$$

The efficiency of a PEMFC is calculated as the ratio between the electrical power and the maximum power obtainable from hydrogen. Although the use of HHV or LHV in efficiency calculation is a controversial point, as explained in *Detlef Stolten: "Hydrogen and Fuel Cells: Fundamentals, Technologies and Applications", Paragraph 10.4.3 (Recommendations) (2010) pp. 216-217,* in this thesis the efficiency is referred to HHV.

$$\eta_{HHV} = \frac{P_{FC}}{h_{H2,HHV}} \tag{4.32}$$

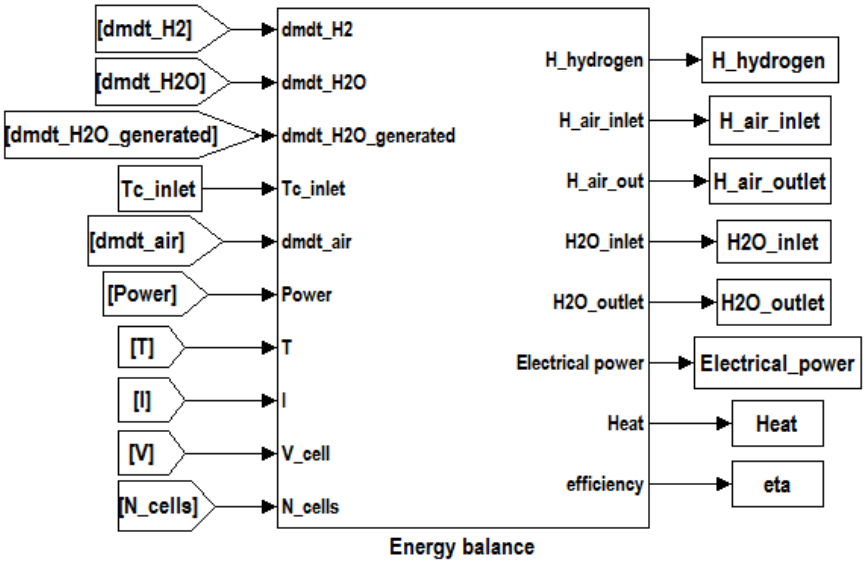

Fig. 4.18: Block diagram in Simulink® model used for energy balance

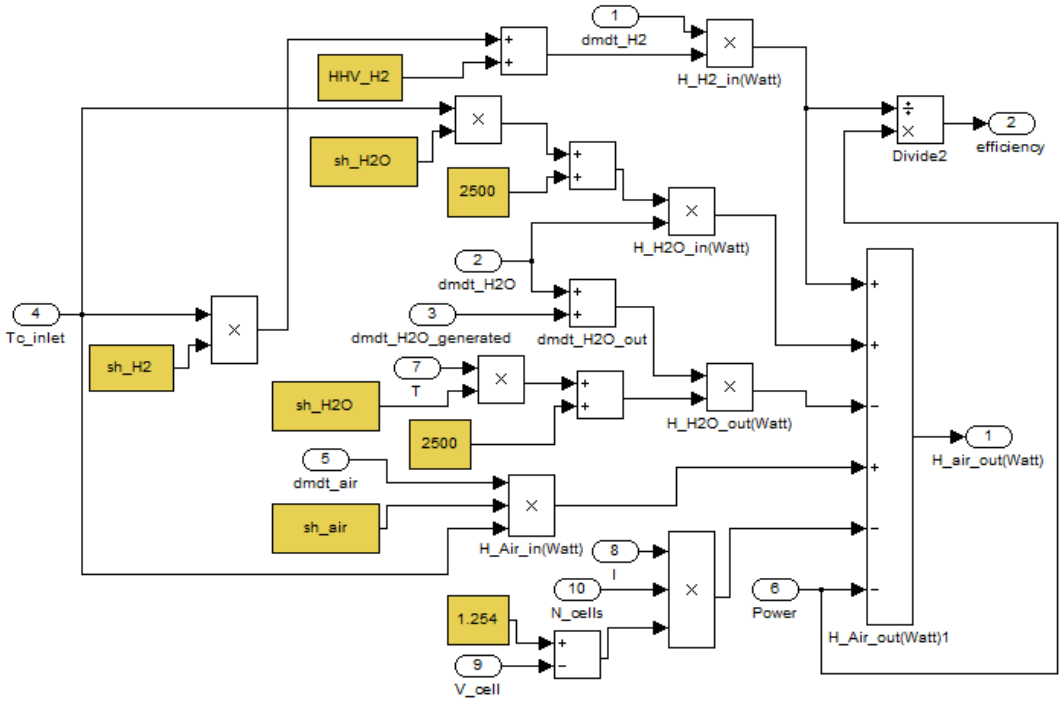

Fig. 4.19: Block diagram detailed in "Energy balance" subsystem

4.2.6 Validation

Veracity of the developed models is validated by previous studies and design data provided by the Fuel Cell manufacturers. Thus, the results of simulation have been verified by comparing them with datasheet provided by the main manufacturers of PEMFC.

In the present study the performances, in terms of voltage and power, and the efficiency of a PEMFC stack has been quantified and assessed using a mathematical model built up in Matlab/Simulink® environment.

The effect of inlet pressure of hydrogen and temperature has been analyzed. Their influence on the polarization curve have been quantified for a single cell. This influence has also an impact on the power curve and on the efficiency of the stack. Particularly, the mass and energy balance showed as reactants and products of chemical reaction are directly proportional. So their ratio is constant at each value of current density. In the other hand, the obtained results showed as electrical power and heat are inversely proportional. Moreover, the impact of energy flows trends on the theoretical efficiency of the PEMFC stack has been examined.

The results of simulation have been verified by comparing them with datasheets provided by Horizon Fuel Cell Technologies which is one of main manufacturers of PEMFC. The

comparison is given in Fig. 6.9 and it contain the match between modeling and real cases of polarization and power curves.

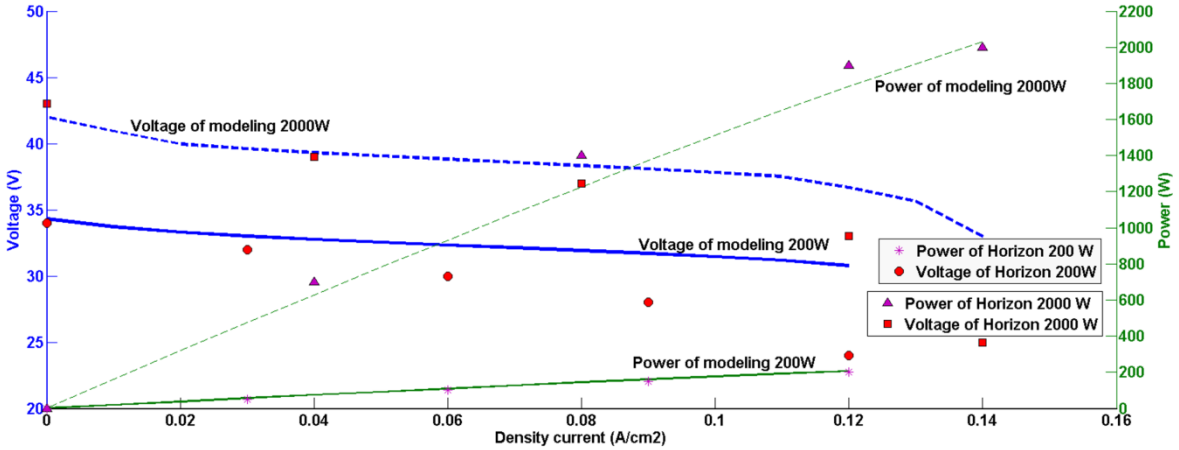

Fig. 4.20: Model graphical validation

The model graphical validation is based on the comparison between results and technical specifications of two different FCs: Horizon H-Series 200 W and Horizon H-Series 2000W. The selected sizes for FCs allow to verify how the model is accurate in its result with two different orders of magnitude. Since the curves provided by Horizon are expressed as function of current, they are changed into a function of current density by dividing the current values by the cell area. So, the FC of 200 W, which is made of 40 cells each of 75 cm^2, reach its maximum power at 9 A that means a current density of around 0.12 A/cm^2. While the FC of 2000W is constitute of 48 cells each of 500 cm^2 and reach the maximum power at 70 A, that means a current density of 0.14 A/cm^2. The model results of FC of 200 W are indicated with continuous lines, while the model results of FC of 200 W are indicated with hatch lines. The values provided by Horizon for commercial FCS are indicated by using marks. In the case of power evaluation the marks have a good correlation with the lines. In the case of polarization curves the marks seem to have a lower profile, but acceptable for difference.

5. Modeling of fuel Cell Hybrid Electric Vehicles

5.1 Modeling methods for HEVs

5.1.1 Creating mathematical models

Compared to conventional vehicles there are more electrical components in FCHEVs, such as electric machines, power electronics, controllers, advanced energy storage devices and energy converters. The dynamic interactions among these components make it difficult to design newly designed FCHEVs because each of the design parameters must be carefully chosen for better fuel economy, enhanced safety, exceptional drivability and a competitive dynamic performance. Since prototyping and testing each design combination is cumbersome, expensive and time consuming, numerical modeling and simulation are indispensable for concept evaluation, prototyping and analysis of FCHEVs [88] [89].

Numerical models should be used to perform vehicle system simulations. They are classified as steady state, quasi-steady or dynamic according to the level of detail of how each component is modeled. On the other hand, models can be classified as “forward-looking” models or “backward-facing” models according to the direction of calculation. Models that start with the tractive effort required at the wheels and work backward towards the engine are called “backward-facing” models. Models that start from the engine and work in transmitted and reflected torque are called “forward-looking” models [90-92].

In this Research an enhanced analysis of three typologies of two-wheeled vehicles equipped with hybrid electric powertrains, FCs and batteries is carried out through a quasi-steady simulation model conducted with a step of 1 second in theoretical and experimental driving cycles. The model has a “backward-facing” direction and a speed profile is used as input data in the model in order to calculate the required power for traction. This type of simulation allows the power flows of the system to be defined in a fast way and with a excellent

accuracy. The "backward-facing" simulation is the preliminary step in the design process of hybrid electric powertrain and is usually carried out in order to define the size of the energy source. In fact, FCHEVs are characterized by a hybrid architecture with two different sources of energy: a primary converter which converts hydrogen into electricity with a unidirectional flow of energy and a Rechargeable Energy Storage System (RESS) which allow energy to be recovered and help the primary converter to reach the peak during motion. The primary converter consists of a PEMFC stack, while the RESS consists of a Lithium-ion battery. These components are dimensioned through the simulation model where the most important operating parameters, such as SOC and hydrogen consumption, are calculated. The key issues of this Research are to calculate the operating parameter of the vehicles during various driving cycles and to set the size of the energy sources and the electric motor. Moreover, the specific consumption, the ratio of energy generated by FC and recovered by RESS, the voltage and current profiles of all electrical components are calculated as result of simulations.

Although it could be useful to insert the data obtained from the PEMFC model into the FCHEV model, in this thesis the input data for FC specifications are taken from User Manual of FC manufacturers. In this way the behavior of FCHEVs is investigated as well as commercial FCs are used for power generation on board of vehicles.

5.2 Matlab/Simulink® model for FCHEVs

5.2.1 Simulink® model

Since FC systems are complex and expensive and dynamic interactions among the electrical components make it difficult to analyze a newly designed hybrid system, accurate models must be created to overcome difficulties of design and building new prototypes.

A flowchart of the simulation consist of the steps indicated in fig. 5.1, which define how the input and the output data are connected each other. In this flowchart the simulation start with the acquisition of the driving cycles. Some important parameters, such as the slope of the road which could be a constant or function, need to be defined in this step. Then, accordingly to the nature of the driving cycle a duration of the simulation and the time during each calculation will be defined. The signal of power, which represent the output signal of the Electric Drive is used as input signal by the Power Management Unit (PMU). The combination of the signal of power requested and the State of Charge (SOC) of battery allow to implement the calculation throughout the Fuel Cell and the battery. Finally, an energy balance will be done.

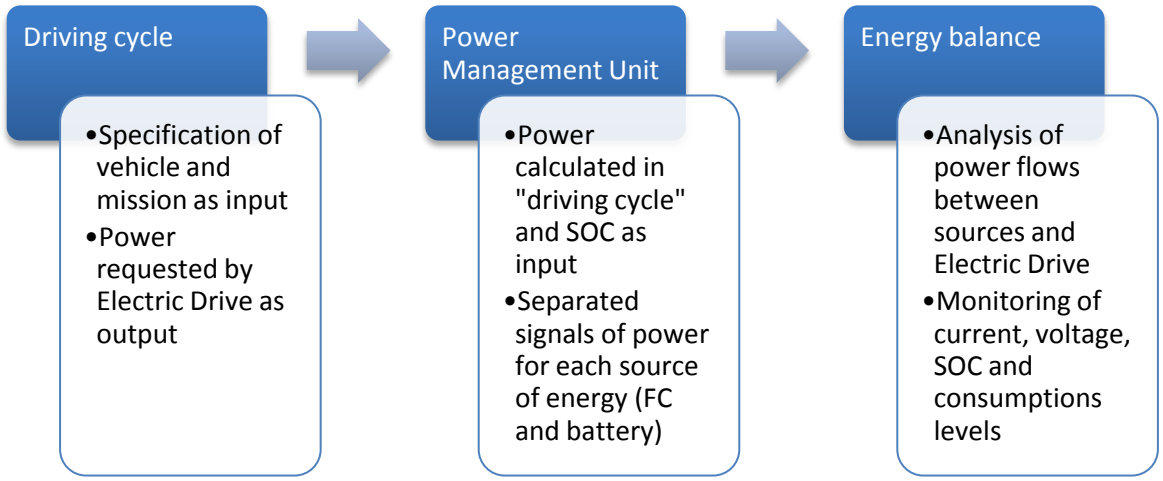

Fig. 5.1: Flowchart of simulation process

In this Research, a Simulink® model is used to investigate the energy flows of the FCHEV. The whole model diagram, presented in Fig. 5.1, consists of several connected blocks. Each block contains physical equations that regulate the behavior of components and sub-systems. The input signal is the time in the "driving cycle" block. Then, all the quantities are calculated as a function of time. In the Matlab/Simulink® workspace additional characteristics and options are loaded, such as efficiencies and specifications of the vehicles, PEMFC and RESS. Some iterations are included in order to verify the correct behavior of the simulator. The power requested by ED is gained through the "Electrical machine with regenerative braking", "Inverter" and "Efficiency and auxiliaries" blocks. Then, its value is used in the "PMU" block as input signal. The "Fuel cell" and "Battery" are regulated by the "PMU". Lastly, the "Energy balance" is done [76].

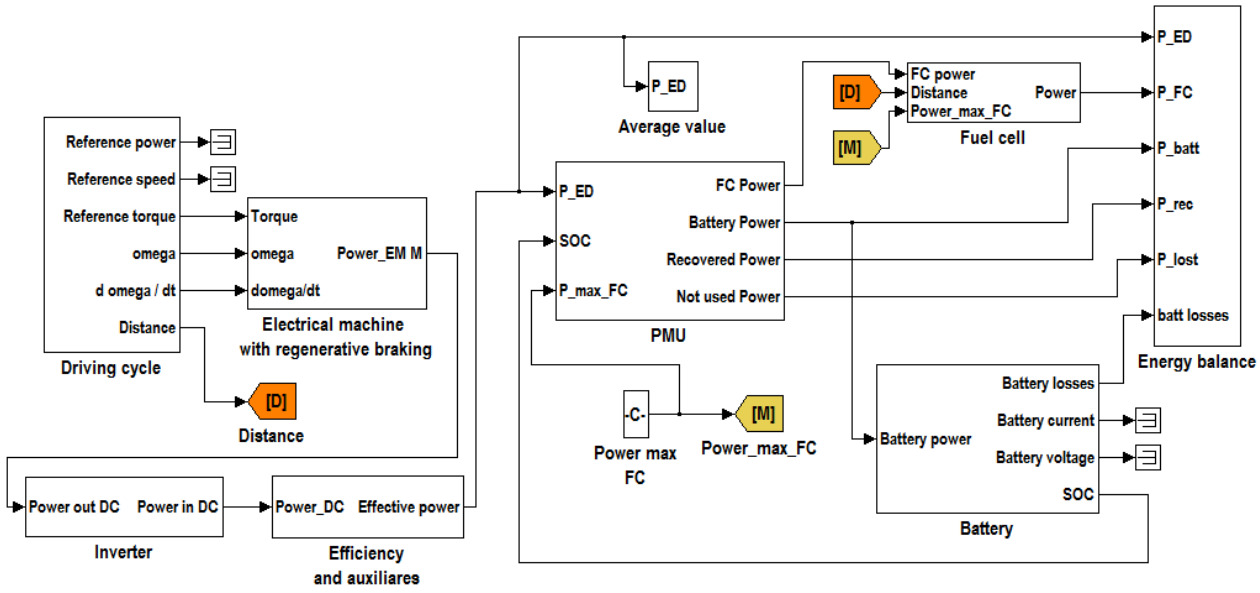

Fig. 5.2: Simulink® model block diagram

The simulations are carried out several times in order to analyze the behavior of the powertrain under different conditions. Some of these simulations are repeated with changed values of input parameters is necessary, as indicated in the following flowchart:

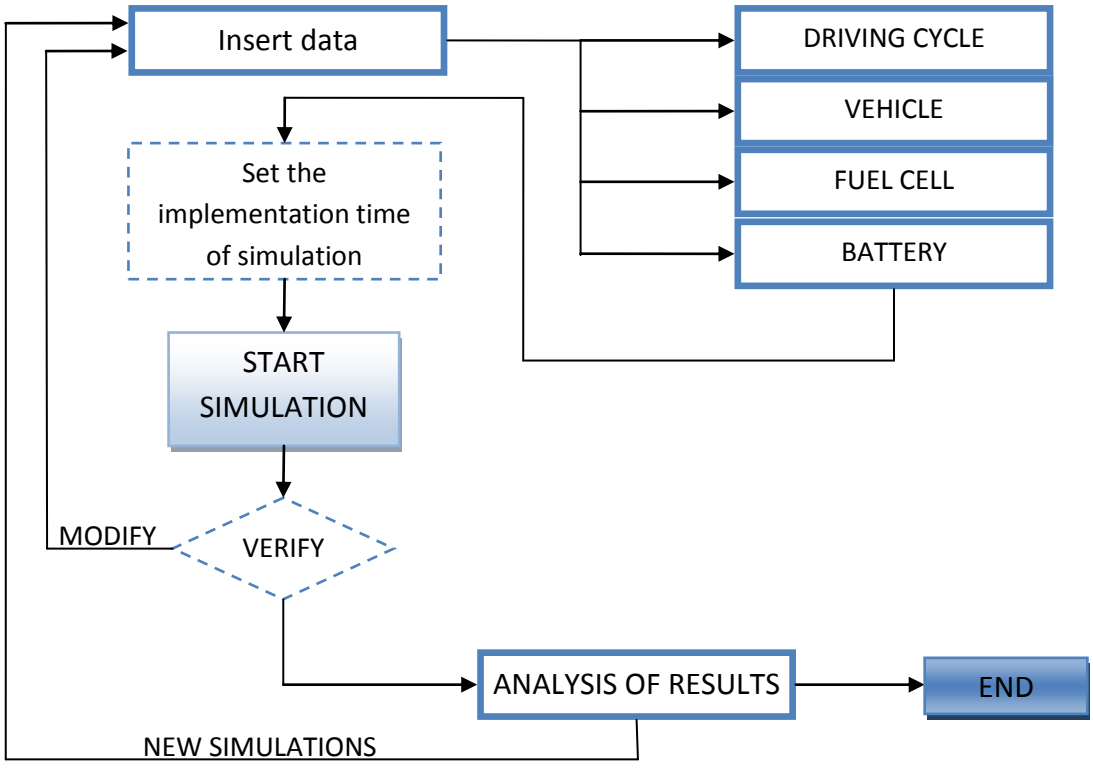

Fig. 5.3: Flowchart of simulation operations

The display of the software, show in Fig. 5.5, contain the workspace with all parameters considered in the simulations. This workspace is, usually, allocated on the right side of the screen, while all files created in the same folder are listed on the left side in a command window. From this command window is possible to open the model block which will be displayed in another page as shown in Fig. 5.2.

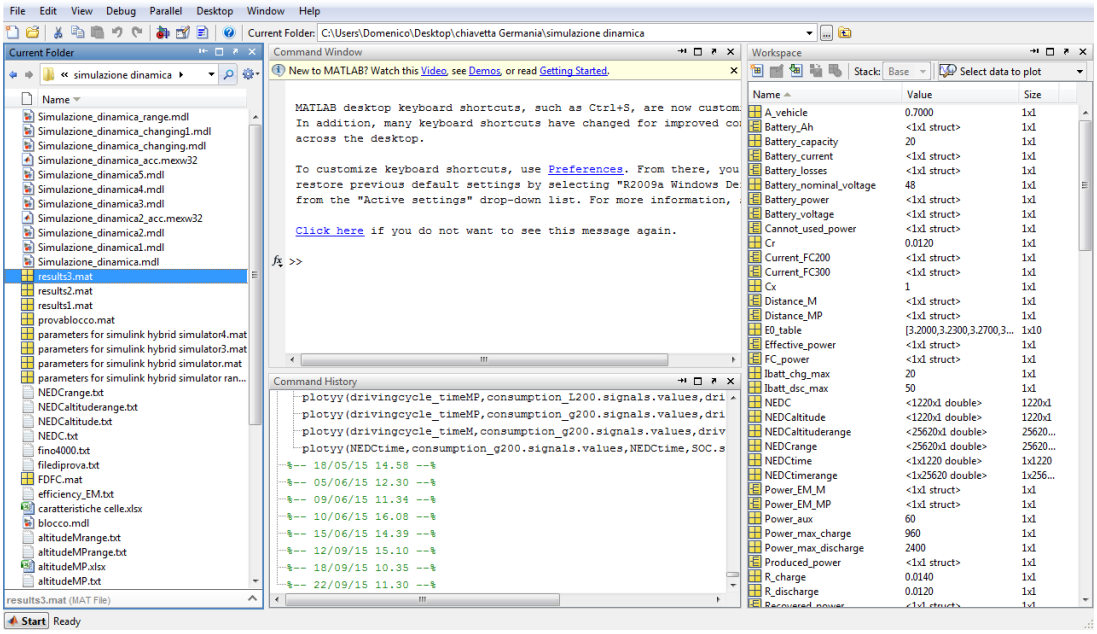

Fig. 5.4: Matlab/Simulink® workspace

5.2.2 Driving cycles

This paragraph approaches the problem of the simulation of the real driving condition for a wide range of vehicles.

A driving cycle is a series of data points representing the speed of a vehicle versus time. They are produced by different countries and organizations to assess the performance of vehicles in various ways, as for example fuel consumption and polluting emissions. An important use for driving cycles is in vehicle simulations in order to predict the performance of internal combustion engines, transmissions, electric drive systems, batteries, fuel cell systems, and similar components [93].

Some driving cycles are derived theoretically, as is preferred in the European Union, whereas others are direct measurements of a driving pattern deemed representative. There are three type of driving cycles: realistic, pseudo-steady-state and stylized [94]:

- realistic driving cycle which has a transient profile according to the type of trip which could be urban, suburban, rural and motorway; a
- stylized driving cycle which has a theoretic profile.
- pseudo-steady-state which has protracted period at constant speed;

Three examples, shown in Fig. 5.5. a, b and c, represent three different type of driving cycles:

- NEDC (New European Driving Cycle) which is a styled cycle;
- TRAMAQ UG214 which is a realistic cycle (for calming traffic);
- EMPA T115 which is pseudo-state.

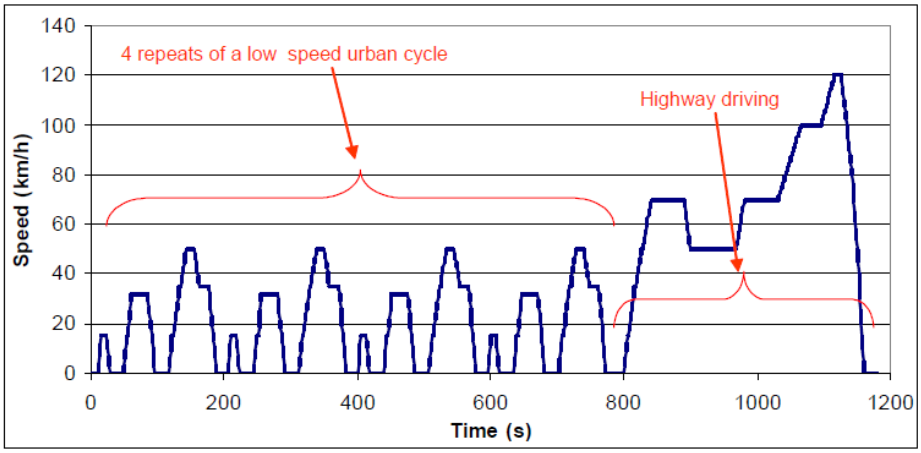

Fig: 5.5.a: NEDC (example of stylized cycle)

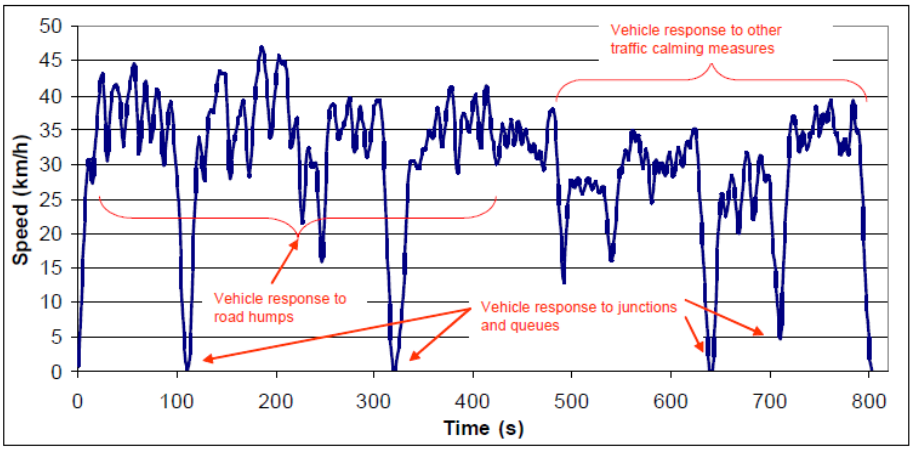

Fig: 5.5.b: TRAMAQ UG214 (example of realistic cycle)

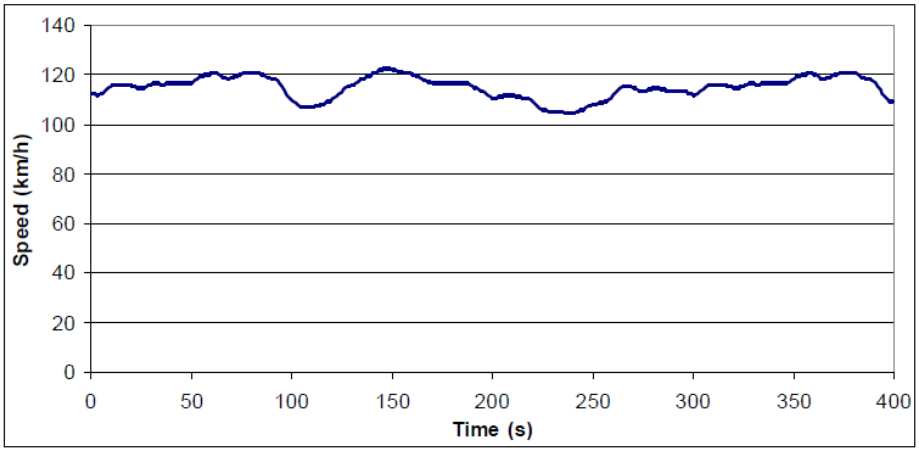

Fig: 5.5.c: EMPA T115 (example of pseudo-steady-state cycle)

Each driving cycle is characterized by a kinematics parameters such as distance, time, speed, acceleration, number of stops and related (positive speed, square speed, cubic speed).
The driving cycles are divided into a group. The most important of them are:

- EU legislative cycles
- US cycles
- Japanese legislative cycles
- Warren Spring Laboratory (WSL) cycles
- TRAMAQ UG214
- Millbrook
- OSCAR (from 5th framework project)
- ARTEMIS (from 5th framework project)
- EMPA
- Handbook
- MODEM
- INRETS (data logger around Lyon)
- MODEM-Hyzem (for hybrid vehicles)
- TRL
- FHB (for motorcycles)

A comprehensive description of these driving cycle and their use for motorcycles, cars, small, medium and large vans, buses in urban, sub-urban, motorways and mixed contexts can be find

in *T. J. Barlow, S. Latham, I. S. McCrae, B. C. Boulter: "A reference book of driving cycles for use in the measurement of road vehicle emission", TRL Project Report PPR 354, 2009.*

An experimental driving cycle is a specific collection of speed data which are directly measured on road. These measurements can be taken over different type of vehicles with a instrumentation and they can include measurements of slope and distance through a GPS technology.

During this Research, some measurements was taken in Esslingen (Germany) with the collaboration of researcher and student of Hochschule Esslingen. These measurements was taken with a Grace One bike, shown in Fig 5.6, equipped with a data logger.

Fig. 5.6: Grace One Bike

The Grace One is a bike equipped with an electrical motor. The electrical motor is directly controlled by the cyclist through an accelerator knob. The electrical motor is powered by a Lithium-Ion battery. A data logger, shown in fig. 5.7, is mounted on the bike in order to the take measurements.

Fig. 5.7: Data logger

The measurements regards speed of vehicle (km/h), voltage (V) and current (A) of battery pack, energy content (Wh) of the battery and total distance (km). Obviously the units of measure can be changed in the numerical model according to their appropriate use in the equations. An example of data in a small part of the measurements are shown in fig. 5.7.

Ah	V	A	S	D
6.4879	45.08	29.21	32.55	8.0047
6.4895	45.08	29.21	32.68	8.0065
6.4911	45.10	27.74	32.75	8.0084
6.4926	45.10	27.74	32.66	8.0102
6.4941	45.10	27.74	32.74	8.0120
6.4957	45.10	27.74	32.36	8.0138
6.4961	45.55	6.87	32.31	8.0156
6.4964	45.55	6.87	32.31	8.0174
6.4968	45.55	6.87	32.51	8.0192
6.4972	45.55	6.87	32.20	8.0210
6.4986	45.15	25.38	32.42	8.0228
6.5000	45.15	25.38	32.36	8.0246
6.5014	45.15	25.38	32.07	8.0264
6.5028	45.15	25.38	32.48	8.0282
6.5034	45.46	11.04	31.99	8.0299
6.5041	45.46	11.04	31.99	8.0317
6.5047	45.46	11.04	31.68	8.0335
6.5053	45.46	11.04	31.48	8.0352
6.5054	45.66	1.40	31.25	8.0370

Fig. 5.8: Example of measurements of data logger

A data logger of GPS is also used in order to have the GPS position of the vehicle, the variation of altitude and a second measurement of the distance. The variation of altitude allow to calculate the slope of the road as function of the time or to have an altitude profile. An example of GPS measurements is shown in fig. 5.9.

```
$PSRFTXT,Version:  GSW3.5.0_3.5.00.00-SDK-3EP2.01A *07
$PSRFTXT,TOW:  146688*10
$PSRFTXT,WK:  1715*67
$PSRFTXT,POS:  4159033 681921 4771605*1F
$PSRFTXT,CLK:  96751*21
$PSRFTXT,CHNL: 12*73
$PSRFTXT,Baud rate: 9600*66
$GPGGA,094213.352,,,,,0,00,,,M,0.0,M,,0000*5F
$GPGLL,,,,,094213.352,V,N*73
$GPGSA,A,1,,,,,,,,,,,,,,*1E
$GPGSV,1,1,00*79
$GPRMC,094213.352,V,,,,,,,201112,,,N*45
$GPVTG,,T,,M,,N,,K,N*2C
$GPGGA,094214.296,,,,,0,00,,,M,0.0,M,,0000*51
$GPGLL,,,,,094214.296,V,N*7D
$GPGSA,A,1,,,,,,,,,,,,,,*1E
$GPGSV,1,1,00*79
$GPRMC,094214.296,V,,,,,,,201112,,,N*4B
$GPVTG,,T,,M,,N,,K,N*2C
$GPGGA,094215.284,,,,,0,00,,,M,0.0,M,,0000*53
$GPGLL,,,,,094215.284,V,N*7F
$GPGSA,A,1,,,,,,,,,,,,,,*1E
$GPGSV,3,1,12,19,90,180,34,03,62,036,,07,44,318,,06,42,043,*7F
$GPGSV,3,2,12,13,40,245,,16,37,061,,11,31,179,,23,24,206,*74
$GPGSV,3,3,12,30,14,085,,01,11,178,,08,09,316,,21,-2,031,*65
$GPRMC,094215.284,V,,,,,,,201112,,,N*49
$GPVTG,,T,,M,,N,,K,N*2C
$GPGGA,094216.286,,,,,0,00,,,M,0.0,M,,0000*52
```

Fig. 5.9: Example of measurements of GPS

The computing program of GPS and data logger have the functionality of analysis of data through several type of diagram. Two examples of them are reported in Fig. 5.10 where the measurement are plotted over the time. In the first diagram all parameters of data logger are reported. In the second one the altitude profile is reported.

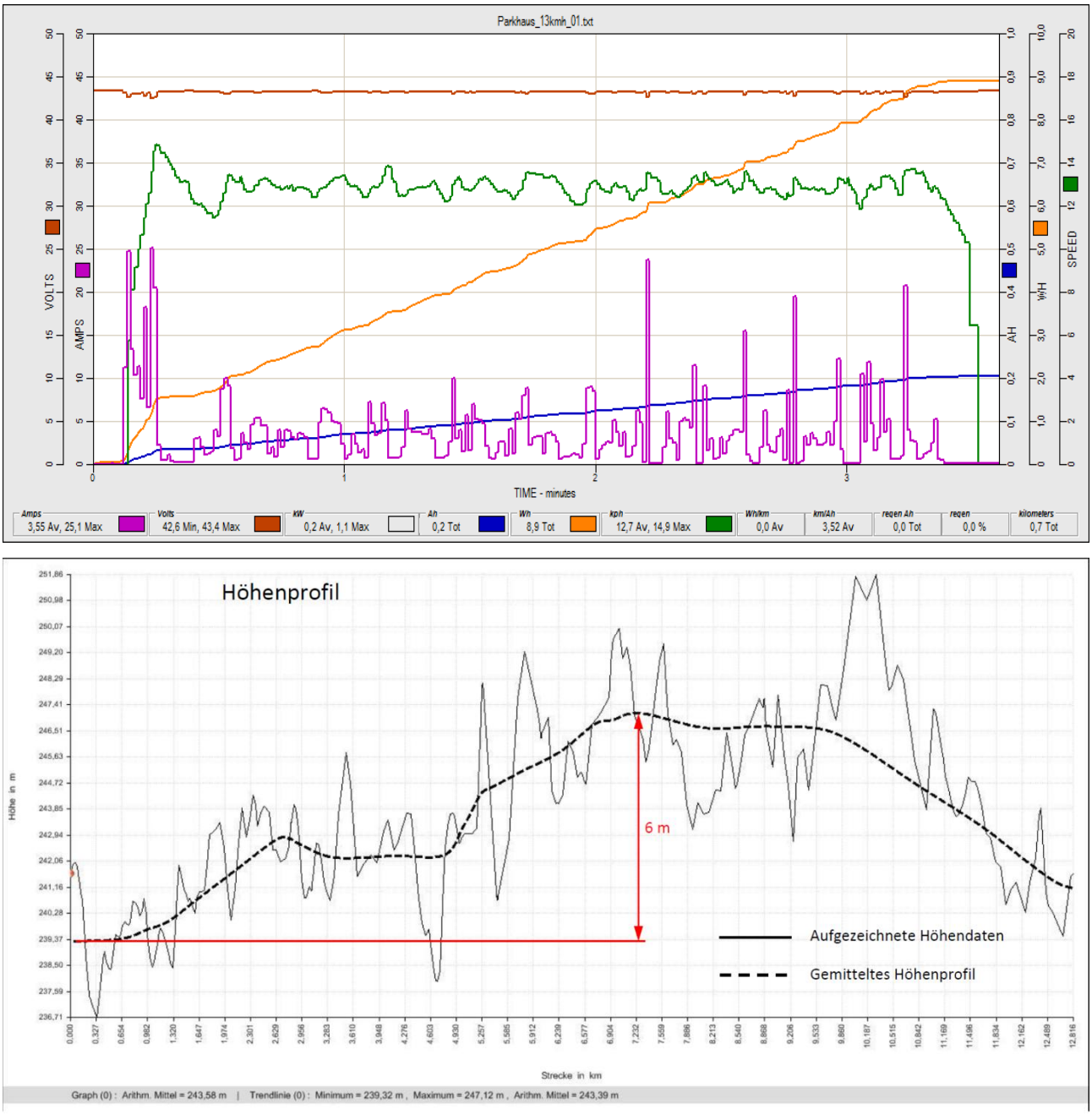

Fig. 5.10: Example of plotting through data logger and GPS software

Different routes were selected in order to have enough data to proceed with a statistical analysis. For instance three different routes were selected in Essingen (Germany) in a urban and sub-urban way. Obviously, the motorway was not taken into consideration due the typology of vehicle. The routes selected are shown in fig. 5.11.(a-b-c).

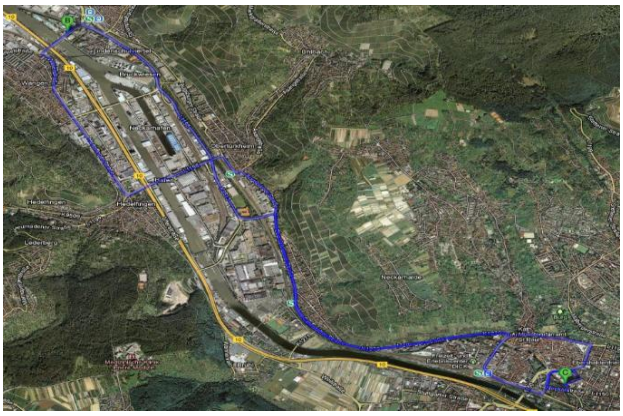

Fig. 5.11.a: Route Hochschule – Untertürkheim

Fig. 5.11.b: Route Hochschule – Festo

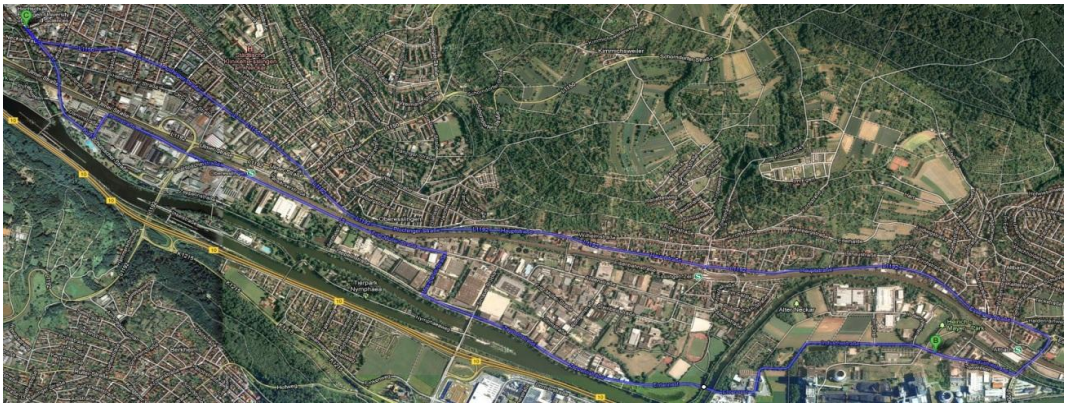

Fig. 5.11.c: Route Hochschule – Altbach

The first block of the Simulink® model, shown in detail in Fig. 5.12, is called the "Driving cycle" and contains the calculations of torque and power requested by the powertrain. A driving cycle is a second-by-second set of speed values that the simulated vehicle is to attain

during the simulation. Drive cycles are used in simulations to predict the performance of a drive system. For instance, a wide range of standard driving cycles are used to test road vehicles for fuel economy optimization and other purposes. Some of them are developed theoretically and others are taken from direct measurements of a representative driving pattern. A driving cycle can include frequent speed changes or extended periods at constant speed.

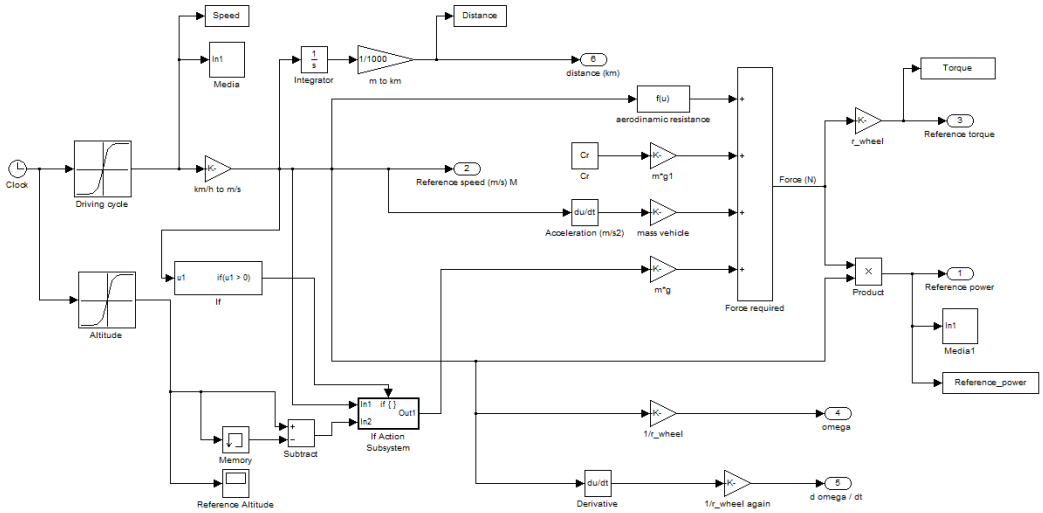

Fig. 5.12: "Driving cycle" block in Simulink® model

Mathematically, the equations which allow to calculate the force needed for traction are indicated as following:

$$F_{AERO} = \frac{1}{2} C_x \cdot A_{vehicle} \cdot \rho \cdot v^2{}_{vehicle} \tag{5.1}$$

$$F_{ROLL} = C_r \cdot m \cdot g \tag{5.2}$$

$$F_{INERTIA} = m \cdot a \tag{5.3}$$

$$F_{GRAV} = m \cdot g \cdot slope \tag{5.4}$$

All of these quantities allow to calculate the power needed for propulsion if multiplied by the vehicle of speed. In these equations C_r is the rolling coefficient, C_x is the drag coefficient, g is the gravitational acceleration, a is the acceleration of vehicle, $A_{vehicle}$ is the frontal surface of vehicle and m is the mass of vehicle.

Summarising, this block follow the numerical procedure receive all contribution shown in Fig. 5.13 as input values or signal available in the workspace of simulation software. This values need to be set accordingly to the choices of the designer.

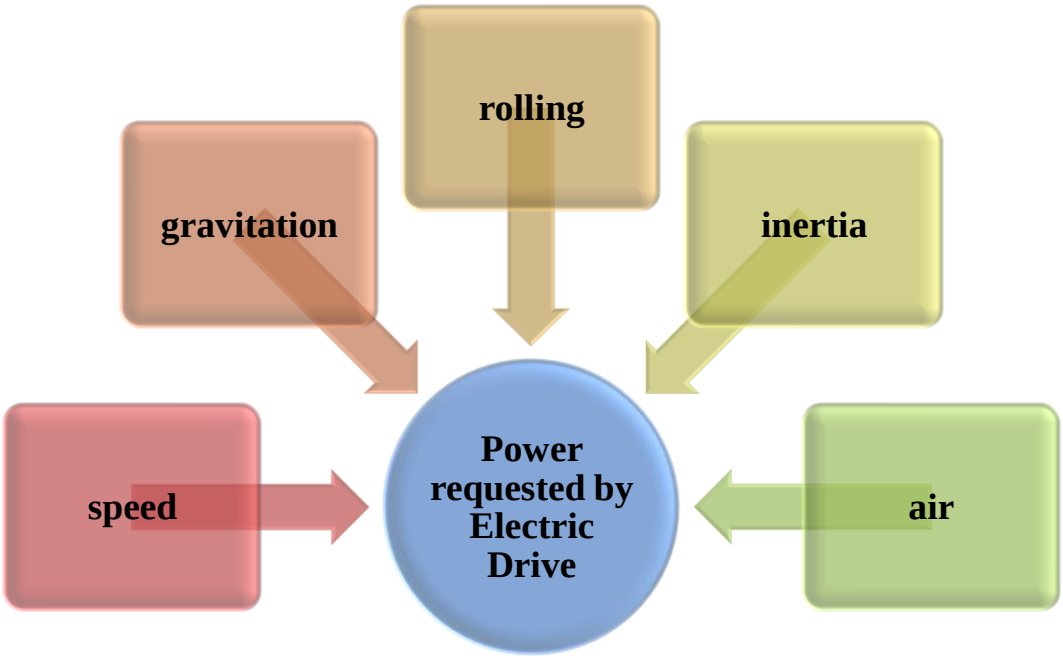

Fig. 5.13: Input contributions for calculations of power requested by Electric Drive

The driving cycle is upload in a "Function Block Parameters" which consist in a set of speed values over the time. In the example below the driving cycle uploaded is ARTEMIS SRL, but several different theoretical and experimental driving cycles are available in the workspace of the model (due previous activities and analysis in this Research).

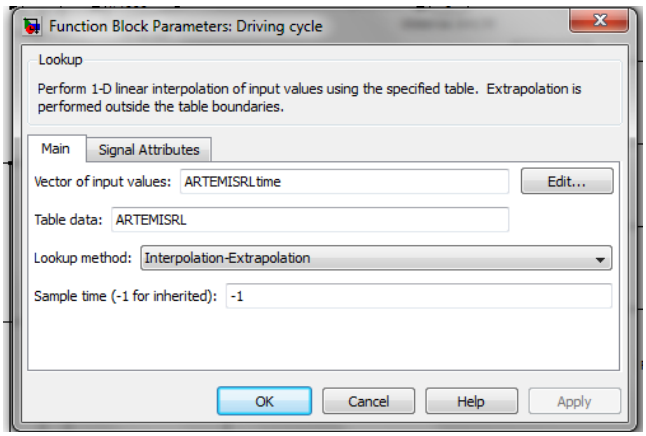

Fig. 5.14: Function Block Parameters of a driving cycle (in this example with ARTEMIS SRL)

The speed values of driving cycles, and the values of altitude which are also uploaded as a function block parameter, are used as input data for the calculation of the requested force needed to overcome the resistances for aerodynamics, rolling, inertia and gravity. This sum of resistances to the traction is the output, in terms of torque and power, of the block. Some other parameters are used in this block, such as the rolling coefficient (C_r), the drag coefficient (C_x), the mass of vehicle (m), the radius of the wheel, etc.

5.2.3 Auxiliaries and efficiencies

The power calculated in the driving cycle need to be increased due the inefficiencies and the presence of auxiliaries. In the model this step is included in three different block: the first one, shown in Fig. 5.15, about the efficiency of the electrical motor (EM); the second one, shown in Fig. 5.16, about the efficiency of inverter/converter; the third one, shown, in Fig. 5.17, about the efficiency of mechanical components and transmission and the amount of power used for auxiliaries. In such way the power requested by the Electric Drive (ED) is calculated and it can be used by Power Management Unit described in the next paragraph.

The electrical motor has a efficiency table which consist in a 2-D function where the efficiency depends on the torque and angular velocity. This table is usually provided by the manufacturers. In any way, the use of the table has a very small influence on the overall efficiency calculation since the value of the table are in a very small range about 0.9÷0,95. For this reason a simplified model can be set using a constant value. In the proposed model, both methodologies can be applied by a manual switch that allow to use the constant value or the lookup table.

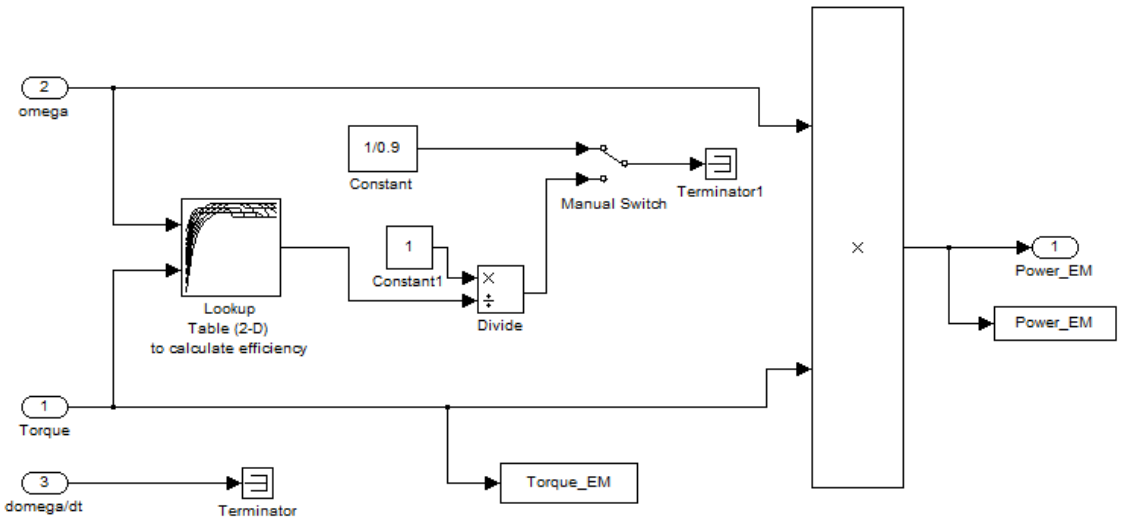

Fig. 5.15: Efficiency of electric motor

The power of the inverter is a constant value which is multiplied or divided to the power depending on the direction of the power flow.

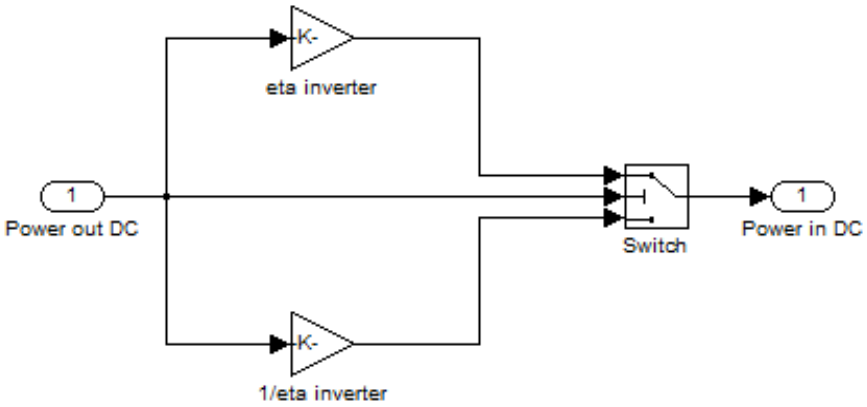

Fig. 5.16: Efficiency of inverter

The mechanical efficiency must be also considered although the adoption of an electrical motor allow to eliminate a gearbox instead of a simplified mechanical transmission between motor and wheels. The auxiliaries are considered as a constant value in this model.

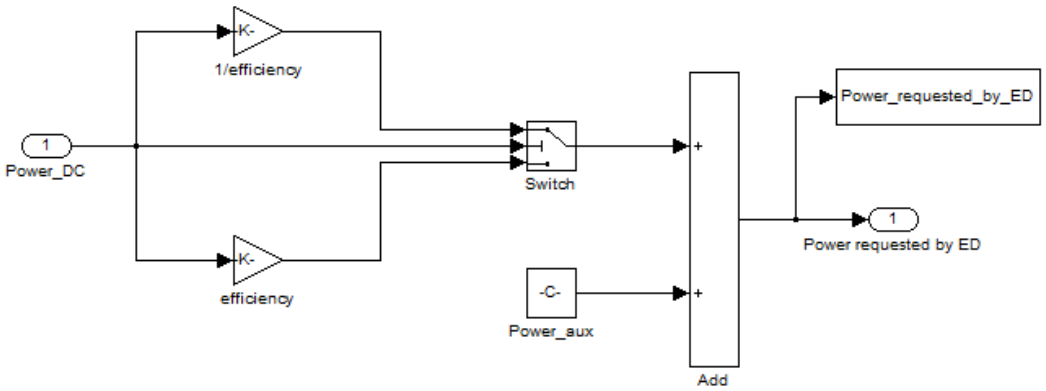

Fig. 5.17: Efficiency of mechanical components and power of auxiliaries

5.2.4 Power Management Unit

The presence of different energy sources in an FCHEV gives the possibility of sharing the power propulsion according to some optimization rules. In the "series" hybrid solution, all power flows are converted into electricity. The power generated in the fuel cell (P_{FC}), the

power stored in the battery (P_{BATT}) and the power requested for traction (P_{ED}) flow into a node as time dependent values.

In Fig. 5.18 the general arrangement of a FCHEV is shown. In this system all traction power is converted to electricity and the sum of energy from two different source is made in terms of electrical quantities. As primary converter is used a FC system which is constitute by a FC stack and all device of Balance of Plant (BoP) such as humidifier, air blower, hydrogen pump heat exchanger and flow valves. Instead of a FC system could be used an Internal combustion engine (ICE) coupled with a three-phase alternator or a gas turbine also coupled with a electricity generator.

The main power fluxes regards the source power (P_{FC}) that is obtained from conversion from fuel, the energy storage system power (P_{RESS}) that represent a secondary source of energy, the power drawn by mechanical and electrical auxiliaries (P_{AUX}) and the power needed for propulsion (P_{ED}) that is requested by the Electric Drive. All these powers are function of the time. Since the power delivered by FC is not directly related to the power requested by the ED, the "Series" hybrid configurations present a certain degree of freedom which allow to dimension the whole system according to some dimensioning rules.

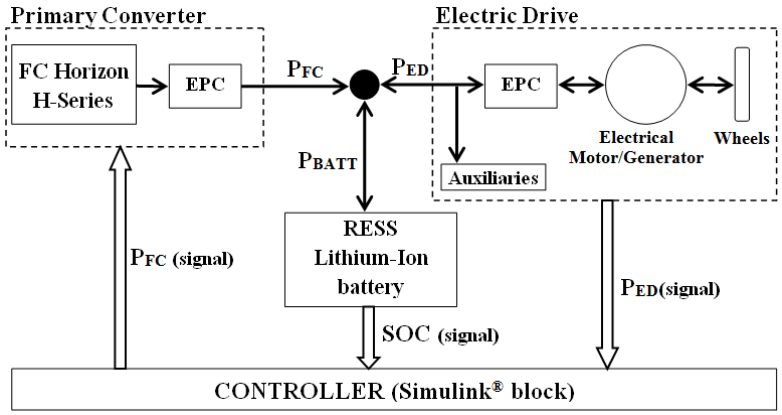

Fig. 5.18: Scheme of FC Hybrid Electric powertrain

These dimensioning rules which allow the definition of the most important operating parameters are as following [95-98]:

- The total power requested from the vehicle is the power requested from the electric drive including the power for auxiliaries (P_{ED}) and is determined by the vehicle parameters, the trip characteristics and the efficiency of all components of the

propulsion system. P_{ED} contains the sum of the power flow requested for propulsion divided by mechanical and electrical efficiency of components plus the power flow requested from auxiliaries (P_{AUX}):

$$P_{ED}(t) = \left[\frac{(F_{AERO} + F_{GRAV} + F_{ROLL} + F_{INERT}) \cdot v_{vehicle}}{\eta_{EM} \cdot \eta_{TRASM}} \cdot \frac{1}{\eta_{INVERTER}} \right] + P_{AUX} \tag{5.5}$$

in the case that P_{ED} is negative with EM in generator mode, the value of produced electricity decreases due to electrical and mechanical efficiencies. It turns out that equation (5.1) become (5.2).

$$P_{ED}(t) = \left[(F_{AERO} + F_{GRAV} + F_{ROLL} + F_{INERT}) \cdot v_{vehicle} \eta_{EM} \eta_{TRASM} \eta_{INVERTER} \right] + P_{AUX} \tag{5.6}$$

- Regarding the RESS, P_{BATT} is calculated as the difference between P_{ED} and P_{FC}.

$$P_{BATT}(t) = P_{ED}(t) - P_{FC}(t); \tag{5.7}$$

The fuel cell produces electricity from hydrogen in a unidirectional way while the power flows between battery and node and electrical machine and node are both bidirectional. For this reason P_{FC} is always positive, while P_{ED} is positive when the electrical machine works as a motor and negative when the electrical machine works as a generator and P_{BATT} is positive during discharging phase and negative during charging phase, shown in fig. 5.8, where all power flows are connected to each other. A Power Management Unit (PMU) regulate the values of power flows entering or leaving each sub-system.
Theoretically, it can be said that the needed power P_{ED} is constituted of an average value and a ripple. The ripple is the difference between the instantaneous power and the average value.

$$P_{ED}(t) = P_{ED\_avg} + r(t), \qquad with \quad avr[r(t)] = 0 \tag{5.8}$$

It is very reasonable to control and dimension the system in a way that the fuel cell provides the average power and the battery provides the ripple (r(t)). It is very important to reduce the

nominal power of the fuel cell in order to reduce the dimension of the system. This can be achieved through an appropriate dimensioning of the fuel cell in consideration of its average power value while in operation, whereby the battery is dimensioned to satisfy the peaks. The energy stored in the battery is used as a control parameter for the control strategy of the fuel cell. This value, called SOC, is maintained below an upper limit (SOC_U), so energy can be recovered during braking, and above a lower limit (SOC_L), to have enough energy to support the propulsion request. The control strategy of the fuel cell is described by equation (5.9).

$$\begin{aligned} &if \quad SOC \geq SOC_U \quad \rightarrow \quad P_{FC} = 0 \\ &if \quad SOC_L \leq SOC \leq SOC_U \quad \rightarrow \quad P_{FC} = P_{ED} \ for \ P_{ED} \geq 0, \quad P_{FC} = 0 \ for \ P_{ED} < 0 \\ &if \quad SOC \leq SOC_L \quad \rightarrow \quad P_{FC} = \max\left[P_{FC}\right] \end{aligned} \tag{5.9}$$

When SOC is below the lower limit, the FC will run at its maximum power to recharge the battery without the need for a plug-in system. Next, when SOC is comprised in the range between the lower and the upper limits the FC run at variable power. The logic of control can optimize the value of the FC power within this range in order to avoid the FC following the typical profiles of driving cycles which are discontinuous, characterized by steep and unscheduled load transients. Lastly, when the SOC is above the upper limit the FC is switched off. The SOC optimal value is in the range SOC_L-SOC_U and it can be determined according to a battery losses minimization criteria or alternatively, as adopted in this thesis, according to typical behavior of vehicle in different driving cycles.

The auxiliary powers are also very important, although they are normally lower than the propulsion power and less variable over time. Their influence depends on the size of the system and the type of vehicle. It will be included as constant in the modeling tools of this Research. In fact, when a new specific powertrain is designed the presence of all mechanical and electrical device which absorb power must be taken into account.

In case of FC-based primary converter, the very high cost of the FC system makes very important to reduce its size. This objective consists in a reduction of the nominal power of the FC stack and can be achieved by making delivered only the average power requested by ED (P_{ED_avg}) and leaving the RESS to delivered the remaining power to reach the peak.

The main purpose of the "Controller", that could be also called Fuel Cell Control Unit (FCCU) or Hybrid Control Unit (HCU), is to determine how to share the propulsion power between the two source available.

The controller is the core of the Simulink® model and allows that the energy management strategy application. As indicated in Fig. 5.18, the input data of this block are SOC and P_{ED}, while the output data are P_{FC}, P_{BATT}, P_{REC} and P_{LOST}. This block contains a logic control in which the power request from ED is used to decide the energy source considering SOC. In fact, the controller defines the operating point of FC and lets the battery provide the remaining power rate. In this way P_{FC} and P_{BATT} are a function of P_{ED} and SOC, according to (5.9). If P_{EFF} is negative, the power flow goes from ED to battery due to recuperative braking. This power flow is called recovered power (P_{REC}). If $P_{REC} \geq P_{CHG(max)}$, the exceeding power ($P_{LOST}$) cannot be recovered, because of the battery charging power limitation. The equations are:

$$P_{REC}(t) = P_{ED}(t) \qquad \text{(only for } P_{ED} \leq 0 \text{ and } P_{REC} \leq P_{CHG(max)}) \qquad (5.10)$$

$$P_{LOST}(t) = P_{REC}(t) - P_{CHG(max)}(t) \qquad \text{(only for } P_{REC} \geq P_{CHG(max)}) \qquad (5.11)$$

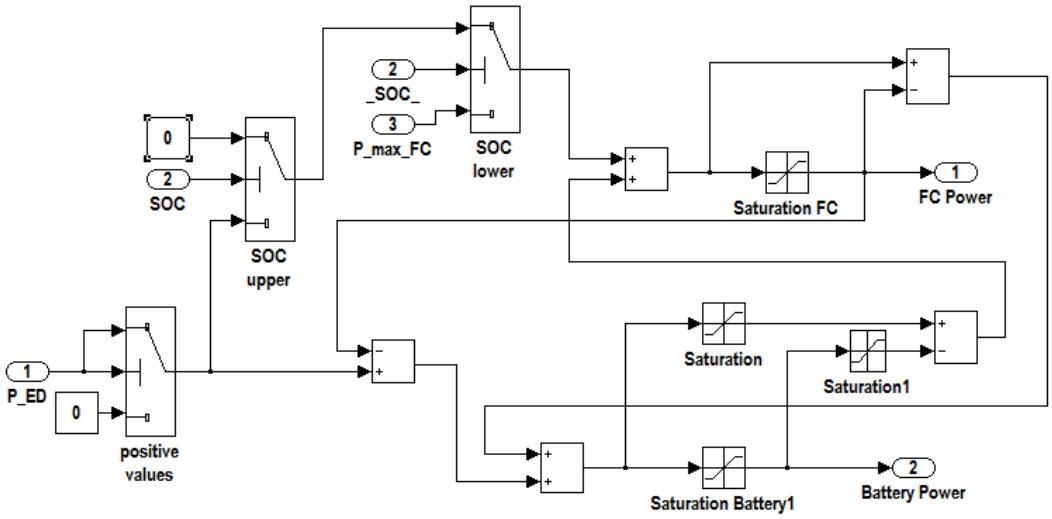

Fig. 5.19: FC and battery logic control in "PMU" block

The PMU block allow the simulation of different logics of control in order to reach a maximum efficiency of the system and to reduce the transient which cause the degradation of membrane. For these reasons the logic proposed above represent only a possible solution which can be analyzed in deep or improved according to specific objective of the research. In

this thesis the logic of control is defined in order to verify how it impact on the overall behavior of the system and the results of this studies are explained in chapter 6. Some conditional instructions are contained in the blocks as well as some limits for parameters. In this logic any change could be done through new conditional instructions or upper or lower limits for operational parameters.

5.2.5 Fuel Cell model

This block, shown in Fig. 5.20, defines the FC stack operating point. The FC characteristics are included as lookup tables provided by the manufacturer. The included tables are: polarization curve (in which voltage is plotted over current), power curve (in which power is plotted over current) and consumption curve (in which consumption is plotted over power or current). The real power of fuel cell is obtained by multiplying voltage with current:

$$P_{FC}(t) = V_{FC}(t) \cdot I_{FC}(t) \tag{5.12}$$

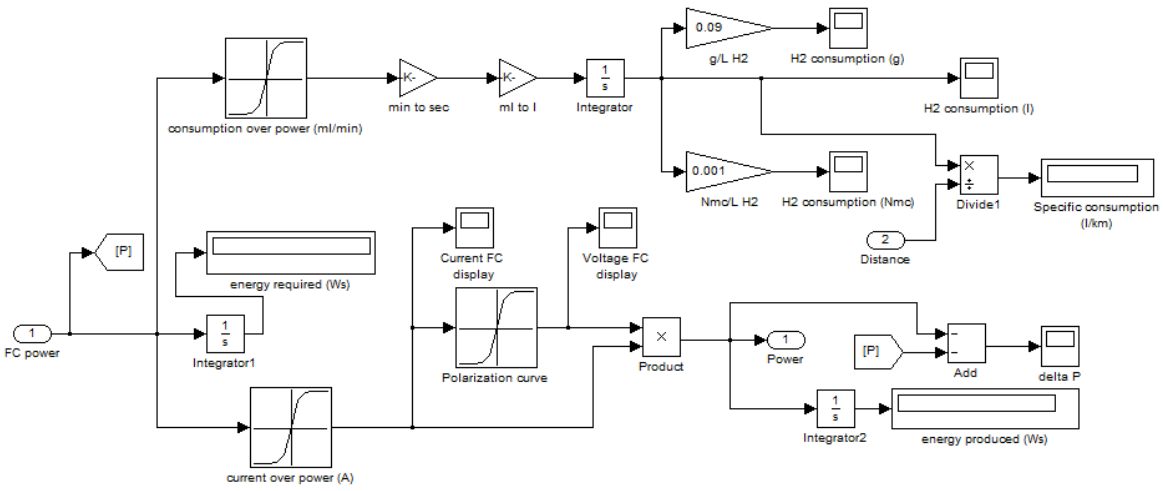

Fig. 5.20: "Fuel cell" block

The fuel cell block is constructed by three "Function Block Parameter" which use the data provided by manufacturer (Horizon fuel Cell Technologies) that consist of the functions of consumption over power, current over power and voltage over current. The last one function is the polarization curve. The input is constituted by the required power from FC stack. This power is obtained by the product of voltage and current. So the "Function Block Parameter"

of current over power allow to define the current level of the FC stack, while the polarization curve allow to calculate the voltage. Also the consumption of hydrogen is calculated. These parameters are defined in a quasi-steady iteration with a step of 1 second. The value of 1 second could be changed, but it seem the most reasonable value to have a good accuracy of the results and a not excessive mole of data.

In the function block parameters the data provided by manufacturer are inserted as indicated in Fig. 5.21 where the example of the polarization curve of a FC of 2000 W is shown.

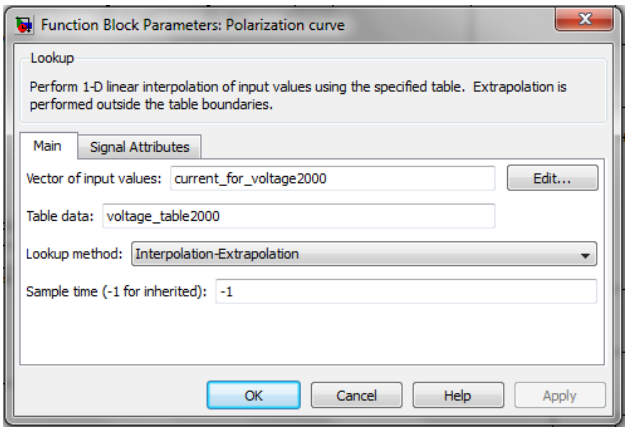

Fig. 5.21: Function block parameters of polarization curve expressed through a function of the voltage over current

Summarizing, the model of FC define the point of functioning of the FC in the polarization curve starting from the power requested by the PMU. In this way the value of requested power allow to define firstly the current and secondly the voltage. As last calculation, the hydrogen flow is calculated by using the consumption curve. This process is described by following flowchart:

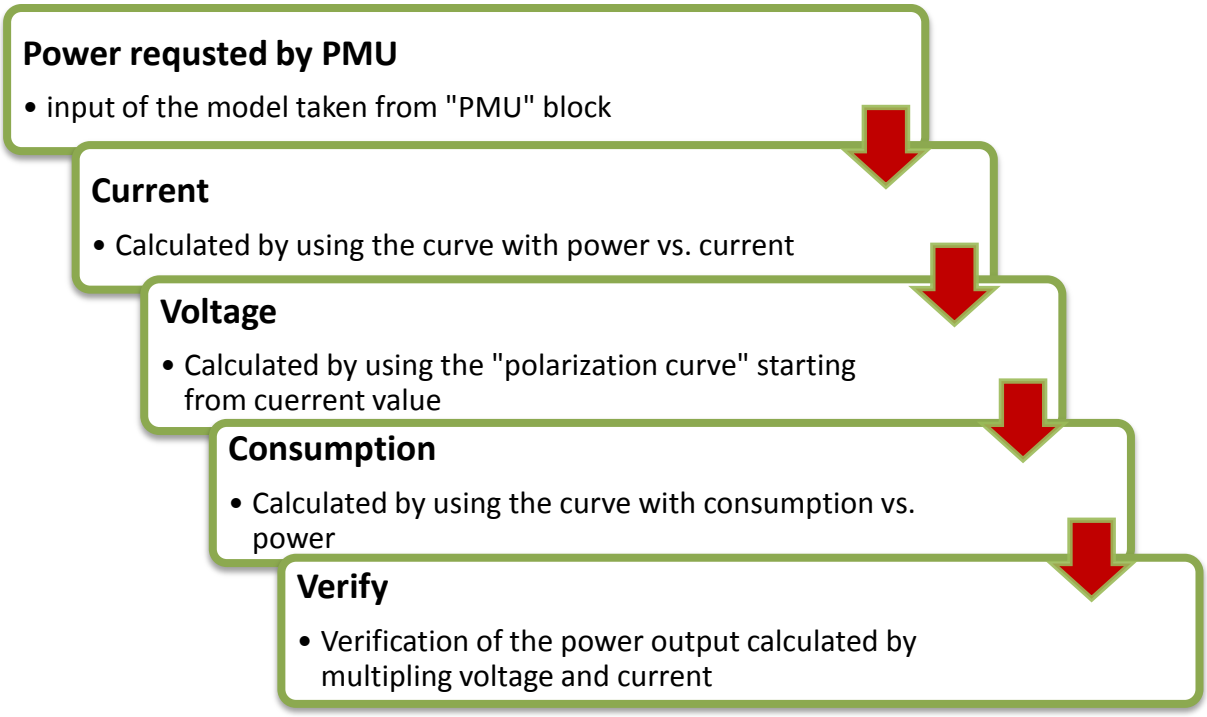

Fig. 5.22: Flowchart of FC model

5.2.6 Battery model

The following electrical scheme allows to represent the behaviour of a lithium-Ion battery is the:

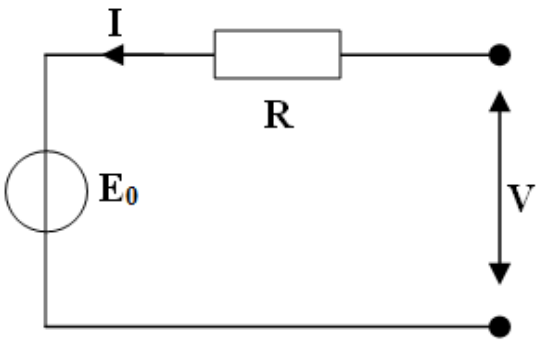

Fig. 5.23: Equivalent circuit of a Lithium-Ion battery

In general, the voltage of a Lithium-Ion battery can be calculated by the equation:

$$V_{BATT} = E_0 - (R \cdot I_{BATT}) \tag{5.13}$$

where E_0 is a function of SOC, which is a very important parameter in FCHEVs because the efficiency of the battery depends on this value. Experimental results have demonstrated that for Lithium-Ion batteries the influence of SOC is very small in comparison with Lead-Acid or Ni-MH batteries. The initial value of the SOC depends on the energy level of the battery which is indicated as capacity. This value increases or decreases as a consequence of a current flow into or from the battery:

$$\Delta SOC = \frac{\int_{t_{n-1}}^{t_n} -\frac{I}{3600}\,dt}{C[Ah]} \tag{5.14}$$

The prefixed minus in the numerator indicates that SOC decrease when battery current is positive during discharge. The time dependent battery current is derived by dividing P_{BATT}, calculated in (5.5), through V_{BATT} calculated in (5.9):

$$I_{BATT}(t) = \frac{P_{BATT}(t)}{V_{BATT}(t)} \tag{5.15}$$

The power flow lost in the battery is:

$$P_{BATT\,(losses)}(t) = R \cdot I^2 \tag{5.16}$$

The equations (5.9), (5.10), (5.11) and (5.12) define the mathematic relations between input parameters (power required, SOC initial, capacity, nominal voltage, internal resistance) and output parameters (SOC, current, voltage, losses) in this block, as shown in fig. 5.23.

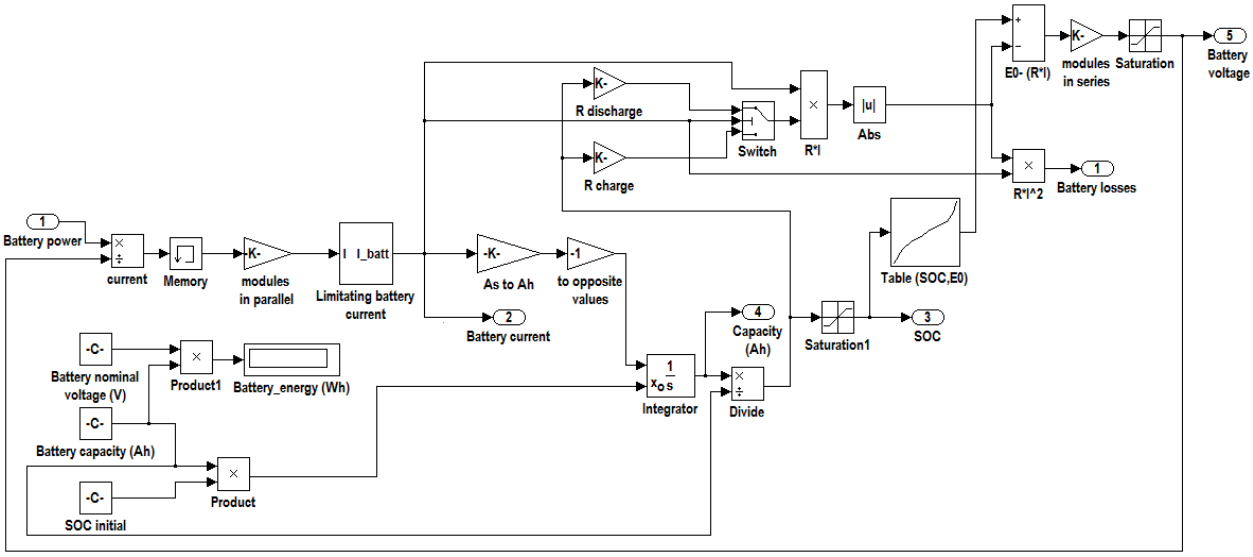

Fig. 5.24: "Battery" block

The battery block define the operating parameters of the battery starting from the initial conditions. The State Of Charge (SOC) is an important parameter which change continuously during operations. In fact, it is defined in the model through an integration. The starting point is defined in terms of initial SOC and power provided or received. An internal resistance is also considered, while the efficiency of the battery is expressed as function of the SOC through the value of E_0.

5.2.7 Energy balance

n this block, the power flows of the FCHEV power train are transformed by integrations to define the values of the total amount of each energy source. The objective is to calculate the amount of generated energy by FC, provided by the battery, lost due to battery limitations and used by ED. All these quantities are expressed in [Wh]. The algebraic sum must be around zero (not exactly because of the nature of simulation), as explained in equation (5.17).

$$\int_0^{t\_end} P_{FC}\,dt + \int_0^{t\_end} P_{BATT}\,dt - \int_0^{t\_end} P_{ED}\,dt = 0 \quad \text{(where } P_{ED} \text{ are taken only if positive)} \qquad (5.17)$$

The energy balance gives an indication about the importance of each component in the system and can be used to choose the best dimension of the whole power train.

Also, in this analysis a verification of the power flows in the electrical node is done. The sum of power flow in the node must be around zero (some oscillation around this value is caused by the nature of simulation):

$$P_{FC}(t)+P_{BATT}(t)-P_{ED}(t)+P_{LOST}(t)=0 \tag{5.18}$$

This balance could be used in order to analyze the percentage of contribution of each source of energy in a hybrid system and in the meantime to verify if the difference between the energy produced and used is equal to the amount of energy stored in the Rechargeable Energy storage system (RESS). Importantly, due the characteristics of the model, the accuracy, the simplification of the electro-chemical phenomena, the result of the algebraic sum is not equal to zero but it will be around zero. This can be considered as a consequence of the approximations.

5.2.8 Considered FC stacks

The Fuel Cells taken into consideration in this Research for simulation in HEVs and for validation of numerical modeling are the HORIZON H-SERIES PEM FC. This family of FC comprises stacks of the following sizes (Watt): 12, 20, 30, 100, 200, 300, 500, 1000, 2000, 3000, 5000.

The manufacturer (Horizon Fuel Cell Technologies) provides the all data sheet with all technical specifications in the manuals, shown in Fig. 5.26, on the website (www.horizonfuelcell.com). The technical specifications are referred to:

- dimensions;
- polarization curve;
- hydrogen consumptions;
- type of reactants;
- points of functioning;
- levels of voltage, power and current;
- instructions for safety, set-up and maintenance.

Fig. 5.25: User manual of a HORIZON FC H-SERIES of 200 W, as indicated in the manufacturer website

Obviously, these stack can be assembled to reach requested levels of power which are not directly reached by a single stack. An example of the technical specifications of the H-SERIES 200 W, as indicated in the manufacturer website, is reported below:

Horizon
Fuel Cell Technologies

4. Technical Specification

Type of fuel cell	PEM
Number of cells	40
Rated Power	200W
Performance	24V @ 8.3A
H2 Supply valve voltage	12V
Purging valve voltage	12V
Blower voltage	12V
Reactants	Hydrogen and Air
External temperature	5 to 30ºC
Max stack temperature	65ºC
H2 Pressure	0.45-0.55bar
Hydrogen purity	≧99.995% dry H2
Humidification	self-humidified
Cooling	Air (integrated cooling fan)
Stack weight (with fan & casing)	2230 grams(±50grams)
Controller weight	400 grams(±30grams)
Dimension	11.8cm x 18.3cm x 9.4cm
Flow rate at max output*	2.6 L/min
Start up time	≦30S at ambient temperature
Efficiency of stack	40% @24V
Low voltage shut down	20V
Over current shut down	12A
Over temperature shut down	65℃
External power supply**	13V (±1V), 5A

Fig. 5.26: Technical specification of a HORIZON FC H-SERIES of 200 W, as indicated in the manufacturer website

The performance characteristics, that consist of three diagram where the voltage is plotted over current, the consumption is plotted over power and power is plotted over current, as indicated in the manufacturer website, are reported below:

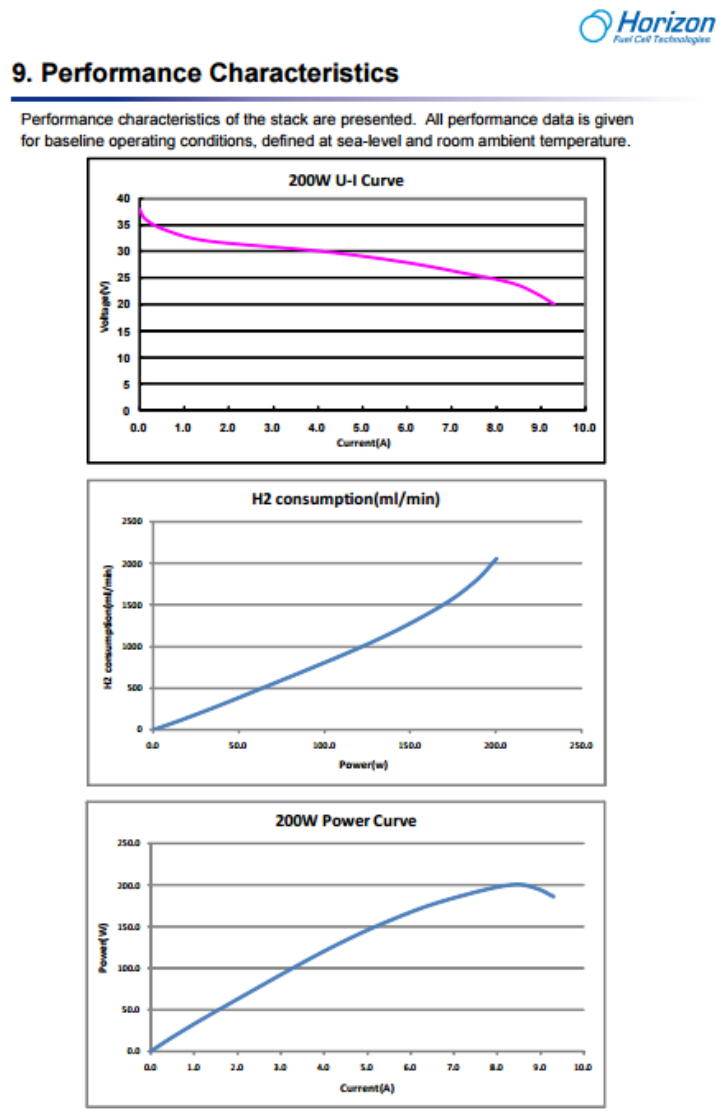

Fig. 5.27: Performance characteristics of a HORIZON FC H-SERIES of 200 W, as indicated in the manufacturer website

This performance are reported in the Matlab/Simulink® model as a library in the workspace. In this way the performance of all H-SERIES FCs are available for simulations. The plotted diagram of the performance characteristics of the FC of 200 W, as a result of the plotting, is shown below:

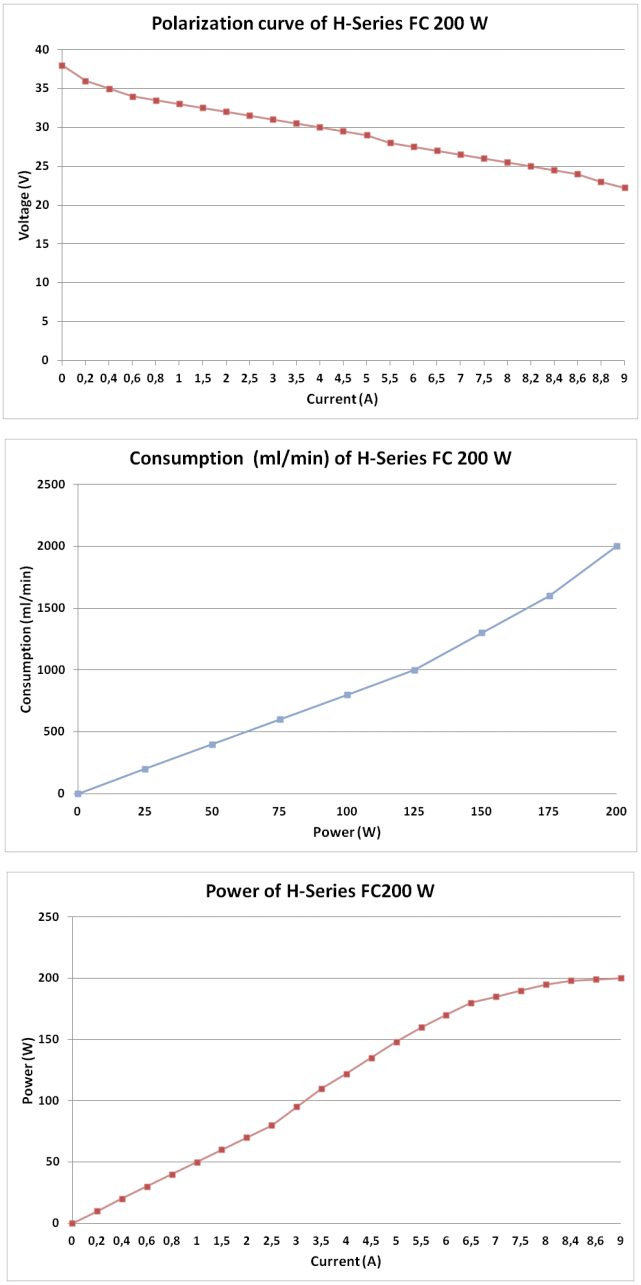

Fig. 5.28: Performance characteristics of a HORIZON FC H-SERIES of 200 W, as obtained by plotting in Matlab/Simulink® model

5.2.9 Validation

The validation was carried out by the comparison of the result with a paper written by Hwang [11], where a fuel cell powered bike was created and tested with a fuel-cell system of 300 W. The system includes FC stack, metal hydride canisters, air pumps, solenoid valves, cooling fans, pressure and temperature sensors and a microcontroller and it is installed on a commercial electric bicycle. Results show that the ratio of travel distance to fuel consumption

of the prototype electric bicycle is about 0.74 g/km which seems reasonable in comparison with the consumptions of FC-E- Grace One.

Moreover, a comparison between the battery voltage profiles of different cases available in scientific literature and the battery voltage profile obtained with the model of this thesis can be done. This comparison show how the voltage follow a similar profile in a rage which is in the range between the maximum value of voltage and 10 % less. Also, the SOC follow the same trend around the SOC_L in a driving cycle with enough time to have a converged value of SOC.

6. Simulation results

6.1 Investigation of power flows in Fuel Cell stacks

6.1.1 Results of simulations for FC stacks

The simulations results give indications about the behavior of PEMFCs through diagrams in which voltage, losses, power, mass flow rates, water for humidification and energy flow rates are plotted over current density or current.

Particularly, the performances have been estimated in three different cases in which the operating temperature and the hydrogen inlet pressure have been varied respectively from 50 °C to 80 °C and from 1 atm to 3 atm. The diagrams are referred to a single cell, but they can be used for a FC stack multiplying the estimated parameters by the numbers of cells. Moreover, the water management analysis has been done under different conditions of relative humidity (0.5, 0.7 and 0.9). Finally, the efficiency of the cell has been studied through the investigation of the energy flow rates into the cell which consist in the mathematical balance of gases enthalpies, heat generated and electricity produced [99].

The model validation has done by the comparison between simulation results and manufactures datasheets.

The simulations has been done in three cases in which cell area, relative humidity, ambient temperature and stoichiometric ratio at the anode and cathode are fixed, while temperature and pressure are variable. This general assumptions are indicated in Table 6-1.

Since a FC stack is made of several cells connected in series, the simulation is referred to one single cell and the results can be used for a stack id multiplied by the number of cells.

Table 6-1. General assumptions

Parameter	CASE A	CASE B	CASE C
A_{cell} (cm^2)	100	100	100
ϕ (relative humidity) (-)	0,5	0,5	0,5
$T_{ambient}$ (°C)	25	25	25
St_{H2} (-) [29]	1.25	1.25	1.25
St_{O2} (-) [29]	2	2	2
N_{cells} (-)	1	1	1
T_c (operating temperature °C)	50	80	80
p_{H2} (atm)	1	1	3

Using the Matlab/Simulink® model explained above, the graphs of Nernst voltage, overvoltages (activation, ohmic and concentration), cell voltage and power over current density are obtained.

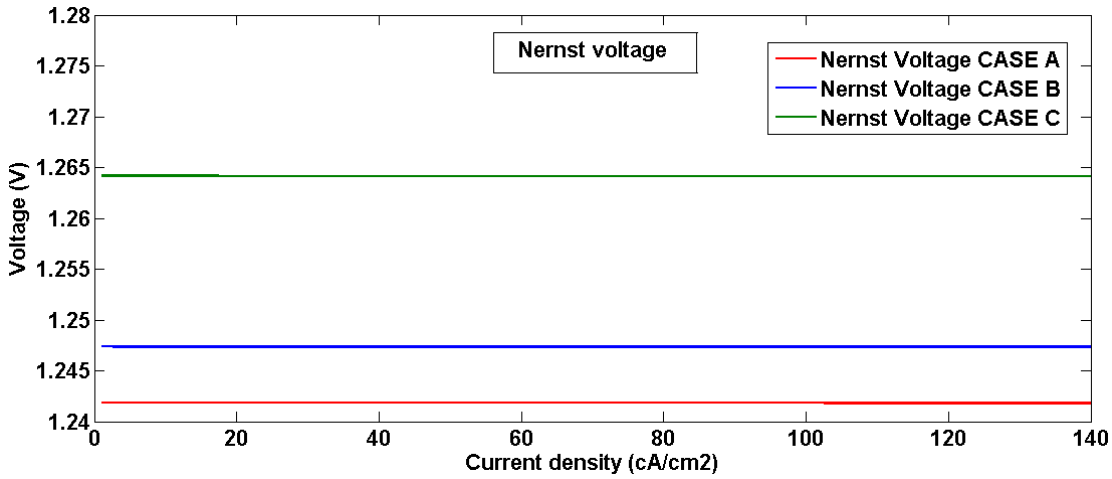

Fig. 6.1: Nernst voltage vs. current density

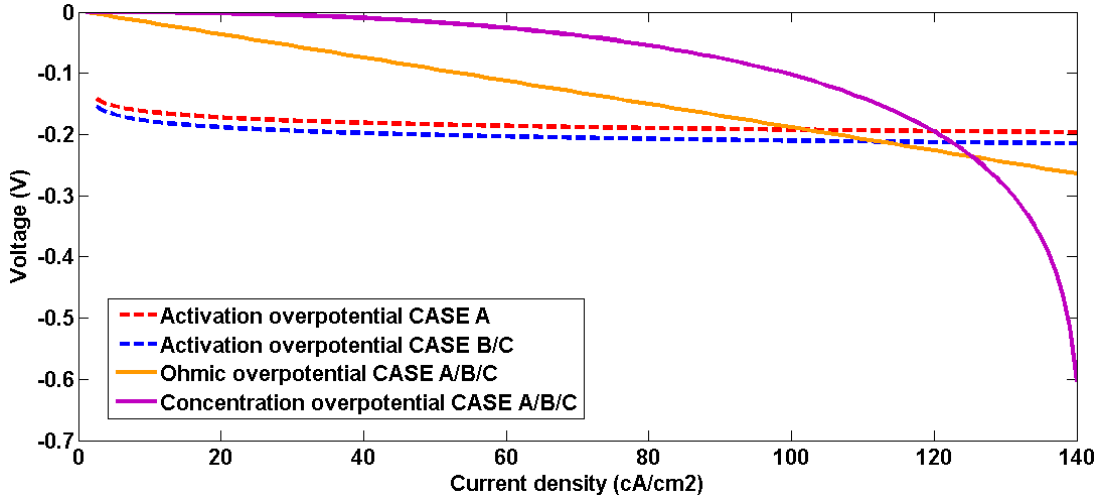

Fig. 6.2: Activation, ohmic and concentration losses (with assumptions of Table 6-1)

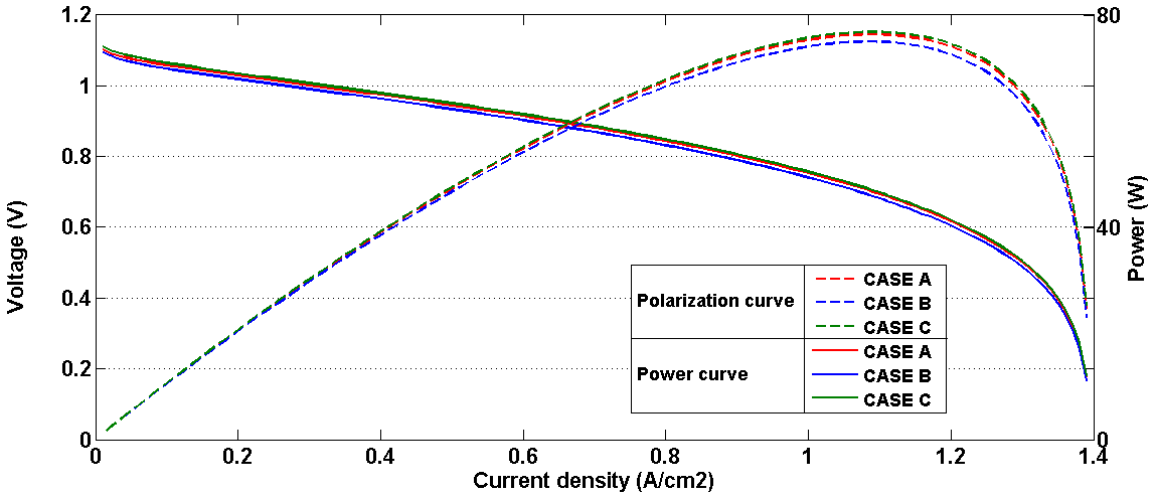

Fig. 6.3: Polarization and power curves (with assumptions of table 6-1)

The diagrams show, in case C, a slight increase of voltage and consequently of power compared to the cases A and B. The electrical power produced by the cell in the case C is higher than cases A and B at the same hydrogen flow. This modest increase has a greater influence with an high number of cells.

In the range between 0÷0.25 A/cm^2 the following diagram show how is the difference in a parametric simulation with three different levels of hydrogen inlet pressure:

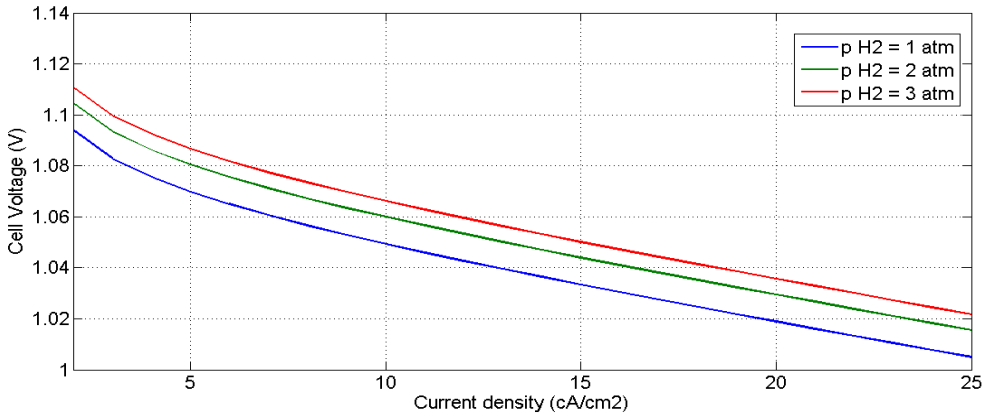

Fig. 6.4: Polarization curve for a parametric analysis regarding three different values of hydrogen pressure

Importantly, the effect of pressure are due only to the hydrogen pressure. The operating pressure in the cell is a weighted average of reactants pressure and, consequently, additional energy is not required to compress the air, while the hydrogen pressure is reduced from the high value of storage system.

Using the general assumptions of Table 6-1 (the simulation give the same results for cases A, B and C), the amount of water injected at three different levels of relative humidity is indicated in Fig. 6.5.

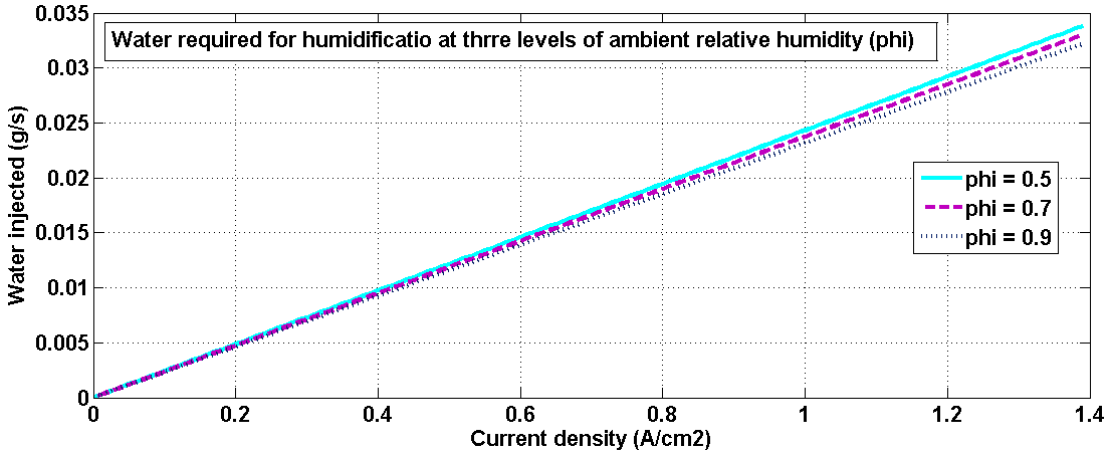

Fig. 6.5: Water injected vs. current density at three different levels of relative humidity.

As a natural consequence of the higher amount of water content in the air used as reactant, an higher value of relative humidity imply a reduction of the water injected.

Using the general assumptions of Table 6-1 (the simulation give the same results for cases A, B and C), the flow rates are:

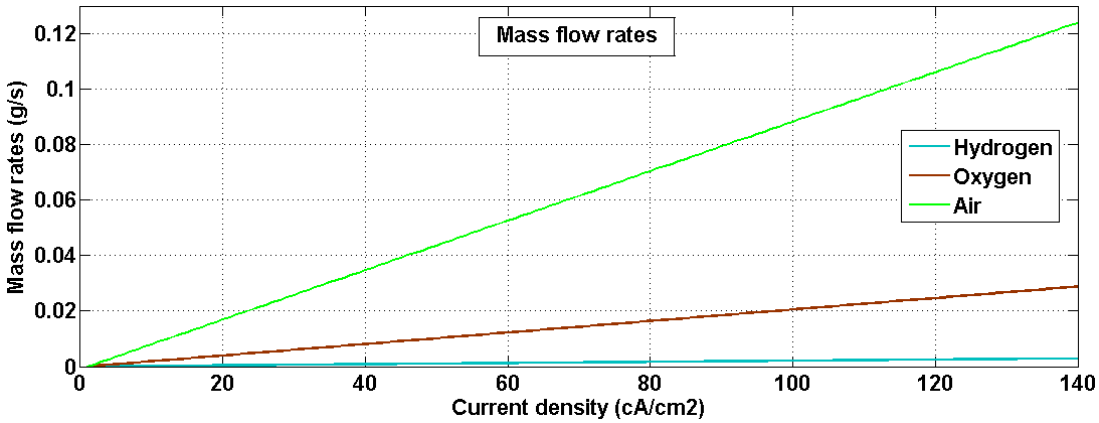

Fig. 6.6: Mass flow rates vs. current density with assumption of Table 1 (CASE A,B and C give the same results)

With the general assumptions of Table 6-1 (CASE B), the energy rates are:

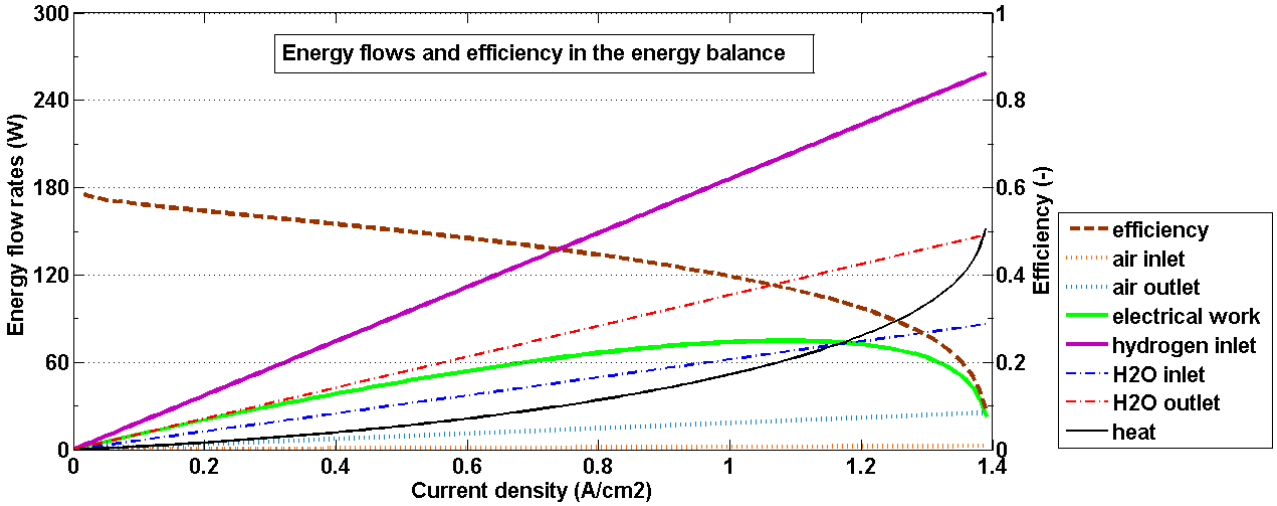

Fig. 6.7 : Energy flow rates vs. current density with assumption of Table 6-13 (CASE B)

The diagram shows a linear trend for energies of reactants and water, a parabolic trend for electrical power and an exponential trend for heat. Since the heat is related to losses, at higher currents the theoretical efficiency decreases.

Importantly, the theoretical efficiency do not consider the presence of auxiliaries devices as compressor or cooling system. In fact the trend of efficiency is steadily decreasing.

In Table 6-2 is indicated the total amount of energy that flow through the FC. The relationship between electrical power and heat is expressed through the percentages of energy flows, indicated in the Table 6-3. This investigation show as the electrical power percentage decrease and heat percentage increase with current density while their sum remain constant.

Table 6-2. Values of energy flow rates (W) for each inlet and outlet flow at various levels of current density.

		Current density (A/cm2)							
		0,1	0,2	0,3	0,4	0,5	0,6	0,7	0,8
Inlet energy flows (W)	air inlet	0,16	0,34	0,52	0,70	0,88	1,06	1,24	1,42
	hydrogen	16,74	35,35	53,95	72,56	91,16	109,76	128,37	146,97
	H2O inlet	5,58	11,77	17,97	24,16	30,36	36,55	42,75	48,94
	Total (inlet flows)	22,48	47,46	72,44	97,42	122,40	147,38	172,36	197,34
Outlet energy flows (W)	air outlet	1,64	3,46	5,29	7,11	8,93	10,76	12,58	14,40
	H2O outlet	9,55	20,17	30,79	41,40	52,02	62,63	73,25	83,87
	electrical work	9,44	19,36	28,75	37,58	45,80	53,33	60,06	65,85
	heat	1,84	4,47	7,62	11,33	15,65	20,66	26,47	33,22
	Total (outlet flows)	22,48	47,46	72,44	97,42	122,40	147,38	172,36	197,34

Table 6-3. Values of percentages of energy flow rates regard the sum of inlet and outlet flows.

		Current density (A/cm2)							
		0,1	0,2	0,3	0,4	0,5	0,6	0,7	0,8
Inlet percentages	air inlet	0,7%	0,7%	0,7%	0,7%	0,7%	0,7%	0,7%	0,7%
	hydrogen	74,5%	74,5%	74,5%	74,5%	74,5%	74,5%	74,5%	74,5%
	H2O inlet	24,8%	24,8%	24,8%	24,8%	24,8%	24,8%	24,8%	24,8%
Outlet percentages	air outlet	7,3%	7,3%	7,3%	7,3%	7,3%	7,3%	7,3%	7,3%
	H2O outlet	42,5%	42,5%	42,5%	42,5%	42,5%	42,5%	42,5%	42,5%
	electrical work	42,0%	40,8%	39,7%	38,6%	37,4%	36,2%	34,8%	33,4%
	heat	8,2%	9,4%	10,5%	11,6%	12,8%	14,0%	15,4%	16,8%

6.2 Theoretical and experimental driving cycles

Before proceed in the selection of theoretical driving cycles or in the analysis of experimental driving cycles for two-wheeled vehicles obtained through the measurement activities carried out at Hochschule Esslingen, some consideration is done. A driving cycles allow to define, according to the procedure explained in the paragraph 3.2.3 about energy management strategies, the required power for motion by vehicles. This quantity is strictly related to the average power during the trip. This analysis is demonstrated though the following calculations in which different theoretical driving cycles are used, in the numerical model, as reference for the same two-wheeled vehicle in a route without slope. The result are shown and listed in Table 6-4 and Fig. 6.8 where the correlations can be noticed.

Table 6-4: Some of the theoretical driving cycles available in literature

Driving cycle	time (s)	Distance (km)	Average speed (km/h)	Average required power (W)
TRL congested urban	1040	1.915	6.6	92
TRL urban	1222	6.145	18.1	276
MODEM 1	1217	5.810	17.2	322
ARTEMIS urban	1028	5.314	18.6	346
INRETS urban fluide 3	1067	7.232	24.4	443
EMPA LSA	770	4.161	19.4	578
EMPA RX	1169	12.390	38.2	860
EMPA Kreisel	513	4.876	34.2	863
HYZEM route 1	700	7.820	40.2	1148
INRETS route 1	888	9.270	37.6	1158
Handbook S3	2537	31.330	44.4	1189
Handbook R3	1208	15.910	47.4	1328
ARTEMIS rural (limited to 80 km/h)	1036	14.880	51.7	2006
TRL suburban & rural (limited to 80 km/h)	1092	15.980	52.7	2017

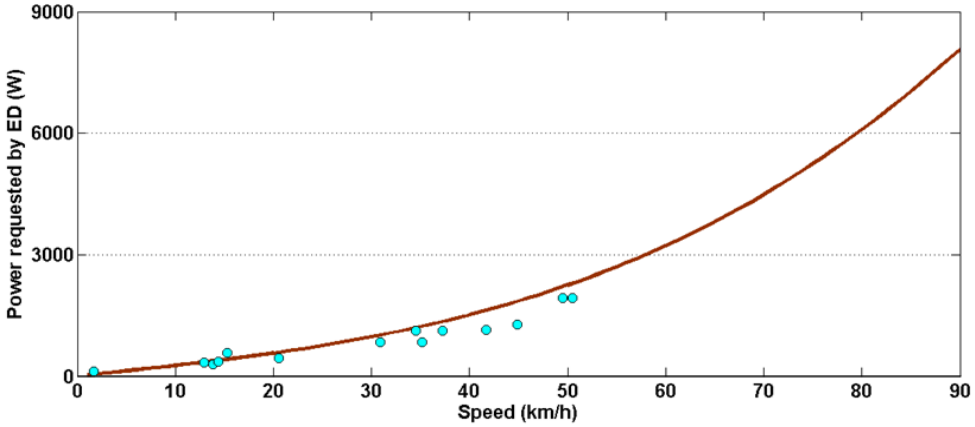

Fig. 6.8: Comparison between the results of average required power listed in the table (markers) and function of power required vs. vehicle speed

Although the power demand depends on several factors, which are variable in driving cycles, such as slope, acceleration and deceleration the average power is strictly related to the average speed. In fact, the results indicated in Table 6-4 follow the same profile as the power required over speed.

Usually driving cycles, that are defined in terms of vehicle speed as a function of time, are employed for conducting test of emission levels. So, hundreds of driving cycles have been used in the measurements of emissions according to the legislation of different countries. In this Research, is not possible to have a comprehensive description of all theoretical available driving cycles because they are high in number, but the emphasis is given to the most used driving cycles.

6.3 Strategies for dimensioning two-wheeled vehicles

6.3.1 Input data for trips and vehicles

The aim of this Research is to design the power train for an FC-driven electric-bike. A GRACE ONE electric bike was used for experimental measurements. The characteristics of GRACE ONE and of the Motorcycle are listed in Table 6-5 [100] [101].

Table 6-5. GRACE ONE E-bike characteristics and Motorcycle characteristics used in Matlab/Simulink® model.

Characteristics	GRACE ONE E-bike	Motorcycle
Mass vehicle (without passengers)	33 kg	180 kg
Mass vehicle (including passengers)	113 kg (1 passenger)	340 kg (2 passengers)
Rolling resistance coefficient C_r	0.005	0.012
Drag coefficient C_x	1	1
Vehicle frontal surface	0.4 m^2	0.7 m^2
Eta inverter	0.90	0.90
Eta electric machine	0.92	0.92
Eta transmission (EM is mounted directly on the rear axis for GRACE-ONE)	0.98	0.95

The simulation model is based on a set of experimental data measured directly on board the vehicle. The data inserted in this Research refer to a specific route from Esslingen to Altbach (Germany). The measurements were taken at Hochschule Esslingen. A data logger is mounted on the E-bike in order to measure consumed total capacity requested, battery voltage, battery

current, speed, distance terrain slope through GPS. The measurements are taken with a step of 1 second. In order to have statistical data, the route was followed several times in two different ways: the first one with the combination of electric motor and pedaling by cyclist (human-electric hybrid) and the second one with the only the contribution of an electric motor for traction (pure electric hybrid). The results are listed in Table 6-6.

Table 6-6. Total capacity [Ah] required from battery in EV in the route Esslingen-Altbach.

Human-electric hybrid		Pure electric
5.60		**9.62**
5.97		**9.69**
7.18		**9.91**
5.64		**10.88**
5.34		**9.49**
Average	**5.94**	**9.91**

The average value is 5.94 Ah under first condition and 9.91 Ah under the second one with a saving of 40 % of energy. Importantly, the simulation with pedaling will be done with a reduction of 40 % of the effective power needed for propulsion. The value of 40 % was defined through a statistical analysis over several different trips and conditions.

The efficiency and the performances of a PEM fuel cell are included in Matlab/Simulink® model through functions in which voltage (V), power (W) and consumption (L) are plotted over current (A). Clearly, the Horizon FC stack H-SERIES is used and its technical specifications are provided from the manufacturer. The Horizon H-SERIES can cover a power range between 10 W and 5 KW. An example of polarization, power and consumptions curves of 200W FC is presented in Fig. 6.9 [102].

Even though in this section the profiles of a 200 W FC are represented, in the Matlab/Simulink® model different FCs of 200, 300, 500, 1000, 2000 and 3000 W are inserted and their use is done by means of the simulator.

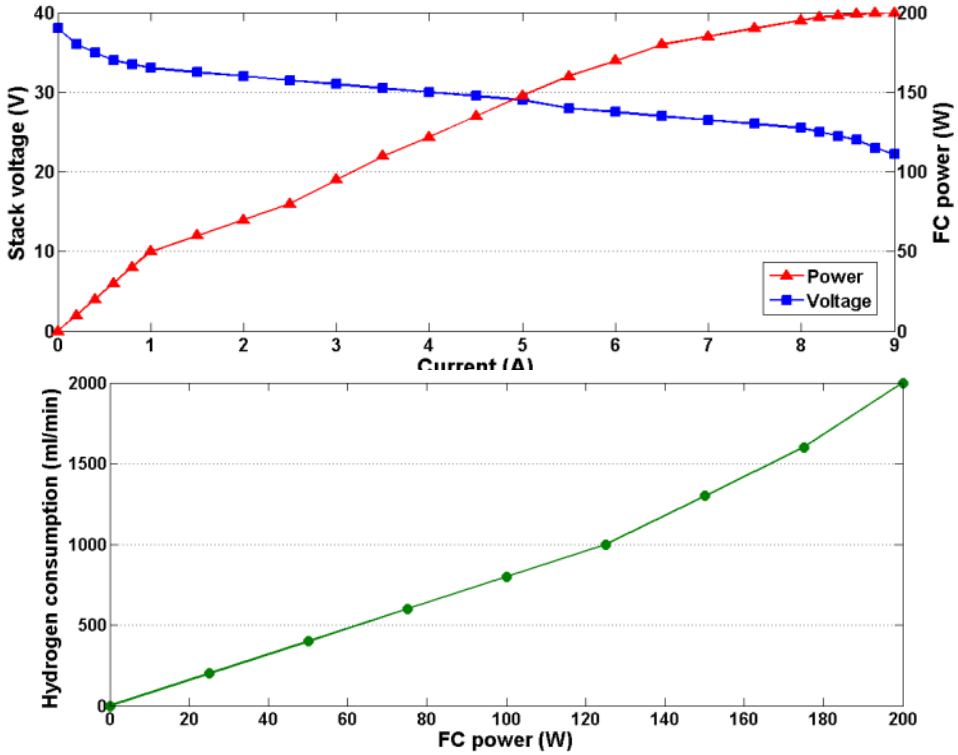

Fig. 6.9: Performance characteristics of the FC stack Horizon H-SERIES 200W

Lithium-Ion batteries are used in the GRACE ONE E-bike to store energy for propulsion. Its characteristics influence the vehicles autonomy whereby charging needs a long time and a plug-in connector is needed. In the Matlab/Simulink® model, a Lithium-Ion battery with the specifications of Table 6-7 is considered.

Table 6-7. Lithium-ion battery specifications.

Parameter	GRACE ONE FC-E-bike	FC-E-motorcycle
Capacity	12 Ah	20 Ah
Nominal Voltage	48 V	48 V
Energy content	576 Wh	960 Wh
Max current in charging	20 A	50 A
Max current in discharging	50 A	120 A
Max power in charging	960 W	2400 W
Max power in discharging	2400 W	5760 W
Internal resistance in charging	0.014 Ω	0.014 Ω
Internal resistance in discharging	0.012 Ω	0.012 Ω

The Matlab/Simulink® model allows a preliminary evaluation of the average power required by ED, which is listed in Table 6-8 for the vehicles of this Research. The average values are very important because the size of the FC must be at least equal or superior to these values. In fact, the energy generated on board by the primary converter must satisfy the total requirement by the entire powertrain in order to avoid any additional source of energy.

Table 6-8. Average power required for propulsion.

Vehicle	Number of passengers	Average power requested by ED
FC-E-bike (human-electric hybrid)	1	186.4 W
FC-E-bike (pure electric hybrid)	1	251.4 W
FC-E-motorcycle	2	1880.5 W

The simulation allows the estimation of the performances, in terms of efficiency and consumption of the FCHEV powertrain considering several different combinations.
Since the efficiency over the SOC curve of Lithium-Ion batteries is rather flat according to [30], the simulation helps a better understanding of control logic. In fact, the efficiency of the battery changes from 86 % (SOC=0.2) to 90% (SOC=0.8). Simulations were carried out using SOC lower and upper limits of 0.7 and 0.8. The driving cycle is related to an Esslingen-Altbach route with a Grace One as pure electric hybrid. The vehicle speed profile (average 24.66 km/h) and the effective power for propulsion (average 314 W) are shown in fig. 6.10.

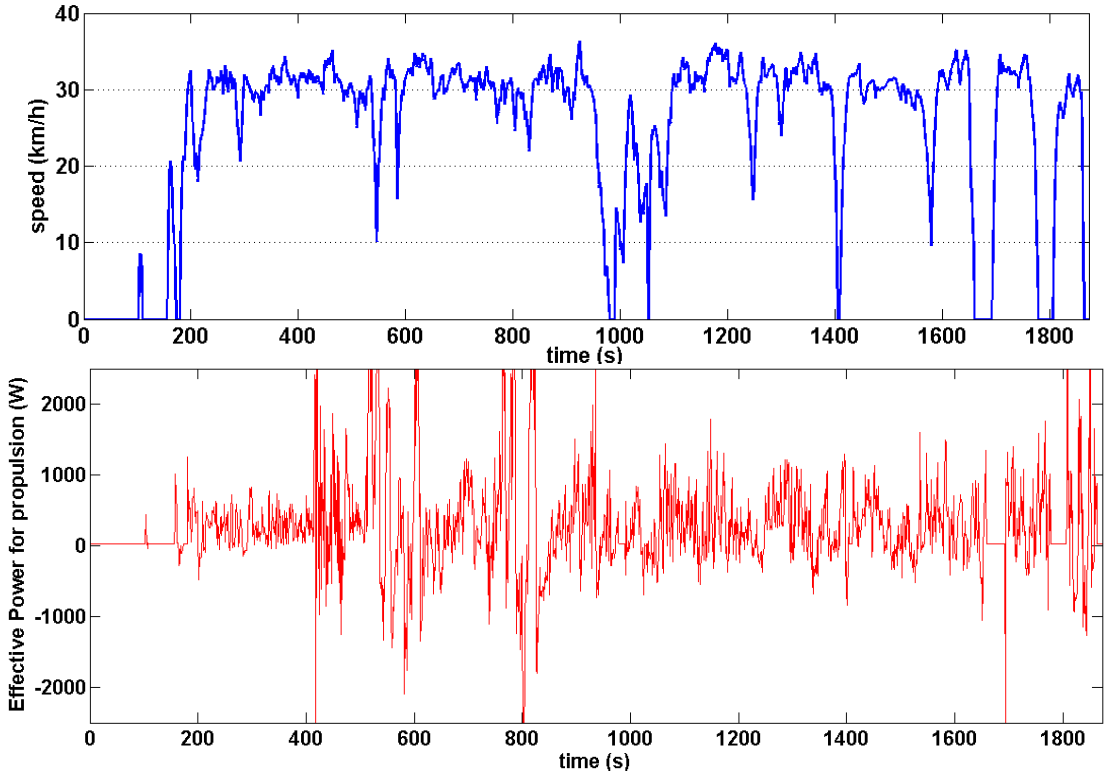

Fig. 6.10: Speed and power of a GRACE ONE (pure electric hybrid) in Esslingen-Altbach route

The values of SOC_L and SOC_U are 0.7 and 0.8 since these values allow recovering the available energy during descent, deceleration by recuperative braking. Furthermore, a high value of the SOC slightly improves the overall efficiency of the system.

The two-wheeled vehicles considered in this thesis are listed below:

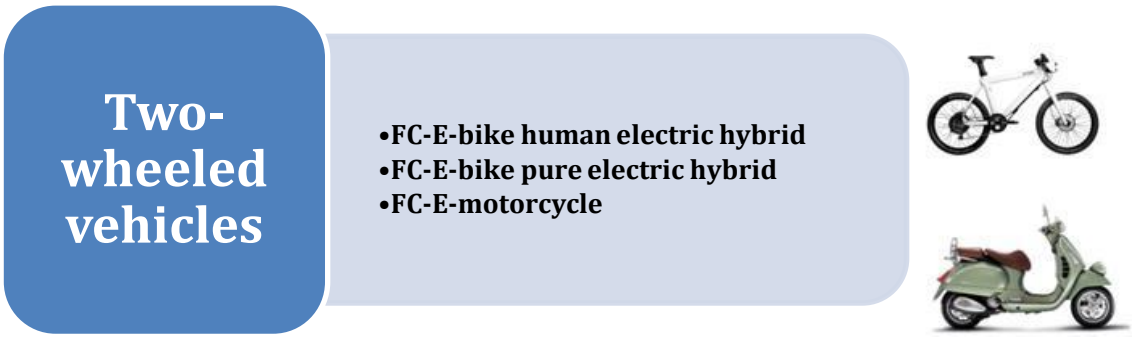

Fig. 6.11: Two-wheeled vehicle considered in this thesis

6.3.2 Results of simulation of the GRACE ONE FC-E-bike (human-electric hybrid)

Firstly, the evaluation of FC sizing was conducted with a repetition of single trips. The results of SOC levels during simulations are shown in Fig. 6.12. The results show that the FC power must be of 200 W for GRACE ONE as human-electric hybrid. In fact, the on-board generated

energy is enough to keep the SOC level up to 0.65 after a trip of 25000 km and a distance of 190.84 km. Consequently, an FC of 200 W, used as primary converter, allows the requirement to be satisfied by ED with a reduction of the size of the system and consumptions of hydrogen.

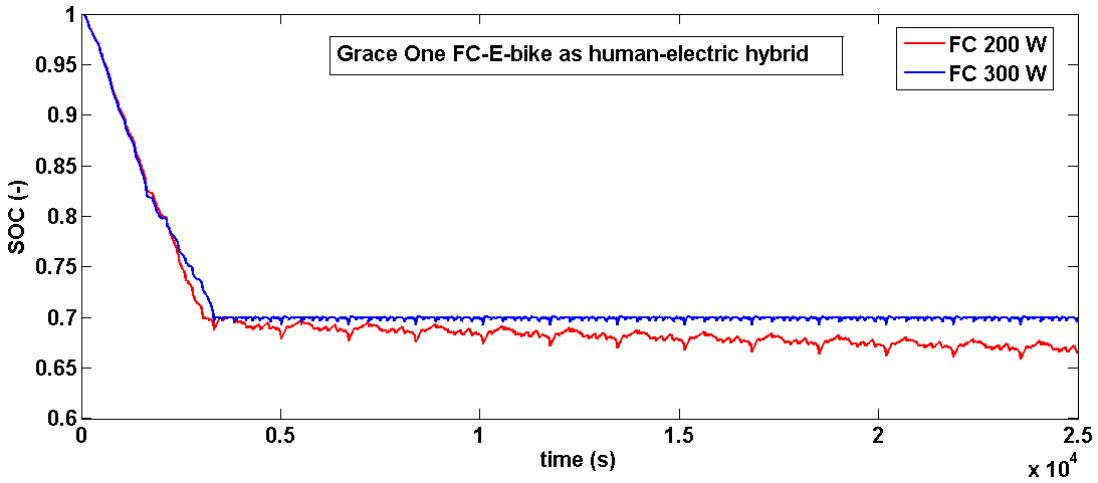

Fig. 6.12: SOC levels for Grace One FC-E-bike

Secondly, the behavior of the hybrid system is analyzed thorough the graphs of SOC and hydrogen consumption, as indicated in Fig. 6.13. The graph of total hydrogen consumption indicates how much hydrogen is used in the FC stack according to the power requested by the ED and the SOC which is also shown in the fig. 6.4. Since the dimension of the primary converter was calculated in a longer driving cycle, the SOC is almost constant due the fact that its range is comprised between 0.68 and 0.70. A total consumption of 4.67 g is needed for a trip of 12.87 following the profiles of speed and slope used in the simulation [103].

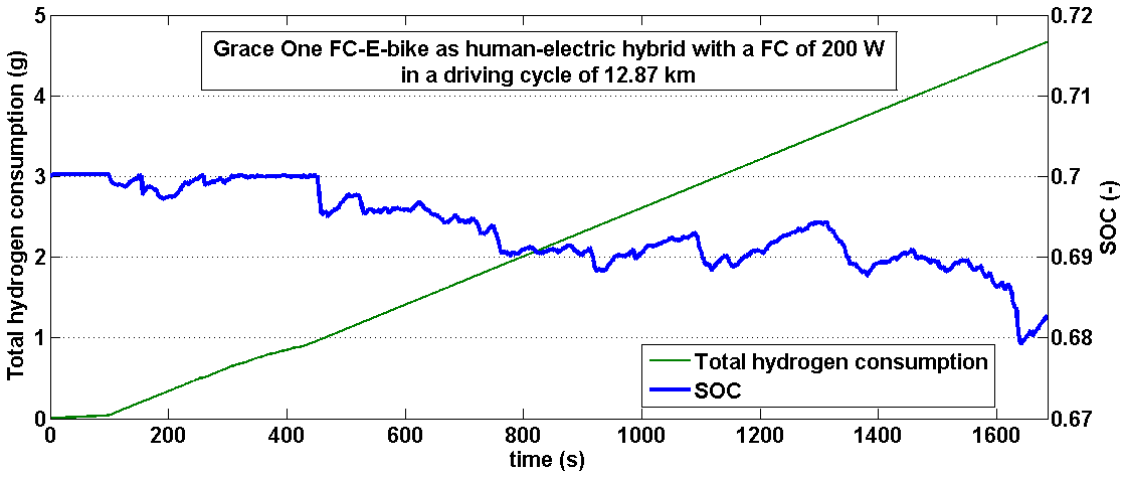

Fig. 6.13: Behavior of powertrain for GRACE ONE as human-electric hybrid

6.3.3 Results of simulation of the GRACE ONE FC E-bike (pure electric hybrid)

Firstly, the evaluation of FC sizing were conducted with a repetition of a single trips. The results of SOC levels during simulations are shown in fig. 6.22. The results show that the FC power has to be 300 W for GRACE ONE as pure electric hybrid. In fact, the on-board generated energy is enough to keep the SOC level up to 0.6 after a trip of 25000 km and a distance of 190.84 km. The value of FC power in this case is superior to the previous case because the Grace-One as pure electric hybrid does not receive energy from the passenger.

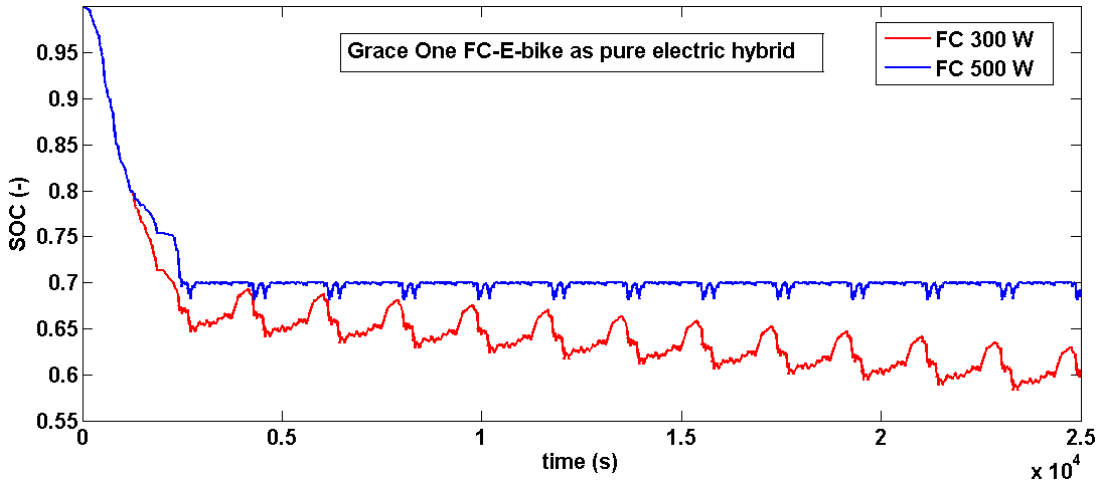

Fig. 6.14: SOC levels for GRACE ONE FC-E-bike

Secondly, the behavior of the hybrid system is analyzed thorough the graphs SOC and hydrogen consumption, as indicated in fig. 6.15. Since the dimension of the primary converter is superior to the human-electric hybrid and the contribution of the passenger is zero, the total consumption of hydrogen is greater than 4.67 g and is equal to 9.11 g. The SOC is maintained in an adequate range due the fact that its range is comprised between 0.64 and 0.70.

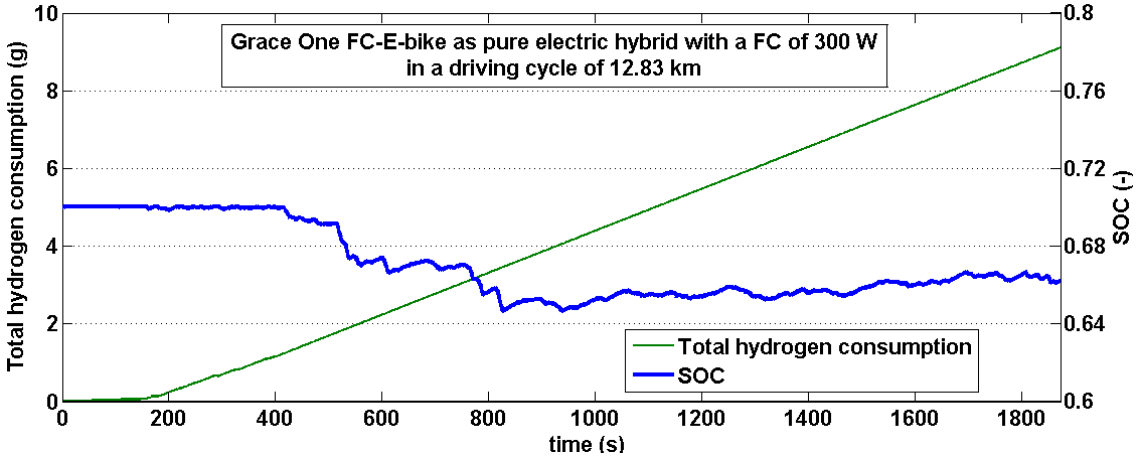

Fig. 6.15: Behavior of the powertrain for Grace One as pure electric hybrid

6.3.4 Results of simulation FC- E-motorcycle.

For this vehicle some parameters must be modified compared to GRACE ONE. In particular, the mass of vehicle is increased from 113 to 340 kg considering 2 passengers, the frontal area is increased from 0.4 to 0.7 m^2 and the rolling resistance coefficient is increased from 0.005 to 0.012.

The New European Driving Cycle (NEDC), limited at 80 km/h, is the basis for this simulation. The altitude profile is related to Esslingen-Altbach route. The driving cycle, in which the average speed is 33.4 km/h, is shown in fig. 6.16.

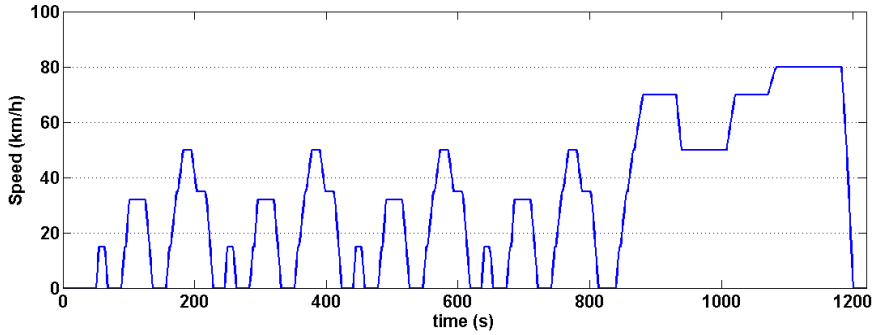

Fig. 6.16: NEDC used in Simulink® model

A simulation is done with several cycles for 25000 seconds to analyze the SOC of battery in a system with a FC of 1000 and 2000 W. As indicated in fig. 6.25, the energy generated from FC is enough for FC-E-motorcycle equipped with a FC of 2000 W because the SOC is maintained in an appropriate range. Moreover, the final SOC, after a range of 223 km, is above 0.65. Indeed, the best hybrid configuration for the motorcycle can be done with a powered FC of 2000 W.

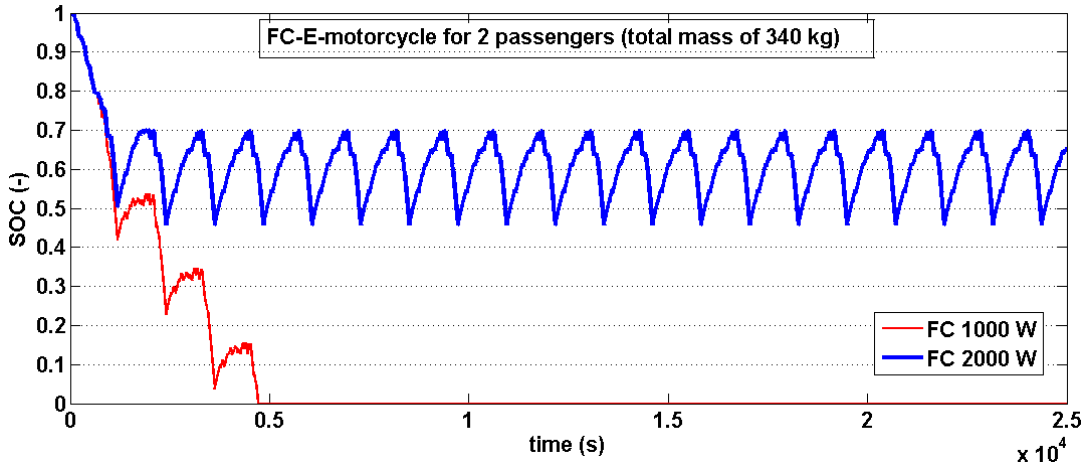

Fig. 6.17: SOC of FC-E-motorcycle during simulation

An enhance analysis of this vehicle, using the NEDC cycle (1220 seconds) is represented in fig. 6.18, where SOC and hydrogen consumption are shown. The profile of total hydrogen consumption is influenced by the logic of control of the FC which work at maximum power when the SOC is below 0.7. The importance of the driving cycle is evidenced in the part after 800 seconds when speed is upper than before. In fact, the architecture of the hybrid system is conceived in order to use both FC and RESS in most demanding phases. Nevertheless the vehicle works with two passengers, high speed and binding slope the SOC remain up to 0.56 at the end of the trip.

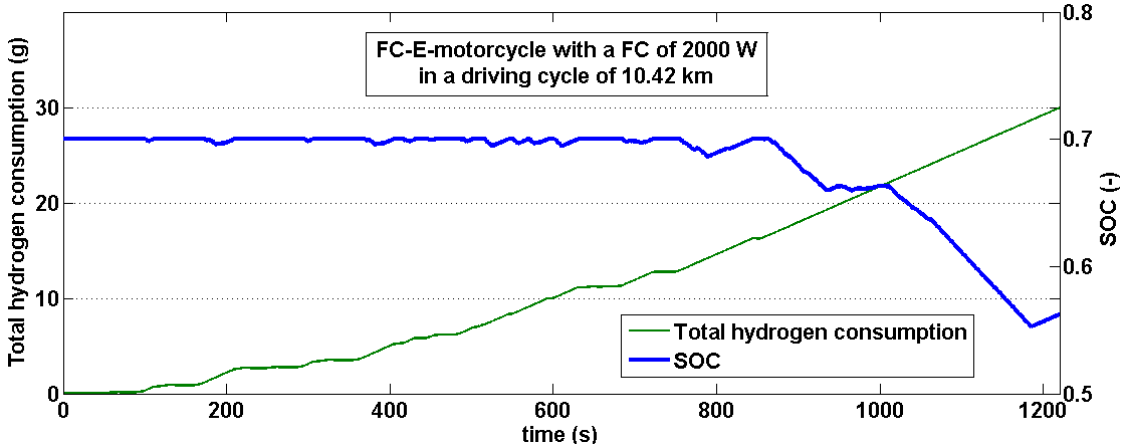

Fig. 6.18: Behavior of the powertrain for FC-E-motorcycle

The higher consumption of the motorbike, compared to GRACE ONE, is acceptable due to the increased amount of hydrogen stored on board.

The layout of the powertrain is proposed in Fig. 6.19 using the external dimensions of the principal components and taking into consideration a Piaggio Vespa scooter, which are

(dimensions are expressed in mm): 350x183x303 for Horizon H-Series 2 kW PEMFC stack, 180x80x300 for Lithium-Ion commercial battery, ϕ220x220 for 5 kW electrical motor and ϕ170x380 for high pressure hydrogen tank.

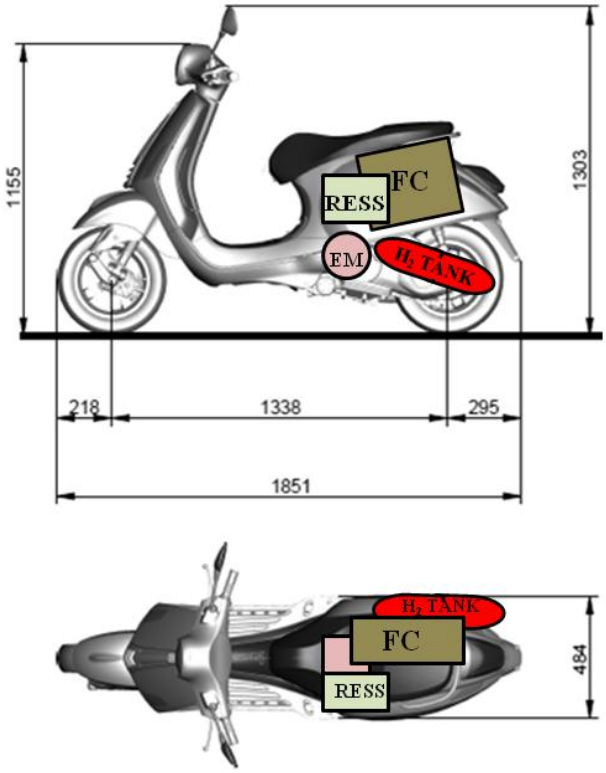

Fig. 6.19: Layout of the powertrain for a FC- E-motorcycle

In this configuration the RESS and the FC are positioned under the seat, the EM is positioned in the housing of the Internal Combustion Engine and the hydrogen tank is positioned on the left side of the rear wheel replacing the exhaust pipe.

6.3.5 Comments

Veracity of the developed models is validated by previous studies and design data available in scientific literature. Assumptions relating to driving cycles and operating conditions are based on open literature and personal communications. Simulation results and associated analysis should therefore be considered in view of all the assumptions presented in the dissertation and papers.

The results of the model exposed in this Research are summarized in Table 6-9 in which the most important working parameters of two-wheeled vehicles, such as average power requested by ED, peak power of EM, maximum power of FC, power and capacity of Lithium-Ion battery and hydrogen consumption, are listed.

Table 6-9. Configuration summary.

Vehicles	RESS capacity	Average P_{ED} requested	RESS max power discharging	FC power (peak)	P_{ED} (peak)	H2 consumption
	(Ah)	(W)	(W)	(W)	(W)	(g/km)
FC-E-GRACE ONE (human-electric hybrid)	12	186.4	2500	200	2500	0.37
FC-E-GRACE ONE (pure electric hybrid)	12	251.4	2500	300	2500	0.71
FC-E-Motorcycle	20	1880.5	7800	2000	7800	2.88

To summarize, in Table 6-10, an overview of the results of simulations is reported in order to compare the energy requirements of three different vehicles.

Table 6-10. Results of simulations.

Vehicles	Time of simulation	Distance	Energy required by ED	Energy from FC	Energy from RESS	SOC_F - SOC_I
	(s)	(km)	(Wh)	(Wh)	(Wh)	(W)
FC-E-GRACE ONE (human-electric hybrid)	1686	12.87	110.4	86.6	23.8	- 2.5%
FC-E-GRACE ONE (pure electric hybrid)	1873	12.83	196.2	145.9	50.3	- 4.1%
FC-E-Motorcycle	1220	10.42	638.8	484.7	154.1	-13.3%

The values 0.40, 0.59 and 2.88 (g/km) are an estimation of the consumption respectively for the bike as human-electric hybrid, the bike as pure electric hybrid and the motorcycle. The energy required by the ED is equal to 110.4, 196.2 and 638.8 (Wh) for the vehicles in the same order as before. This amount of energy is provided by the FC and the RESS with the contributions indicated in the table. The ratio of the energy provided by the FC is equal to 78.4 %, 74.3 % and 75.8 % respectively for the three vehicles, while the ratio of energy provided by the RESS is the remaining percentage until obtaining 100%. The ratio of the energy provided by the FC defines the relationship between the energy generated by the FC and the energy requested by the ED. Since the propulsion systems were designed with the same criteria, similar values of this percentage were expected. Consequently, the efficiency of

the entire drive system is almost the same for the three vehicles of this study. The SOC variation indicates how much energy will be available in the RESS at the end of the trips. The P_{FC}, for all vehicles, is higher than the average required power by ED in order to satisfy the energy requirements in the most demanding cases.

The value of the maximum power requested for traction allows the same drivability of traditional vehicles to be maintained, such as electric bikes and ICE-based motorcycles. Since the peak power of the EM must be provided for a limited time, the nominal power of the EM is lower than the peak and it is equal to 1300 W for FC-E-GRACE ON human-electric hybrid, to 2400 W for FC-E-GRACE ONE pure electric hybrid and to 5000 W for FC-E-Motorcycle that means a degree of hybridization respectively equal to 65 %, 67 % and 64 % for the vehicle indicated before.

6.4 Strategies for dimensioning four-wheeled vehicles

6.4.1 Components sizing of hybrid electric powertrains with fuel cell for passengers cars

In this research a technical analysis about a wide range of Fuel Cell Hybrid Electric Vehicles (FCHEVs) has been conducted with the focus on the passenger cars of European segments, indicated in Fig. 6.20.

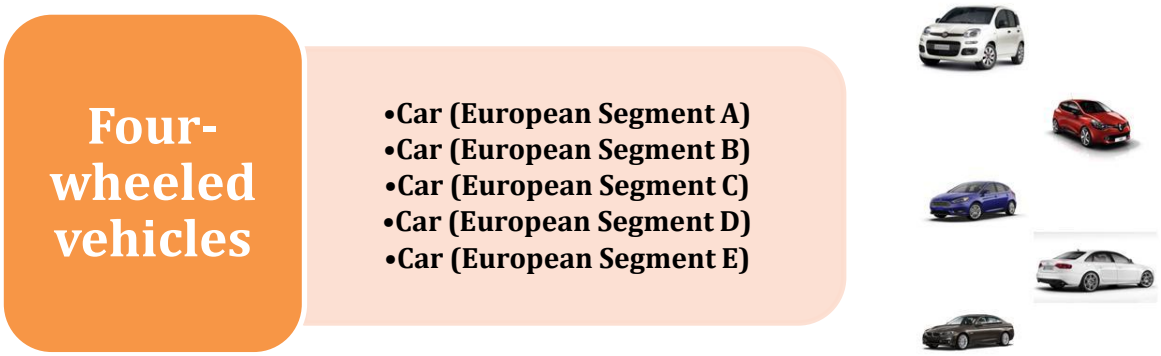

Fig. 6.20: Four-wheeled vehicle considered in this thesis

The performance of the vehicles was tested with six theoretical driving cycles which are referred to as rural, urban and highway routes using a Matlab/Simulink® model in order to determine the most convenient configurations of the system. The results of the simulations give indications about the power required for traction and auxiliaries, the State Of Charge (SOC) of RESS and the hydrogen consumption of FC.

In this Research, the dimensioning of FCHEVs has been optimized starting from the acquisition of theoretical driving cycles in different conditions for a wide range of car segments. Simulations have been conducted using the parameters which characterize the vehicles and the missions in order to define the average power required by the wheels. Then, this value is used as a reference for the dimensioning of the FC stack and the car configurations are proposed and analyzed.

The calculations were implemented using a block diagram, shown in Fig. 6.21, in which the power and the torque required by the wheels (P_{ED}) was calculated by the sum of the aerodynamic, rolling, gravitational and inertial forces occurring during the motion. This value was adopted due to the presence of mechanical and electrical losses before its use in PMU as the input parameter. The task of PMU is to define the ratio of power provided by FC and RESS. The power of FC, hydrogen consumption, current and battery voltage and SOC are continuously monitored [76].

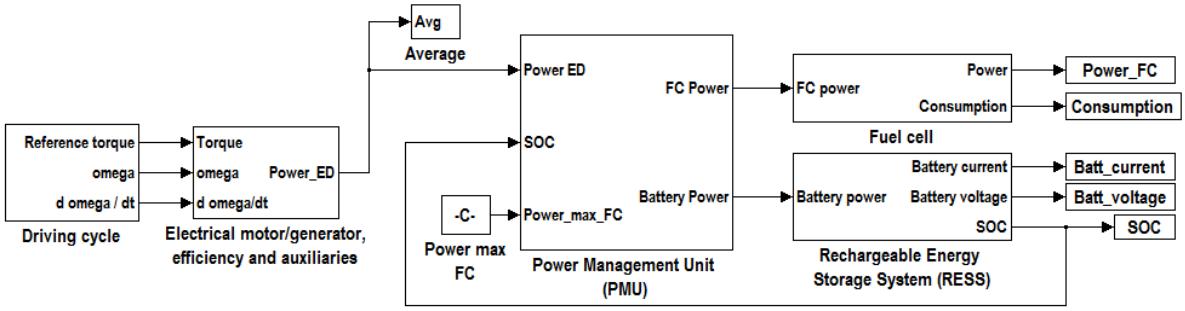

Fig. 6.21 Matlab/Simulink® block diagram used for FCHEV simulation

6.4.2 Input data and classifications for driving cycles and cars

A driving cycle is a series of data points representing the speed of a vehicle versus time. They are produced by different organizations to assess the performance of vehicles in various way [104].

The driving cycles considered in this Research are listed in Table 1 which contains the total distance, duration, average speed, slope and variation of altitude for each driving cycle. The slope was assumed constant with values of 1%, 2% and 5% according to the average speed.

Table 6-11. Specifications of driving cycles used in this Research [105]

Driving cycle	Distance (km)	Time (s)	Average Speed (km/h)	Slope (%)	Variation of altitude (m)
MODEM Urban5	6.34	1027	22.2	5%	317
NEDC	11.02	1220	33.6	5%	551
Handbook R2	55.30	2572	77.7	2%	1106
MODEM Hyzem highway	46.21	1804	92.2	2%	924
Artemis High motorway	30.21	1065	102.1	2%	604
EMPA BAB	32.64	1000	117.5	1%	326

Vehicle segments in Europe do not have formal characterization or regulations, but they tend to be based on the document of the European Commission about the merger regulation between two cars manufactures (Hyundai and Kia) in which the vehicles are classified in segments with letters A, B, C, D, E according to the American classification [106].
The segments taken into consideration in this Research are listed in Table 6-12, in which the cargo volume is also indicated.

Table 6-12. European classification of cars (American classification in the brackets).

Segment	Definition	Examples	Cargo volume
A	MINI (CITY CARS)	Fiat 500, Toyota Aygo, Citroen C1.	< 2.4 m^3
B	SMALL (SUBCOMPACT CARS)	Opel Corsa, VW Polo, Renault Clio.	2.41<m^3<2.83
C	MEDIUM (COMPACT)	Audi A3, Alfa Romeo Giulietta, Peugeot 308.	2.83<m^3<3.11
D	LARGE (ENTRY-LEVEL-LUXURY)	Audi A4, Mercedes C, Mazda 6.	3.11<m^3<3.40
E	EXECUTIVE (MID-SIZE-LUXURY)	VOLVO S80, BMW 5, Mercedes E.	>3.40 m^3

A complete description of European car segments is reported in the following scheme:

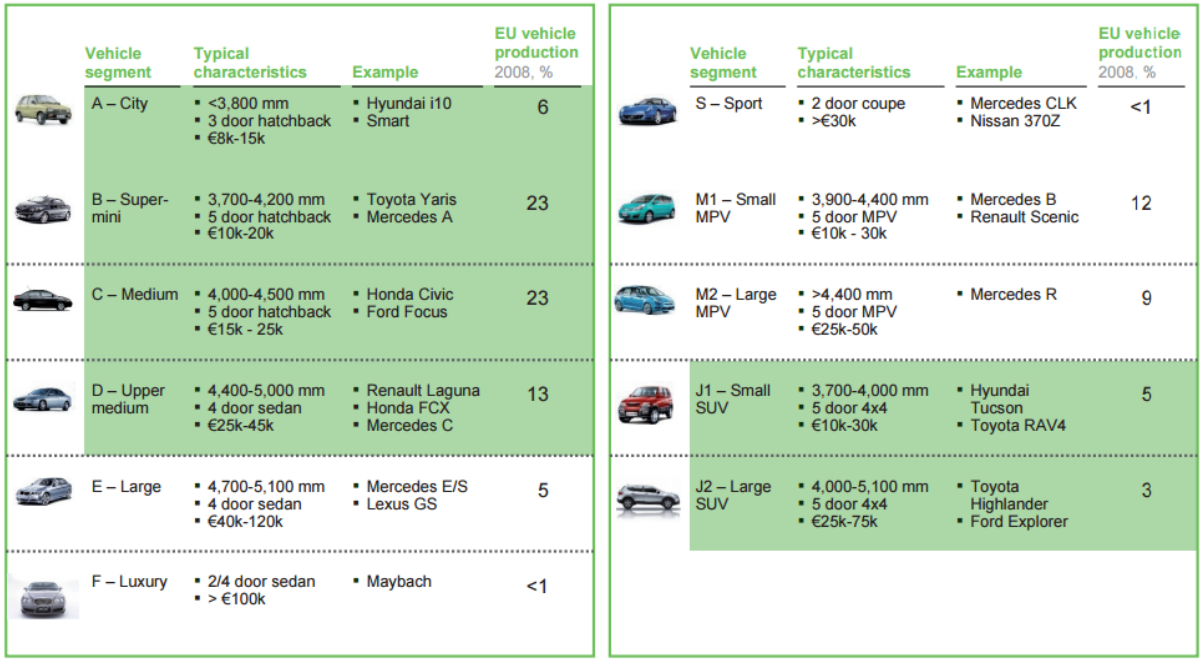

Vehicle segment	Typical characteristics	Example	EU vehicle production 2008, %
A – City	▪ <3,800 mm ▪ 3 door hatchback ▪ €8k-15k	▪ Hyundai i10 ▪ Smart	6
B – Super-mini	▪ 3,700-4,200 mm ▪ 5 door hatchback ▪ €10k-20k	▪ Toyota Yaris ▪ Mercedes A	23
C – Medium	▪ 4,000-4,500 mm ▪ 5 door hatchback ▪ €15k - 25k	▪ Honda Civic ▪ Ford Focus	23
D – Upper medium	▪ 4,400-5,000 mm ▪ 4 door sedan ▪ €25k-45k	▪ Renault Laguna ▪ Honda FCX ▪ Mercedes C	13
E – Large	▪ 4,700-5,100 mm ▪ 4 door sedan ▪ €40k-120k	▪ Mercedes E/S ▪ Lexus GS	5
F – Luxury	▪ 2/4 door sedan ▪ > €100k	▪ Maybach	<1

Vehicle segment	Typical characteristics	Example	EU vehicle production 2008, %
S – Sport	▪ 2 door coupe ▪ >€30k	▪ Mercedes CLK ▪ Nissan 370Z	<1
M1 – Small MPV	▪ 3,900-4,400 mm ▪ 5 door MPV ▪ €10k - 30k	▪ Mercedes B ▪ Renault Scenic	12
M2 – Large MPV	▪ >4,400 mm ▪ 5 door MPV ▪ €25k-50k	▪ Mercedes R	9
J1 – Small SUV	▪ 3,700-4,000 mm ▪ 5 door 4x4 ▪ €10k-30k	▪ Hyundai Tucson ▪ Toyota RAV4	5
J2 – Large SUV	▪ 4,000-5,100 mm ▪ 5 door 4x4 ▪ €25k-75k	▪ Toyota Highlander ▪ Ford Explorer	3

Fig. 6.22: Scheme of European Car segments

The input data of the vehicles are listed in Table 6-13. The mass of the vehicle includes a mass of 280 kg for passengers and bags. The auxiliaries include air condition, compressor of FC stack, lights and converters. The maximum power of FCHEVs must be inside the ICE power range, indicated in Table 6-13, in order to maintain the same drivability as traditional vehicles [107].

Table 6-13. Vehicle parameters used as input data.

Parameter	A	B	C	D	E
Mass simulated (kg)	1290	1430	1590	1840	2020
Drag Area = Cx·A (m^2)	0.625	0.639	0.665	0.623	0.644
Rolling coefficient (-)	0.010	0.011	0.012	0.012	0.012
ICE power range (kW)	36÷44	44÷66	66÷88	88÷110	110÷169
Auxiliaries power (kW)	1000	1000	1200	1400	1400

The calculation of the power needed in a vehicle mission was made using the following equation:

$$P_{ED\_avr} = \frac{1}{t_{tot}} \int_0^{t_{tot}} P_{ED} dt \qquad (6.1)$$

In fig. 6.23 the values of average power required for propulsion, in the driving cycles considered in this Research, are graphically exposed. Obviously, a higher demand of power was requested by larger vehicles in faster driving cycles.

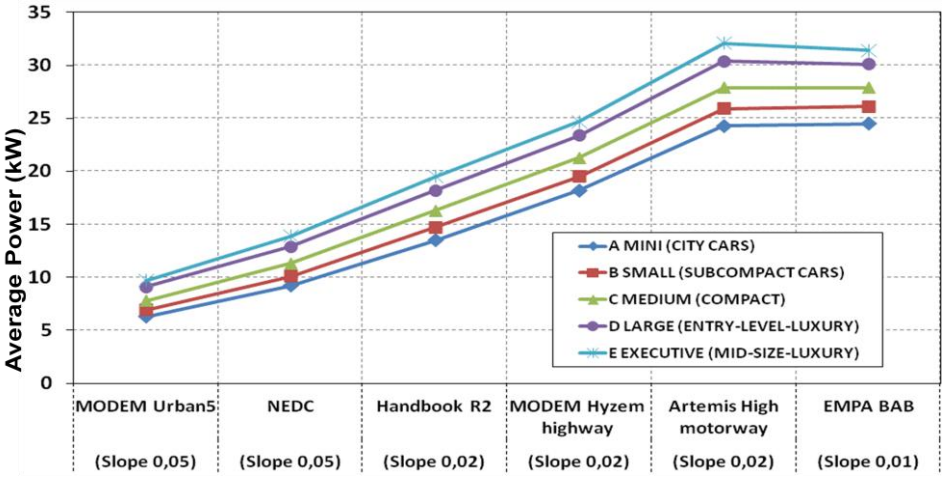

Fig. 6.23: Average power required from ED and auxiliaries in various driving cycles

The values of average power required shown in fig. 6.30 are used as reference in the proposed configurations of Table 6-14. The dimensioning of the hybrid architecture follows two basic rules: the power of FC must be equal or higher than the average required power in the most demanding driving cycle and the degree of hybridization must be in an appropriate range.

Table 6-14. Hybrid Electric configurations selected for car segments

Parameter	A	B	C	D	E
EM nominal power (kW)	29	44	59	73	100
EM peak power (kW)	44	66	88	110	150
FC power (kW)	25	32	38	45	60
Degree of hybridization (-)	0.85	0.73	0.65	0.61	0.60
RESS power (kW)	19	34	50	65	90
RESS voltage	400	400	400	400	400
RESS capacity (Ah)	40	50	60	70	80
RESS max current in discharging (A)	48	85	125	163	225
RESS max current in charging (A)	19	34	50	65	90

6.4.3 Results of simulations for passengers cars

The behaviour of powertrains has been analyzed for the configurations of Table 6-14 and the most important parameters are monitored during the driving cycles of table 1. In this section the results in terms of SOC and total hydrogen consumption are graphically exposed for the mission of the vehicles in three driving cycles (NEDC, MODEM Hyzem highway and EMPA BAB), graphically exposed in Fig. 6.24.

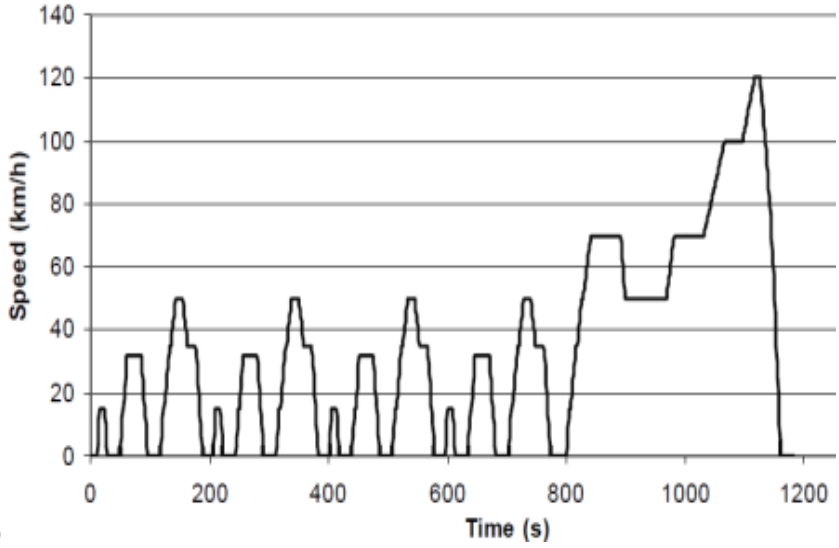

a)

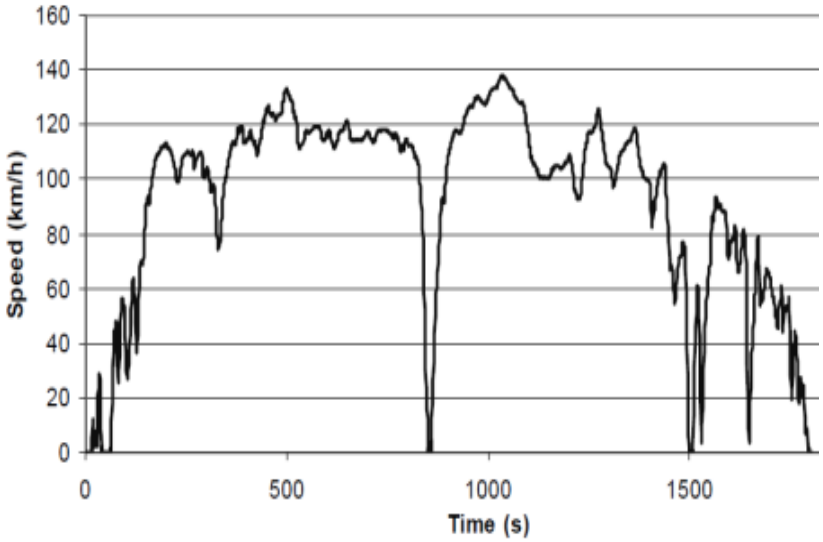

b)

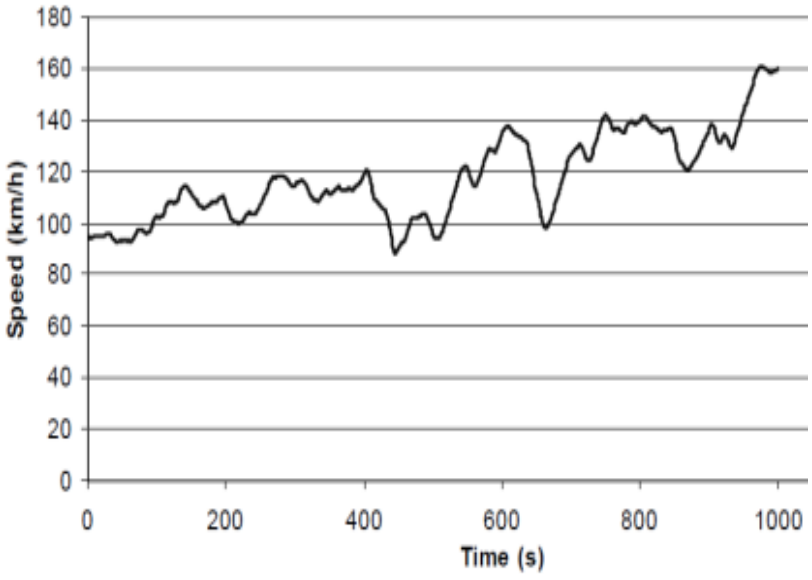

c)

Fig. 6.24 Driving cycles: a) NEDC b) MODEM Hyzem highway c) EMPA BAB, with speed (km/h) vs. time (s) [99]

The SOC graphs indicate how the energy content of the battery varies over time: it remains higher than 0.64 in all cases due to the size of the primary converter. The graph of the total hydrogen consumption indicates how much hydrogen is required for each driving cycle and it is greater for car segment E, then decrease till car segment A. When the power demand has a high level the SOC decrease but it remain always in a range between 0.6-0.7, as indicated in figures 6.25, 6.26 and 6.27 [108].

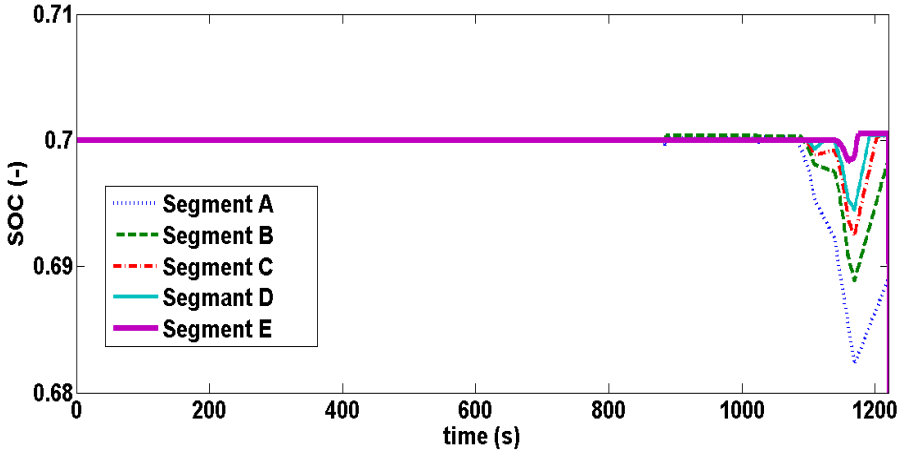

a)

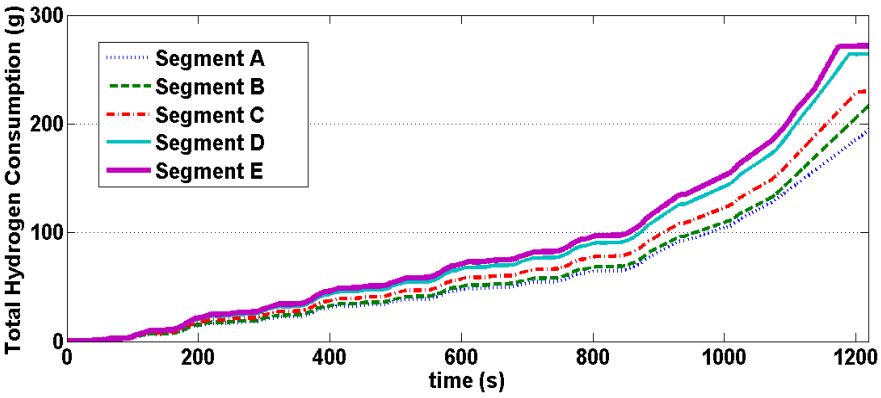

b)

Fig. 6.25: a) State of charge of battery, b) total hydrogen consumption, in NEDC.

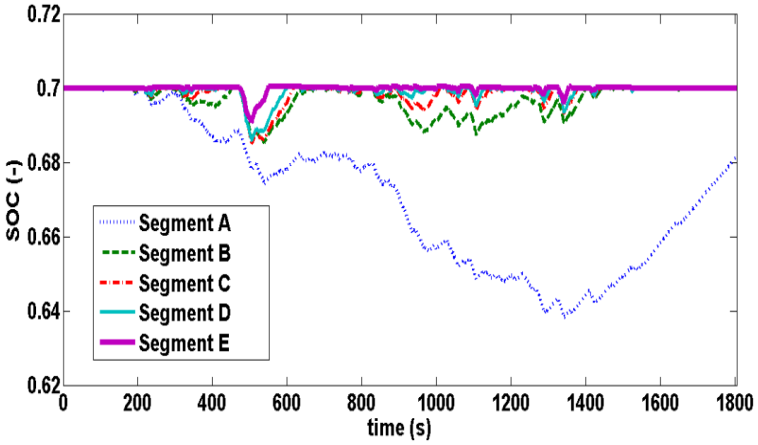

a)

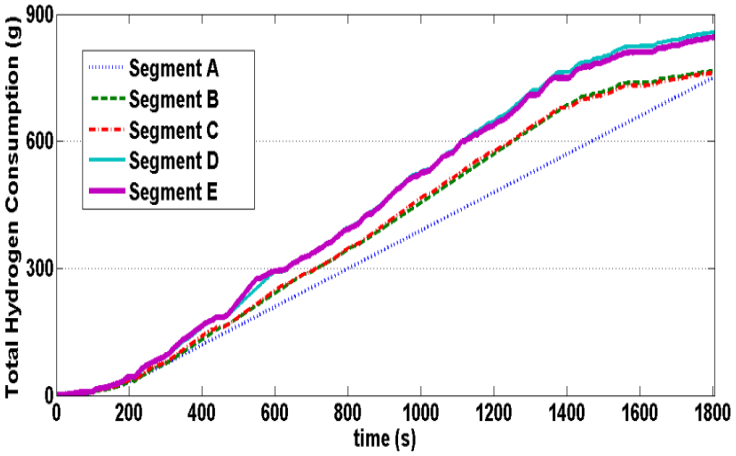

b)

Fig. 6.26: a) State of charge of battery, b) total hydrogen consumption, in MODEM Hyzem highway.

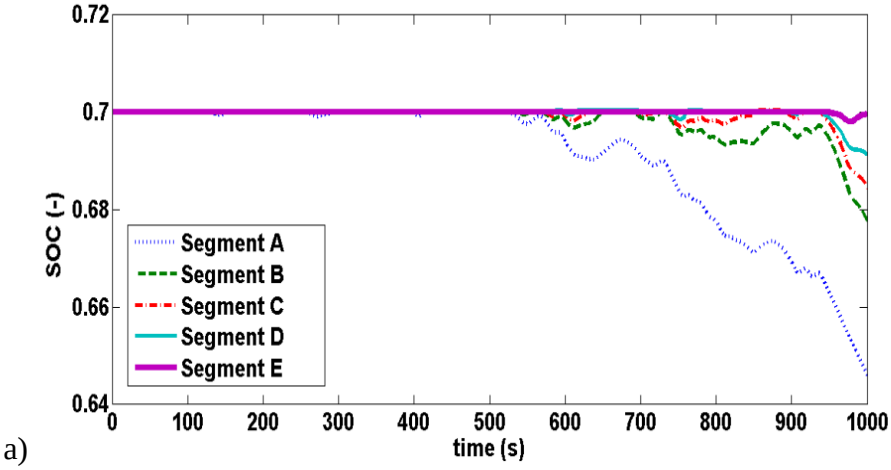

a)

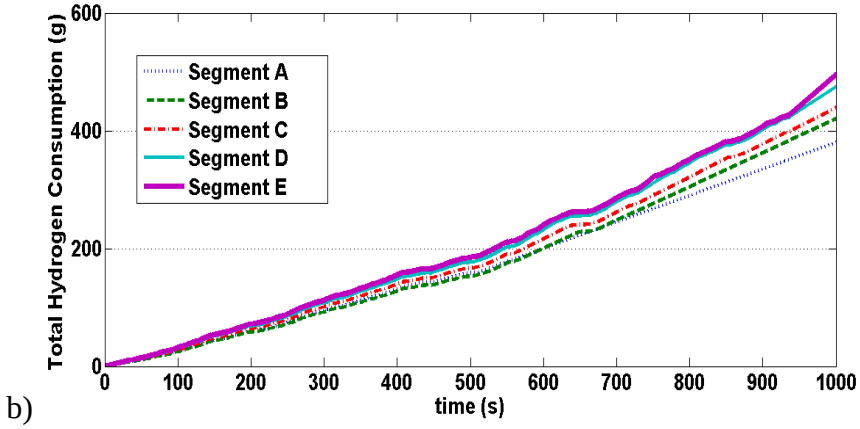

b)

Fig. 6.27: a) State of charge of battery, b) total hydrogen consumption, in EMPA BAB.

The specific consumption indicated in grams of hydrogen per kilometer is reported in the table 6-11, which give indications about the consumptions in different working conditions. For instance, although the EMPA BAB present a higher average speed, the consumptions in this driving cycle are lower than NEDC and MODEM Hyzem highway due the lower slope of the road and the reduction in numbers of accelerations and stops&goes [109].

Table 6-15. Specific consumption with different slope of road (g/km).

Driving cycle	A	B	C	D	E
NEDC (slope 5%)	17.7	19.8	20.9	24.0	24.7
MODEM Hyzem highway (slope 5%)	17.6	18.0	18.1	20.0	20.2
EMPA BAB (slope 1%)	11.7	12.9	13.5	14.6	15.2

Since the consumptions for vehicle are usually calculated without slope because almost the totality of trips starts and finish at the same altitude, the results of Table 6-15 are calculated with a value of slope equal to zero. The obtained values of consumptions are listed in Table 6-16 and they can be used for comparison with consumptions of ICE-based vehicles.

Table 6-16. Specific consumption with slope equal to zero (g/km).

Driving cycle	A	B	C	D	E
NEDC	11.9	13.8	15.8	17.1	19.2
MODEM Hyzem highway	11.6	12.7	13.1	13.9	14.6
EMPA BAB	9.0	9.7	10.8	11.2	12.2

These values give indications about the consumptions of a vehicle in the listed driving cycles with a slope equal to zero. Although the slope should be considered as an important parameter in simulations, its influence need to be considered in the dimensioning of the ED and the primary converter in order to guarantee enough power for challenging values of slope. By the way, mostly of real driving cycles starting from and finish to the same place. In other words, mostly of real driving cycles has an algebraic sum equal to zero which allow to carry out the simulations with a value of zero for slope.

7. Concluding remarks

7.1 Summary of analysis

7.1.1 Modeling of fuel Cell stacks

In the present thesis the performances, in terms of voltage and power, and the efficiency of a PEMFC stack has been quantified and assessed using a mathematical model built up in Matlab/Simulink® environment.

The effect of inlet pressure of hydrogen and temperature has been analyzed. Their influence on the polarization curve have been quantified for a single cell. This influence has also an effect on the power curve and on the efficiency of the stack. Specifically, the mass and energy balance showed as reactants and products of chemical reaction are directly proportional. So their ratio is constant at each value of current density. On the other hand, the obtained results showed how electrical power and heat are inversely proportional. Moreover, the effect of energy flow trends on the theoretical efficiency of the PEMFC stack was examined.

So, the results show how all parameters have a certain influence on the overall behavior of the FC system in terms of efficiency, consumptions, durability and performances. In particular, it is possible to notice which parameters must be increased or reduced in order to have a better dimensioning of the stack.

7.1.2 Modeling of two-wheeled vehicles equipped with Fuel Cells

The dimensioning of a hybrid architecture and the logic of control of energy management strategy have a great influence on the improvement of FC technology and the applications in transportations. As discussed above, in the design phase a hybrid electric powertrain needs a numerical model in order to configure the system arrangement and the components size properly and to predict the behavior of the powertrain. For this scope, a simulation model was constructed using Matlab/Simulink® software by following a hybrid electric “series”

configuration equipped with a PEMFC stack and a Lithium-Ion battery. The model validation confirms the accuracy of the mathematic model which is suitable for the development of the logic strategy control and the dimensioning of the system. Simulation results demonstrate that the proposed model can be used for the dimensioning and optimization of FCHEVs.

In this Research, the best configuration of the hybrid electric powertrain was defined for 2-wheeled vehicles in three case studies. Both sources of energy were dimensioned in term of power (FC of 200, 300, 2000 W and RESS of 2500 and 7800 W for cases studies) and capacity (RESS of 12 and 20 Ah). These vehicle are used for different purposes and although they present a different system configuration, they have similar efficiency. Moreover, the performance of these vehicles was analyzed in experimental driving cycles which reproduce the real mobility needs.

The optimization of the working parameters, such as upper and lower limits of state of charge, point of functioning of the FC, voltage and current of electrical components were monitored during the driving cycles. The dimensioning of the FC and lithium-Ion battery were tested in a long simulation in which a single driving cycle was repeated several times up to a total duration of 25000 seconds. In these simulations the energy generated on board appeared sufficient to meet the traction needs characterized by the driving cycles with challenging speed and slope.

The results of the study are summarized as follows:

1) Two different power sources were connected in a hybrid configuration, such that both types of power can be delivered simultaneously. The presence of an energy storage system allows dimensioning of the primary converter, which has a unidirectional flow, on the average power required for traction and auxiliaries. The storage system can compensate for the deficiencies of the primary converter in the case of higher demand for power.
2) The control strategy managed a model in which the power provided by the FC is able to satisfy the requirement of the ED although the control strategy must consider also a deep analysis of durability of the FC stack during changing working conditions.
3) The enhanced analysis of a “long” mission of the vehicle during repeated driving cycles allowed the behavior of the powertrain in range extender conditions to be assessed.

4) A low value of the relationship of the power generated by the FC over the power provided by the RESS was used in order to reduce the size of the hybrid powertrain.
5) The voltage and the current of all the electric components was monitored and consumption was estimated for the two-wheeled vehicle considered in this Research.

7.1.3 Modeling of four-wheeled vehicles equipped with Fuel Cells

In this Research the hybrid electric configurations of vehicles of European car segments were defined. The solutions proposed were tested through the numerical simulation of the principal parameters of the vehicles over time: SOC and hydrogen consumption. An enhanced analysis which includes the monitoring of the current and voltage of FC and RESS was described in this thesis.

Since a hybrid electric powertrain has two different sources of energy, the relationship between the primary converter and the energy storage can be defined by the designer of the vehicle. In any case, the primary converter must be higher than the average value of the power required in the most demanding case. If this relationship is satisfactory the SOC will be maintained above a lower limit for all driving cycles and the energy content of the energy storage will be enough to supply energy to the EM, as in the cases in this Research. On the other hand the size of the primary converter should not exceed the minimum requirement in order to reduce the cost of the powertrain.

Bibliography

1. Peighambardoust S.J., Rowshanzamir S., Amjadi M.: “Review of the proton exchange membranes for fuel cell applications”, *International Journal of Hydrogen Energy*, Vol. 35 (2010), pp. 9349-9384.

2. Yun Wang, Ken S., Chen, Jeffrey Mishler, Sung Chan Cho, Xavier Cordobes Adroher: “A review of polymer electrolyte membrane fuel cells: Technology, applications, and needs on fundamental research”, *Applied Energy*, Vol. 88 (2011), pp. 981–1007.

3. L. Rambaldi, A. Santiangeli: “Innovative design of a hydrogen powertrain via reverse engineering”, *International Journal of Hydrogen Energy*, Vol. 36 (2011), pp. 8003-8007.

4. Nikolce Murgovski, Lars Johannesson, Jonas Sjöberg, Bo Egardt: “Component sizing of a plug-in hybrid electric powertrain via convex optimization”, *Mechatronics*, Vol. 22 (2012), pp. 106-120.

5. G. Pede, A. Iacobazzi, S. Passerini, A. Bobbio, G. Botto: “FC vehicle hybridization: an affordable solution for an energy-efficient FC powered drive train”, *Journal of Power Source*, Vol. 125 (2004), pp. 280-291.

6. C. Sapienza, L. Andaloro_, F.V. Matera, G. Dispenza, P. Cretì, M. Ferraro, V. Antonucci: “Batteries analysis for FC-hybrid powertrain optimization”, *International Journal of Hydrogen Energy, Vol.* 33 (2008), pp. 3230-3234.

7. Clint Alex Cottrell, Scott E. Grasman, Mathew Thomas, Kevin Braun Martin, John W. Sheffield: “Strategies for stationary and portable fuel cell markets”, *International Journal of Hydrogen Energy*, Vol. 36 (2011), pp. 7969-7975

8. C.C. Chan: “The state of the art of electric and hybrid vehicles”, *Proceedings of the IEEE*, Vol. 90, n.2.

9. Yun Haitao, Zhao Yulan, Sun Zechang, Wan Gangb: “Model-based power control strategy development of a fuel cell hybrid vehicle”, *Journal of Power Sources*, Vol. 180 (2008), pp. 821-829.

10. Xiangjun Li, Liangfei Xu, Jianfeng Hua, Xinfan Lin, Jianqiu Li, Minggao Ouyang: “Power management strategy for vehicular-applied hybrid fuel cell/battery power system”, *Journal of Power Sources*, Vol. 191 (2009), pp. 542-549.

11. J.J. Hwang, D.Y. Wang, N.C. Shih, D.Y. Lai, C.K. Chenb “Development of fuel-cell-powered electric bicycle”, *Journal of Power Sources,* Vol. 133 (2004), pp. 223–228.

12. Bruce Lin “Conceptual design and modeling of a fuel cell scooter for urban Asia”, *Journal of Power Sources*, Vol. 86 (2000), pp. 202–213.

13. Wikipedia PHB bicycle. [Online] Available: http://en.wikipedia.org/wiki/PHB_(bicycle). [Accessed Mar. 08, 2015].

14. Gabele H., Panik F., Ziegler M.: “Brennstoffzellenscooter Hydrofight Fuels”, 7th Int. Colloquium, 2009 January 14-15, TAE Esslingen.

15. Signachem. [Online] Available: http://www.signachem.com/wp-content/uploads/2013/10/3.5_eBike-Fact-Sheet-WEB2.pdf [Accessed Gen. 08, 2015].

16. Intelligent energy. [Online] Available: http://www.intelligent-energy.com/automotive/case-studies/suzuki. [Accessed Gen. 15, 2015].

17. Asia Pacific Fuel Cell Technology. Available: http://www.apfct.com/goods_cat.php?act=view&no=31. [Accessed Gen. 15, 2015].

18. Pragma industries. [Online] Available: http://www.pragma-industries.com/about-us/press-releases/alter-bike/. [Accessed Gen. 15, 2015].

19. J. Larminie, A. Dicks, “Fuel Cell Systems explained”, Wiley, 2003.

20. M. Ceraolo, C. Miulli, P. Cravini: “A Comparison of different fuel-cell based drive train typologies to be used on two-wheel vehicles”, *European Ele-drive Transportation Conference & Exhibition”*, Estoril (Portugal) 17-20 March 2004, paper n.°19_2004 eet.pdf.

21. Jung-Ho Wee “Applications of proton exchange membrane fuel cell systems”, *Renewable and Sustainable Energy Reviews*, Vol. 11 (2007), pp. 1720–1738.

22. Wang, Y., et al., "A review of polymer electrolyte membrane fuel cells: Technology, applications, and needs on fundamental research," *Applied Energy,* vol. 88, pp. 981-1007, (2011).

23. Larminie, J., Dicks, A., "Fuel Cell Systems Explained," Hoboken: John WILEY & Sons Inc., ISBN: 0-470-84857-X, (2003).

24. Hosseinzadeh E, Rokni M: Development and validation of a simple analytical model of the Proton Exchange Membrane Fuel Cell (PEMFC) in a fork–lift truck power system. *International Journal of Green Energy* (2013) pp. 23–43.

25. M. Ceraolo, C. Miulli, A. Pozio, Modelling static and dynamic behaviour of proton exchange membrane fuel cells on the basis of electro–chemical description, *Journal of Power Sources*, Vol. 113 (2003), pp- 131–144.

26. Tsai, B., et al., "Effects of flow field design on the performance of a PEM fuel cell with metal foam as the flow flow distributor," *International Journal of Hydrogen Energy,* vol. 37 (2012), pp. 13060-13066.

27. Scientific Computing World. 2013.http://www.scientific–computing.com/features/feature.php?feature_id=126

28. Bin-Tsang Tsai, Chung-Jen Tseng, Zhong-Sheng Liu, Chih-Hao Wanga, Chun-I Lee,Chang-Chung Yang, Shih-Kun Lo: “Effects of flow field design on the

performance of a PEM fuel cell with metal foam as the flow distributor", *International Journal of Hydrogen Energy*, Vol. 37 (2012), pp. 13060-13066

29. Springer, T.E., et al., "Polymer electrolyte fuel cell model," *Journal of The Electrochemical Society*, vol. 138 (1991), no. 8, pp. 2334-2342.

30. Yuan, W., et al., "Porous metal materials for polymer electrolyte membrane fuel cells - A review," *Applied Energy*, vol. 94 (2012), pp. 309-329.

31. Yun Wanga, Ken S. Chen, Jeffrey Mishler, Sung Chan Cho, Xavier Cordobes Adroher: "A review of polymer electrolyte membrane fuel cells: Technology, applications, and needs on fundamental research", *Applied Energy*, Vol. 88 (2011) pp. 981–1007.

32. Ronald F. Mann, John C. Amphlett, Michael A.I. Hooper, Heidi M. Jensen, Brant A. Peppley, Pierre R. Roberge: "Development and application of a generalized steady-state electrochemical model for a PEM fuel cell", *Journal of Power Sources*, Vol. 86, (2000) pp. 173-180.

33. Amphlett, J. C., et al., "Performance Modeling of the Ballard Mark IV Solid Polymer Electrolyte Fuel Cell," *Electrochemical Science and Technology*, Vol. 142 (1995) no. 1, pp. 9-15.

34. Colleen Spiegel PEM Fuel Cell modeling and simulation using Matlab, Academic Press Elsevier, 2008.

35. Honda's FCX fuel cell concept vehicle. AutoTechnology 2007.

36. Friedlmeier G, Friedrich J, Panik F. Test Experiences with the DaimlerChrysler Fuel Cell Electric Vehicle NECAR 4. *Fuel Cells* 2001;1:92–96.

37. Thomas CE. Fuel cell and battery electric vehicles compared. *International Journal of Hydrogen Energy* Vol. 34 (2009), pp. 6005–6020.

38. Steven G. Chalk, James F. Miller, Key challenges and recent progress in batteries, fuel cells, and hydrogen storage for clean energy systems. *Journal of Power Sources*, Vol. 86, (2000) pp. 173-180.

39. Houchins C, Kleen GJ, Peterson D, Garland NL, Ho DL, Marcinkoski J, *et al.* U.S. doe progress towards developing low–cost, high performance, durable polymer electrolyte membranes for fuel cell applications. *Membranes* Vol. 159 (2006), pp. 73–80.

40. Baschuk, Li X. Carbon monoxide poisoning of proton exchange membrane fuel cells. *International Journal of Energy Research,* Vol. 25 (2001), pp. 695–713.

41. Elham Hosseinzadeh, Masoud Rokni, Abid Rabbani, Henrik Hilleke Mortensen: "Thermal and water management of low temperature Proton Exchange Membrane Fuel Cell in fork-lift truck power system", *Applied Energy*, Vol. 104 (2013), pp. 434-444.

42. Chung-Hsing Chao, Jenn-Jong Shieh: "A new control strategy for hybrid fuel cell-battery power systems with improved efficiency", *International Journal of Hydrogen Energy,* Vol. 37 (2012) pp. 13141-13146.

43. Schiavetti M., Mattoli V., Lutzemberger G., Dario P., Carcassi M.: "Experimental study of hydrogen releases in the passenger compartment of a Piaggio Porter", *International Journal of Hydrogen Energy,* Vol. 37, Issue 22 (2012), pp. 17470–17477.

44. Q. Ning, D. Xuan, Y. Kim: "Modeling and control strategy development for fuel cell hybrid vehicles", *International Journal of Automotive Technology*, Vol. 11, No. 2 (2010) pp. 229-238.

45. G. Pede, A. Iacobazzi, S. Passerini, A. Bobbio, G. Botto: " FC vehicle hybridization: an affordable solution for an energy-efficient FC power drive train", *Journal of Power Source,* Vol. 125 (2004), pp. 280-291.

46. Walker, Linda, Motorcycling and Leisure; Understanding the Recreational PTW Rider, (May 6, 2009)Ashgate Publishing, Ltd.

47. Melissa Holbrook Pierson, The Perfect Vehicle: What It is about Motorcycles, 1997, W.W. Norton & Company, New York

48. Bruce Lin "Conceptual design and modeling of a fuel cell scooter for urban Asia", *Journal of Power Sources* Vol. 86 (2000), pp. 202–213.

49. Whitney G. Colella: "Market prospects, design features, and performance of a fuel cell-powered scooter", *Journal of Power Sources*, Vol. 86 (2000) pp. 255-260.

50. Chunto Tso, Shih-Yun Chang: "A viable niche market-fuel cell scooters in Taiwan", *International Journal of Hydrogen Energy*, Vol. 28 (2003), pp. 757-762.

51. J.J. Hwang, D.Y. Wang, N.C. Shih, D.Y. Lai, C.K. Chenb "Development of fuel-cell-powered electric bicycle", *Journal of Power Sources* Vol. 133 (2004) pp. 223–228.

52. Wikipedia website: http://en.wikipedia.org/wiki/PHB_(bicycle), 16/12/2014.

53. Gabele H., Panik F., Ziegler M.: "Brennstoffzellenscooter Hydrofight Fuels", 7th Int. Colloquium, 2009 January 14-15, TAE Esslingen.

54. Signachem : http://www.signachem.com/wp-content/uploads/2013/10/3.5_eBike-Fact-Sheet-WEB2.pdf, 16/12/2014.

55. Intelligent energy: http://www.intelligent-energy.com/automotive/case-studies/suzuki, 16/12/2014.

56. Asia Pacific Fuel Cell Technology: http://www.apfct.com/goods_cat.php?act=view&no=31, 16/12/2014.

57. Laurianne Ménard, Guillaume Fontès, Stéphan Astier: "Dynamic energy model of a lithium-ion battery", *Mathematics and Computers in Simulation*, Volume 81, Issue 2, October 2010, Pages 327-339.

58. Diego Feroldi, Maria Serra, Jordi Riera: “Design and Analysis of Fuel-Cell Hybrid Systems Oriented to Automotive Applications”, *IEEE Transactions On Vehicular Technology*, Vol. 58, N. 9 (2009).

59. R. Sutula, K.L. Heitner, S.A. Rogers, T.Q. Dong, R.S. Kirk (OATT), V. Battaglia, G. Henriksen, N.L. Argonne, F. McLarnon, N.L. Lawerence Berkeley, B.J. Kumar, C. Schonefeld (Energetics Inc.), *Recent Accomplishment of the Electric and Hybrid Vehicle Storage R&D Programs at the U.S. Department of Energy: A Status Report, EVS-17*, Montreal, October 2000.

60. G. Pede, V. Sglavo, F. Vellucci, C. Villante:” Report su test di ricarica rapida di batterie a Litio*”, Ricerca di sistema elettrico Rd*S, ENEA, 2011.

61. G. Lo Bianco, G. Pede, E. Rossi, A. Puccetti (ENEA), G. Mantovani (ALTRA), Vehicle Testing in ENEA Drive-train Test Facility, *Advanced Hybrid Vehicles Powertrains*, SAE SP-1607, Detroit, March 2001.

62. Mohammad Ali Karbaschian, Dirk Soffker: “Review and Comparison of Power Management Approaches for Hybrid Vehicles with Focus on Hydraulic Drives”, *Energies*, Vol. 7 (2014), pp. 3512-3536.

63. Hellmann, M., et al., "Required Operating Temperature of a Mobile Fuel Cell System and Consequences for the Dimensioning of the System," f-cell Stuttgart, BOSCH (2012).

64. Bruno G. Polleta, Iain Staffellb, Jin Lei Shangc: “Current Status of Hybrid, Battery and Fuel Cell Electric Vehicles: from Electrochemistry to Market Prospects”, Electrochimica Acta, *Special Issue of International Year of Chemistry 2011 "Electrochemical Science and Technology - State of the Art and Future Perspectives"* ID 03.172, 2012.

65. State of the Art on Alternative Fuels Transport Systems in the European Union, Final Report, European Commission, July 2015.

66. Caiying Shen, Peng Shan, Tao Gao: “A Comprehensive Overview of Hybrid Electric Vehicles” *International Journal of Vehicular Technology*, Article 571683 (2011) 7 pages.

67. State of the States: Fuel Cells in America 2014 5th Edition Fuel Cell Technologies Office U.S. Department of Energy, December 2014

68. Nan Qin, Ali Raissi, Paul Brooker: “Analysis of Fuel Cell Vehicle Developments”, Electric Vehicle Transportation Center Report Number FSEC-CR-1987-14, 2014

69. FCH JU: http://www.fch.europa.eu/, 15/09/2015

70. Programme Review Report 2014, European Union, FCH JU, 2014

71. Fuel Cell and Hydrogen technologies in Europe 2011: financial and technology outlook on the European sector ambition 2014-2020, European Union, FCH JU, 2011.

72. A portfolio of power-trains for Europe: a fact-based analysis. The role of Battery Electric Vehicles, Plug-in Hybrids and Fuel Cell Electric Vehicles, European Union, FCH JU, 2014.

73. Faheem Khan, Arshad Nawaz, Malik Ansar Muhammad, Muhammad Ali Khadim: “ Review And Analysis of MATLAB/Simulink Model Of PEM Fuel Cell Stack”, *International Journal of Engineering & Computer Science* IJECS-IJENS Vol:13 No:03 pp. 31-34.

74. Abid Rabbani, Masoud Rokni: “Effect of nitrogen crossover on purging strategy in PEM fuel cell systems”, *Applied Energy*, Vol. 111, November 2013, Pages 1061-1070.

75. Abid Rabbani, Masoud Rokni: “Dynamic characteristics of an automotive fuel cell system for transitory load changes”, *Sustainable Energy Technologies and Assessment*s, Vol. 1, March 2013, Pages 34-43.

76. D. De Luca, P. Fragiacomo, G. De Lorenzo, T.W. Czarnetski, W. Schneider, "A MATLAB/SIMULINK® design procedure for proton exchange membrane fuel cells", *9th International Symposium Hydrogen & Energy* 25-30 January 2015, Emmetten, Switzerland. (abstract).

77. M.G. Santarelli, M.F. Torchio, P. Cochis: "Parameters estimation of a PEM fuel cell polarization curve and analysis of their behavior with temperature", *Journal of Power Sources*, Vol. 159 (2006) pp. 824-835.

78. Abd El Monem, Ahmed Azmy, Mahmoud: "Dynamic Modelling of Proton Exchange Membrane Fuel Cells for Electric Vehicle Applications.", *Petroleum & Environmental Biotechnology*, Vol. 5 (2014).

79. R.Seyezhai, B.L.Mathur: "Mathematical Modeling of Proton Exchange Membrane Fuel Cell", *International Journal of Computer Application* Vol. 20, N.5, April 2011

80. Xiuqin Zhang, Juncheng Guo, Jincan Chen: "The parametric optimum analysis of a proton exchange membrane (PEM) fuel cell and its load matching", *Energy*, Vol. 35 (2010) pp. 5294-5299.

81. Shuguo Qu, Xiaojin Li, Ming Hou, Zhigang Shao, Baolian Yi: "The effect of air stoichiometry change on the dynamic behavior of a proton exchange membrane fuel cell", *Journal of Power Sources*, Vol. 185 (2008) pp. 302-310.

82. Lin Wang, Attila Husar, Tianhong Zhou, Hongtan Liu: "A parametric study of PEM fuel cell performances", *International Journal of Hydrogen Energy*, Vol. 28 (2003) pp. 1263-1272.

83. Satoshi Takaichi, Hiroyuki Uchida, Masahiro Watanabe: "In situ analysis of oxygen partial pressure at the cathode catalyst layer/membrane interface during PEFC operation", Electrochimica Acta, Vol. 53 (2008) pp. 4699-4705.

84. Jason Marcinkoskia, Brian D. Jamesb, Jeff A. Kalinoskib, Walt Podolskic, Thomas Benjaminc, John Kopaszc: “Manufacturing process assumptions used in fuel cell system cost analyses”, *Journal of Power Sources*, Vol. 196 (2011) pp. 5282-5292

85. Xiuqin Zhang, Juncheng Guo, Jincan Chen: “The parametric optimum analysis of a proton exchange membrane (PEM) fuel cell and its load matching”, *Energy*, Vol. 35 (2010) pp. 5294-5299

86. J. Wishart, Z. Dong, M. Secanell: “Optimization of a PEM fuel cell system based on empirical data and a generalized electrochemical semi-empirical model”, *Journal of Power Sources*, Vol. 161 (2006) pp. 1041-1055

87. Joeri Van Mierlo, Peter Van den Bossche, Gaston Maggetto: “Models of energy sources for EV and HEV: fuel cells, batteries, ultracapacitors, flywheels and engine-generators”, *Journal of Power Sources*, Vol. 128 (2004) pp. 76-89.

88. David Wenzhong Gao, Senior Member IEEE, Chris Mi, Senior Member IEEE, Ali Emadi, Senior Member IEEE: “Modeling and Simulation of Electric and Hybrid Vehicles”, *Proceeding of IEEE*.

89. Jenn-Jiang Hwang, Yu-Jie Chen, Jenn-Kun Kuo: “ The study on the power management system in a fuel cell hybrid vehicle”, *International Journal of Hydrogen Energy*, Vol. 37 (2012), pp. 4476-4489.

90. P. Struss, C. Price: “Model-based systems in the automotive industry”, AI Magazine, Vol. 24, n. 4, pp. 17-34, Winter 2004.

91. B. Powell, K. Bailey, S. Cikanek: “Dynamic modeling and control of hybrid electric vehicle powertrain systems”, Control Systems, Vol. 18, n. 5, pp. 17-22, October 1998.

92. K. L. Butler, M. Ehsani, P. Kamath: “Matlab-based modeling and simulation package for electric and hybrid electric vehicle design”, *Vehicular Technology*, November 1999, Vol. 48, n. 6, pp. 1770-1118.

93. Michel André: “The ARTEMIS European driving cycles for measuring car pollutant emissions”, *Science of the Total Environment*, Vol. 334-335 (2004), pp. 73-84.

94. T. J. Barlow, S. Latham, I. S. McCrae, B. C. Boulter: “A reference book of driving cycles for use in the measurement of road vehicle emission”, *TRL Project Report PPR 354*, 2009.

95. Jeffrey Wishart, Yuliang Leon Zhou, Zuomin Dong “Review of multi-regime hybrid vehicle powertrain architecture”, *International Journal of Electric and Hybrid* Vehicles”, 2008 Vol.1, No.3, pp.248 – 275.

96. L. V. Pérez, G. R. Bossio, D. Moitre, G. O. García: “Optimization of power management in an hybrid electric vehicle using dynamic programming“, *Mathematics and Computers in Simulation*, Volume 73, Issues 1–4, 6 November 2006, pp. 244-254.

97. L. V. Pérez, E. A. Pilotta: “Optimal power split in a hybrid electric vehicle using direct transcription of an optimal control problem“, *Mathematics and Computers in Simulation*, Volume 79, Issue 6, February 2009, pp. 1959-1970.

98. Bernard J., Delprat S., Guerra T.M., Buchi F.N.: “A Fuel efficient power management strategy for fuel cell hybrid powertrains”, *Control Engineering Practice*, Vol. 18 (2010) pp. 408-417.

99. D. De Luca, P. Fragiacomo, G. De Lorenzo, “Investigation of energy flow rates in Proton Exchange Membrane Fuel Cells using numerical model”, *5th European PEFC & H_2 Forum (EFCF)* 30 June - 3 July 2015, Lucerne, Switzerland. (abstract).

100. Grace One. (Online) Available: http://www.grace-bikes.com/Bikes/One. (Accessed Feb. 18, 2015).

101. Jason Thomas Parks: “Simulation of Riding a Bicycle Using Simulink”, California State university, Sacramento (2010) pp.174.

102. Horizon Fuel Cell Stack H-Series User Manuals. (Online) Available: http://www.horizonfuelcell.com/#!h-series-stacks/c52t. (Accessed Feb. 20, 2015).

103. D. De Luca, P. Fragiacomo, G. De Lorenzo, T.W. Czarnetzki, W. Schneider, "Development of a Hybrid Electric 2-wheeled Vehicle equipped with Fuel Cell", *6th International Conference on Fundamentals & Development of Fuel Cells (FDFC)* 3-5 February 2015, Toulouse, France. (abstract).

104. T. J. Barlow, S. Latham, I. S. McCrae, B. C. Boulter: "A reference book of driving cycles for use in the measurement of road vehicle emission", *TRL Project Report PPR 354*, 2009.

105. Becherif, Claude, Harvier, Boulon,: "Multi-stack Fuel Cells Powering a Vehicle", *Energy procedia,* Vol. 74 (2015) pp. 308-319.

106. European Commission , *Regulation N. 4064/89*, Brussels 17.03.1999.

107. Oscar P.R. van Vliet, Thomas Kruithof, Wim C. Turkenburg, Andre P.C. Faaij: "Techno-economic comparison of series hybrid, plug-in hybrid, fuel cell and regular cars", *Journal of Power Sources*, Vol. 195 (2010), pp. 6570-6585.

108. D. De Luca, P. Fragiacomo, G. Pede, "Components sizing of hybrid electric powertrains with fuel cell for passenger cars", *The Energy & Materials Research Conference (EMR)* 25-27 February 2015, Madrid, Spain. (abstract).

109. D. De Luca, P. Fragiacomo, G. Pede, "Components sizing of hybrid electric powertrains with fuel cell for passenger cars", *Materials and technologies for energy efficiency*, Vol.1, pp.73-77, 2015.